Western Australia 2-D Marine Seismic Survey

Acoustic Modelling for Assessing Marine Fauna Sound Exposures

Submitted to:

Joe Edgell
INPEX Operations Australia Pty Ltd
PO: 4500039837 and 4500039843

Authors:

Craig McPherson
Jennifer Wladichuk
Zahraalsadat Alavizadeh
Karen Hiltz

27 February 2019

P001457-001
Document 01696
Version 1.0

JASCO Applied Sciences (Australia) Pty Ltd.
Unit 1, 14 Hook Street
Capalaba, Queensland, 4157
Tel: +61 7 3823 2620
www.jasco.com

Disclaimer:

The results presented herein are relevant within the specific context described in this report. They could be misinterpreted if not considered in the light of all the information contained in this report. Accordingly, if information from this report is used in documents released to the public or to regulatory bodies, such documents must clearly cite the original report, which shall be made readily available to the recipients in integral and unedited form.

Suggested citation:

McPherson, C.R., J.L. Wladichuk, Z. Alavizadeh and K. Hiltz. 2018. *Western Australia 2-D Marine Seismic Survey: Acoustic Modelling for Assessing Marine Fauna Sound Exposures*. Document 01696, Version 1.0. Technical report by JASCO Applied Sciences for INPEX Operations Australia Pty Ltd.

Contents

Figures

Tables

Executive Summary

JASCO Applied Sciences performed a numerical estimation study of underwater sound levels associated with the planned INPEX Western Australia (WA) 2-D Marine Seismic Survey (MSS) to assist in understanding the potential acoustic impact on key regional receptors including fish, marine mammals, benthic invertebrates (including pearl oysters), plankton, and turtles. The planned Acquisition Area is focused on two exploration permits, WA-533-P and WA-532-P, and Production Licence, WA-50-L, in northwest WA. Three seismic sources were initially considered, with the propagation modelling considering the source with the loudest far-field representative signature, a 3080 in^3 seismic source towed at a 7 m depth behind a single vessel.

A specialised airgun array source model was used to predict the acoustic signature of the three seismic sources, and complementary underwater acoustic propagation models were used in conjunction with the modelled array signature of a 3080 in^3 to estimate sound levels over a large area around the source. Single-impulse sound fields were predicted at defined locations within the entire Acquisition Area, and accumulated sound exposure fields were predicted for three representative scenarios for likely survey operations over 24 hours. The modelling methodology considered source directivity and range-dependent environmental properties in each of the areas assessed. Estimated underwater acoustic levels are presented as sound pressure levels (SPL, L_p), zero-to-peak pressure levels (PK, L_{pk}), peak-to-peak pressure levels (PK-PK; $L_{pk\text{-}pk}$), and either single-impulse (i.e., per-pulse) or accumulated sound exposure levels (SEL, L_E) as appropriate for different noise effect criteria. A conservative sound speed profile that would be most supportive of sound propagation conditions for the period of the survey was defined and applied to all modelling.

The analysis considered the distances away from the seismic source at which several effects criteria or relevant sound levels were reached. The results are summarised below for the representative single-impulse sites and accumulated SEL scenarios. Additionally, sound levels were predicted at five locations relevant to the pearl oyster fishery and four locations relevant to calving and resting humpback whales.

Marine mammal injury and behaviour

- The maximum distance where the NMFS (2014) marine mammal behavioural response criterion of 160 dB re 1 µPa (SPL) could be exceeded varied between 5.52 and 11.19 km (Site 8, 45 m and Site 12, 103 m, permit WA-532-P).
- The maximum received SPL, LF-weighted SPL and per-pulse SEL at any of the four locations relevant to calving and resting humpback whales were received at Tasmanian Shoal considering a modelled site 79 km away. The respective levels were 134.6 (L_p; dB re 1 µPa), 120 ($L_{p,LF}$; dB re 1 µPa) and 126.2 (L_E; dB re 1 µPa²·s).
- The results for the criteria applied for marine mammal Permanent Threshold Shift (PTS), NMFS (2018), consider both metrics within the criteria (PK and SEL_{24h}). The longest distance associated with either metric is required to be applied. The table below summarise the maximum distances for PTS, along with the relevant metric and the location of the results within this report.
- The furthest distance from the array that high-frequency cetaceans could experience PTS was 440 m at Site 12 (103 m, permit WA-532-P), a site in a different location to any of the SEL_{24h} scenarios.

Table 1. Summary of maximum marine mammal PTS onset distances for SEL_{24h} modelled scenarios

Relevant hearing group	Metric associated with longest distance to PTS onset	R_{max} (km)		
		Scenario 1 (WA-533-P Shallow)	Scenario 2 (WA-533-P Deep)	Scenario 3 (WA-532-P)
Low-frequency cetaceans†	SEL_{24h}	0.7	1.35	2.13
Mid-frequency cetaceans†	PK	< 0.02	< 0.02	< 0.02
High-frequency cetaceans	PK	0.27	0.22	0.39
Sirenians	PK	NA	NA	0.02

† The model does not account for shutdowns.

- The 24-h SEL is a cumulative metric that reflects the dosimetric impact of noise levels within 24 hours based on the assumption that an animal is consistently exposed to such noise levels at a fixed position. The corresponding 24-h SEL radii for low-frequency cetaceans were larger than those for peak pressure criteria, but they represent an unlikely worst-case scenario. More realistically, marine mammals (and fish) would not stay in the same location or at the same range for 24 hours. Therefore, a reported radius for 24-h SEL criteria does not mean that marine fauna travelling within this radius of the source will be injured, but rather that an animal could be exposed to the sound level associated with injury (either PTS or TTS) if it remained in that range for 24 hours

Turtle Behaviour

- The maximum distance where the United States NMFS criterion (NSF 2011) for behavioural effects in turtles of 166 dB re 1 µPa (SPL) could be exceeded varied between 3.09 and 6.13 km (Site 8, 45 m and Site 11, 70 m, permit WA-532-P).

Fish, turtle injury, fish eggs, and fish larvae

- The modelling study assessed the seafloor and water column ranges for quantitative criteria based on Popper et al. (2014) and considering both PK and SEL_{24h} metrics associated with mortality and potential mortal injury and impairment in:
  - Fish without a swim bladder (also appropriate for sharks in the absence of other information)
  - Fish with a swim bladder that do not use it for hearing
  - Fish that use their swim bladders for hearing
  - Turtles
  - Fish eggs and fish larvae
- Water column receptors, assessed at four modelling sites:
  - The maximum distance to sound levels associated with mortality and potential mortal injury on most the sensitive fish groups are associated with the PK metric, and range from 120 m (Sites 1, 5 and 12) to 220 m (Site 7). For fish without a swim bladder, the distance is 60 m at all four sites.
- Seafloor receptors, assessed at five modelling sites, along with sites representative of different depths and geoacoustic parameters, three in WA-533-P and five in WA-532-P (depths from 30 to 103 m):
  - The maximum distance to sound levels associated with mortality and potential mortal injury in fish, turtles, fish eggs and fish larvae is associated with the PK metric in all cases.
  - The maximum distance for the most sensitive fish groups (associated with a PK threshold of 207 dB re 1 µPa) varies between 154 and 185 m.

  - The maximum distance for the less sensitive fish groups (associated with a PK threshold of 213 dB re 1 µPa) varies between 54 and 114 m.
- Considering the three 24-hour SEL scenarios, and based on Popper et al. (2014), the SEL_{24h} metric criteria for potential TTS could be exceeded within the following distances:
  - 1.58 km of the array at both the seafloor for maximum-over-depth during Scenario 1,
  - 4.94 km for maximum-over-depth during Scenario 2
  - within 2.92 km at the seafloor and 3.5 km for maximum-over-depth during Scenario 3.

Crustaceans and Bivalves, Sponges and Coral, and Plankton

To assist with assessing the potential effects on these receptors, the following have been determined:

- The maximum received SPL and per-pulse SEL at any of the five locations relevant to the pearl oyster fishery were received at the closest lease to modelling Site 1, 74.5 km away. The respective levels were 101.9 (L_p; dB re 1 µPa) and 121.1 (L_E; dB re 1 µPa²·s).
- Crustaceans: The sound level of 202 dB re 1 µPa PK-PK from Payne et al. (2008) was considered; it was reached at ranges between 461 and 666 m depending on the modelled site, with range generally increasing with bottom depth.
- Sponges and coral: The PK sound level at the seafloor directly underneath the seismic source was estimated at all modelling sites considered for seafloor fish receptors, and compared to the sound level of 226 dB re 1 µPa PK for sponges and corals (Heyward et al. 2018); it was found to reach or just exceed the criterion only at sites with a water depth less than 45 m, with the maximum distance being < 12 m (30 m depth).
- Plankton: The distance to the sound level of 178 dB re 1 µPa PK-PK from McCauley et al. (2017) was estimated at all modelling sites through full-waveform modelling using FWRAM; the results ranged from 7.94 km to 12.23 km.

1. Introduction

JASCO Applied Sciences (JASCO) performed a numerical estimation study of underwater sound levels associated with the planned INPEX Western Australia (WA) 2-D Marine Seismic Survey (MSS) to assist in understanding the potential acoustic impact on key regional receptors including fish, marine mammals, benthic invertebrates (including pearl oysters), plankton, and turtles. The survey plan Acquisition Area is focused on two exploration permits, WA-533-P and WA-532-P, and Production Licence, WA-50-L, in northwest WA. Three seismic sources were initially considered, with the propagation modelling considering the source with the loudest far-field representative signature, a 3080 in^3 seismic source towed at a 7 m depth behind a single seismic source vessel.

JASCO's specialised Airgun Array Source Model (AASM) was used to predict the acoustic signature of all three arrays. AASM accounts for individual airgun volumes and array geometry. Complementary underwater acoustic propagation models were used in conjunction with the selected modelled array signature to estimate sound levels over a large area around the source. Single-impulse sound fields were predicted at defined locations within the entire Acquisition Area, and accumulated sound exposure fields were predicted for three representative scenarios for likely survey operations over 24 hours. A conservative sound speed profile that would be most supportive of sound propagation conditions for the period of the survey was defined and applied at each of the modelling locations.

The modelling methodology considered source directivity and range-dependent environmental properties in each of the areas assessed. Estimated underwater acoustic levels are presented as sound pressure levels (SPL, L_p), zero-to-peak pressure levels (PK, L_{pk}), peak-to-peak pressure levels (PK-PK; $L_{pk\text{-}pk}$), and either single-impulse (i.e., per-pulse) or accumulated sound exposure levels (SEL, L_E) as appropriate for different noise effect criteria.

2. Modelling Scenarios

Six standalone single impulse sites and three likely scenarios of survey operations over 24 hours to assess accumulated SEL were initially defined, with an additional six modelling sites (a combined total of 12 sites) defined to ensure a robust assessment of accumulated SEL. The locations of all modelling sites are provided in Table 2, with all sites shown in Figure 1 along with the exploration permits and survey boundaries. Seafloor sound levels were examined at depths of 45, 55, and 65 m in WA-533-P, and 30–70 m in WA-532-P using geological profiles consistent with associated water depths.

Single impulse sound fields were also sampled at fixed receiver locations relevant to humpback whale resting, calving and nursing grounds (Figure 1, Table 3) and pearl oyster fishery lease and fishing grounds (Figure 1, Table 4).

Three representative scenarios (Scenarios 1–3) for acquisition within the Acquisition Area were considered for 24 hours of operation, the period relevant considering the various criteria applied in this study. Two scenarios are located in permit WA-533-P, located in the shallowest (Scenario 1) and deepest (Scenario 2) sections of the permit, and the third scenario is in WA-532-P, close to shoals and Australian Marine Parks. The track lines for each scenario are shown in Figures 2–4. The modelling assumes that the vessels sail along the survey lines at ~4.5 knots, with an impulse interval of 18.75 m. The considered survey lines take between ~3.75–11.3 h to traverse, with ~1.86–1.92 h of turn time required between the lines depending upon the scenario, this is likely a faster turn than for the actual survey. The scenarios account for 9840, 9046, and 9591 impulses, respectively. For Scenario 3, the time history of sound exposure accumulation at the seafloor was also estimated at static receivers located at eight offset distances (50, 100, 300, 500, 1000, 2000, 3000, and 5000 m) from both survey lines within the scenario.

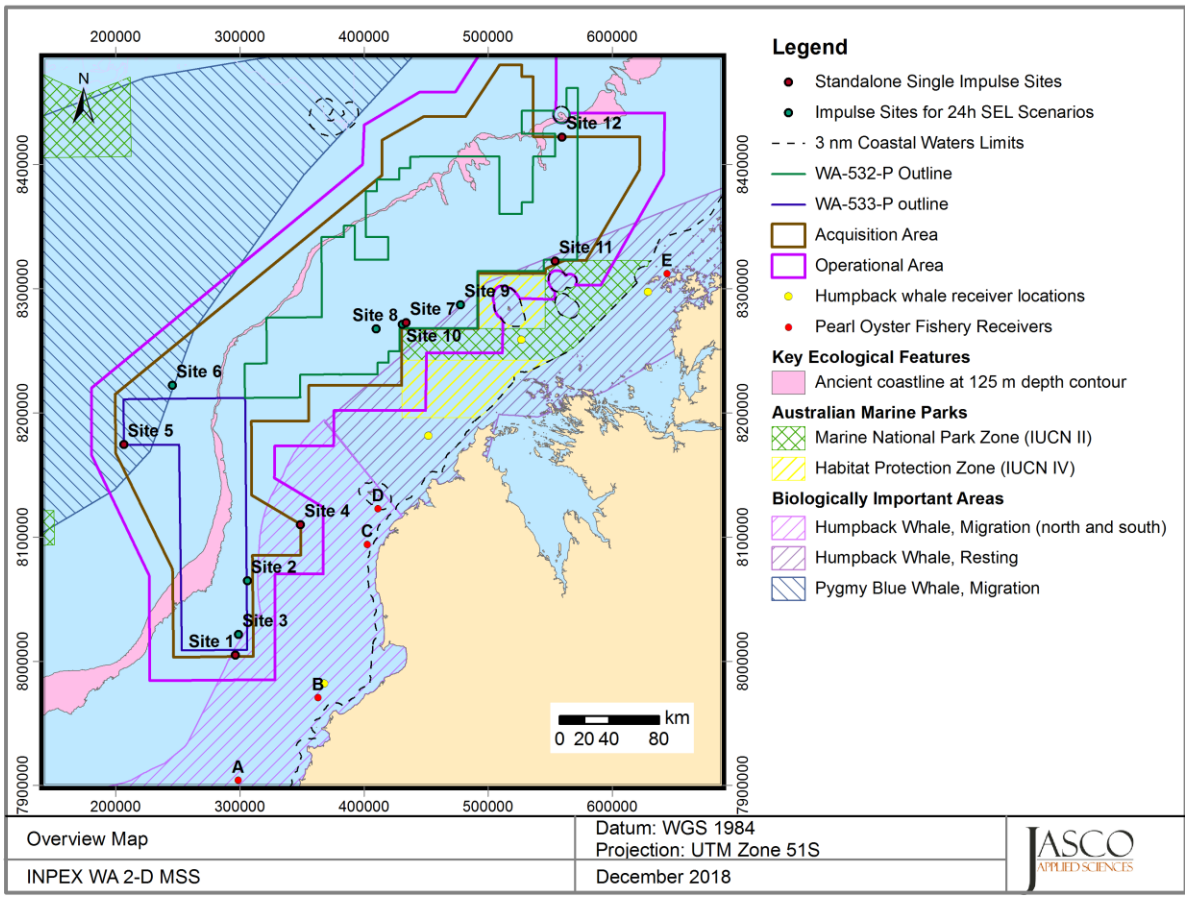

Figure 1. Overview of the modelling sites and features for the WA 2-D marine seismic survey modelling.

Table 2. Location details for the standalone single impulse sites.

Site	Latitude (S)	Longitude (E)	UTM (WGS84), Zone 51 S		Water depth (m)	Representative tow direction (°)	Associated 24-hour Scenario
			X (m)	*Y* (m)			
1	18° 02' 13.9900"	121° 04' 33.4297"	296326.9	8004637	67	189.9/9.9	Scenario 1
2	17° 29' 49.1347"	121° 10' 22.9614"	306025.7	8064535	98		
3	17° 53' 14.1409"	121° 06' 07.7760"	298932.4	8021264	89		
4	16° 29' 36.2192"	120° 15' 10.6251"	206726.2	8174490	37	121.3	NA
5	17° 05' 25.8942"	121° 34' 42.8679"	348758.8	8109879	451	210.9/30.9	Scenario 2
6	16° 04' 07.4590"	120° 37' 26.6740"	245821.2	8222002	360		
7	15° 37' 26.7291"	122° 23' 02.9719"	433987.3	8272549	59	71.5/251.5	Scenario 3
8	15° 40' 10.9159"	122° 09' 33.6274"	409907.5	8267422	45		
9	15° 29' 40.4578"	122° 47' 35.8906"	477830.4	8286960	84		
10	15° 38' 15.4254"	122° 21' 15.4894"	430791.4	8271043	34		
11	15° 10' 29.8828"	123° 30' 06.3271"	553899.2	8322260	70	160.9	NA
12	14° 16' 20.9080"	123° 33' 04.0528"	559446.5	8422069	103	339.5	NA

Table 3. Humpback whale receiver locations and relevant modelling sites.

Receiver location	Latitude (S)	Longitude (E)	UTM (WGS84), Zone 51 S		Relevant modelling site	Distance (km)
			X (m)	*Y* (m)		
Camden Sound	15° 24' 00.0000"	124° 12' 00.0000"	628774.2	8297073	11	93.8
					12	142.9
Tasmanian Shoal	15° 45' 00.0000"	123° 15' 00.0000"	526781	8258702	7	79.0
					11	69.1
Pender Bay	16° 27' 00.0000"	122° 33' 00.0000"	451962.6	8181234	4	125.4
					7	93.1
Gourdon Bay	18° 15' 00.0000"	121° 45' 00.0000"	367851	7981704	1	75.1
					4	129.5

Table 4. Pearl oyster fishery receiver locations and relevant modelling sites.

Pearl oyster fishery receiver	Latitude	Longitude	Relevant modelling site	Location description	Distance (km)
A	18° 56' 51.1990" S	121° 05' 11.6198" E	1	Compass Rose fishing ground	100.8
B	18° 21' 06.1200" S	121° 42' 06.1200" E	1	Port Smith farm lease	74.8
C	17° 14' 18.2400" S	122° 05' 02.7600" E	4	North Coulomb Pt farm lease	56.0
D	16° 58' 48.7447" S	122° 09' 54.4718" E	4	Lacepede Channel fishing ground	63.6
E	15° 15' 52.9045" S	124° 20' 32.5257" E	11	Pearl Transport Exempt Area / Kuri Bay farm leases	90.7

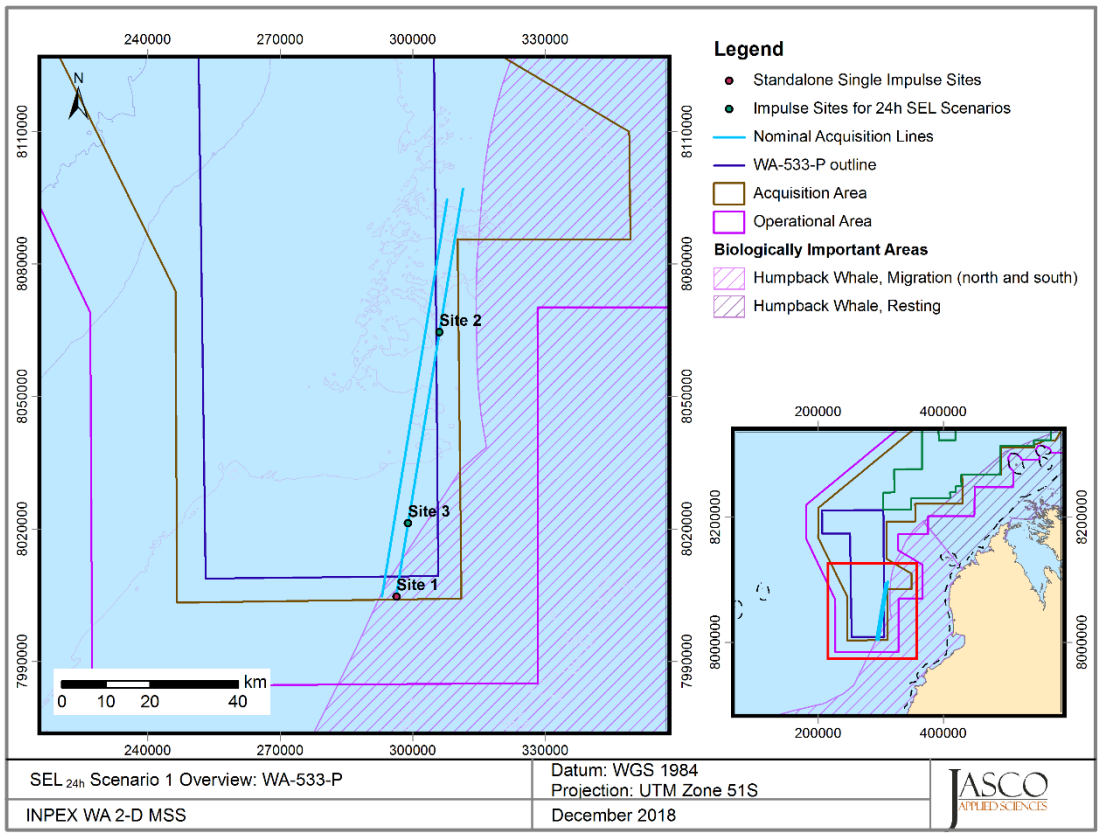

Figure 2. *Scenario 1*: Acquisition lines and static receiver locations considered for SEL_{24h} calculations, WA-533-P Shallow.

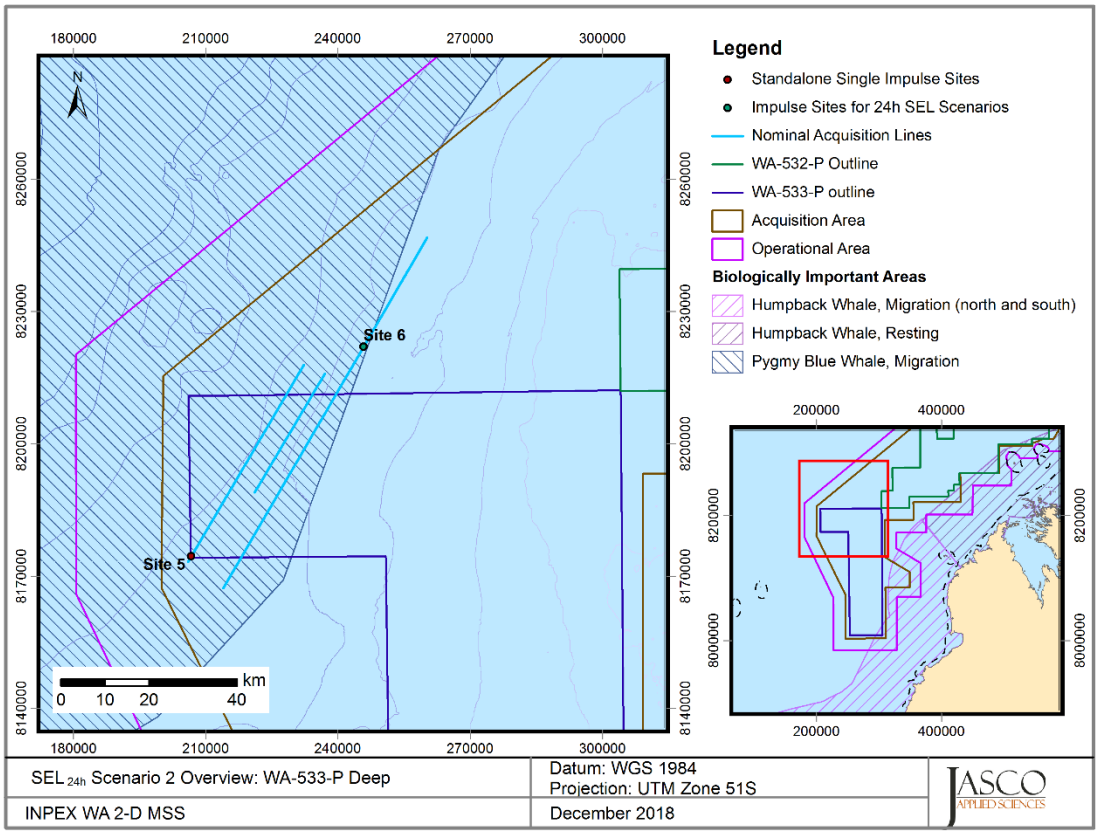

Figure 3. *Scenario 2*: Acquisition lines and static receiver locations considered for SEL_{24h} calculations, WA-533-P deep.

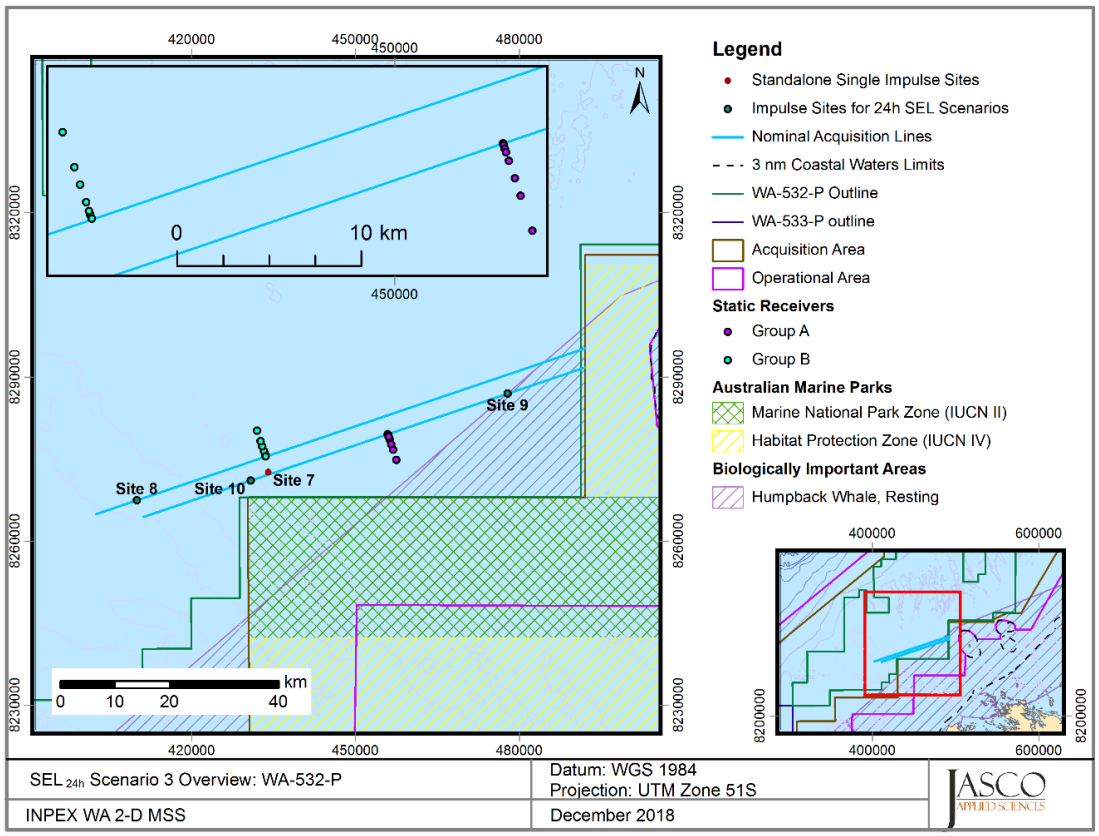

Figure 4. *Scenario 3*: Acquisition lines and static receiver locations considered for SEL_{24h} calculations, WA-532-P.

3. Noise Effect Criteria

The perceived loudness of sound, especially impulsive noise such as from seismic airguns, is not generally proportional to the instantaneous acoustic pressure. Rather, perceived loudness depends on the pulse rise-time and duration, and the frequency content. Several sound level metrics, such as PK, SPL, and SEL, are commonly used to evaluate noise and its effects on marine life (Appendix A). The period of accumulation associated with SEL is defined, with this report referencing either a "per pulse" assessment or over 24 hours. Appropriate subscripts indicate any applied frequency weighting; unweighted SEL is defined as required. The acoustic metrics in this report reflect the updated ISO standard for acoustic terminology, ISO/DIS 18405.2:2017 (2017).

Whether acoustic exposure levels might injure or disturb marine mammals is an active research topic. Since 2007, several expert groups have investigated an SEL-based assessment approach for injury, with a handful of key papers published on the topic. The number of studies that investigated the level of disturbance to marine animals by underwater noise has also increased substantially.

We chose the following noise criteria and sound levels for this study because they include standard thresholds, thresholds suggested by the best available science, and sound levels presented in literature for species with no suggested thresholds (Sections 3.1–3.2 and Appendix A):

1. Peak pressure levels (PK; L_{pk}) and frequency-weighted accumulated sound exposure levels (SEL; $L_{E,24h}$) from the U.S. National Oceanic and Atmospheric Administration (NOAA) Technical Guidance (NMFS 2018) for the onset of Permanent Threshold Shift (PTS) in marine mammals.
2. Marine mammal behavioural threshold based on the current interim U.S. National Marine Fisheries Service (NMFS) (2014) of 160 dB re 1 µPa SPL (L_p) for impulsive sound sources.
3. Sound exposure guidelines for fish, fish eggs and larvae, and turtles (Popper et al. 2014).
4. Threshold for turtle behavioural response (NSF 2011), 166 dB re 1 µPa SPL (L_p), applied by the U.S. NMFS.
5. A sound level 178 dB re 1 µPa PK-PK in the water column, reported for comparing to McCauley et al. (2017) for plankton.
6. Peak-peak pressure levels (PK-PK; L_{pk-pk}) at the seafloor to help assess effects of noise on crustaceans and bivalves, through comparing to results in Payne et al. (2008), and Day et al. (2016).
7. A sound level of 226 dB re 1 µPa PK (L_{pk}) reported for comparing to Heyward et al. (2018) for sponges and corals.

Additionally, to assess the size of the low-power zone required under the Australian Environment Protection and Biodiversity Conservation (EPBC) Act Policy Statement 2.1, Department of the Environment, Water, Heritage and the Arts (DEWHA) (2008), the distance to an unweighted per-pulse SEL of 160 dB re 1 µPa^2·s is reported.

The following section expands on the thresholds and sound levels for marine mammals, fish, turtles, fish eggs, and fish larvae and benthic invertebrates.

3.1. Marine Mammals

The criteria applied in this study to assess possible effects of airgun noise on marine mammals are summarised in Table 5 and detailed in Sections 3.1.1 and 3.1.2, with frequency weighting explained in Appendix A.3.

Table 5. Unweighted SPL, SEL_{24h}, and PK thresholds for acoustic effects on marine mammals.

Hearing group	NMFS (2014)	NMFS (2018)			
	Behaviour	PTS onset thresholds* (received level)		TTS onset thresholds* (received level)	
	SPL (L_p; dB re 1 µPa)	Weighted SEL_{24h} ($L_{E,24h}$; dB re 1 µPa^2·s)	PK (L_{pk}; dB re 1 µPa)	Weighted SEL_{24h} ($L_{E,24h}$; dB re 1 µPa^2·s)	PK (L_{pk}; dB re 1 µPa)
Low-frequency cetaceans	160	183	219	168	213
Mid-frequency cetaceans		185	230	170	224
High-frequency cetaceans		155	202	140	196
Sirenians (Dugong)		190	226	175	220

* Dual metric acoustic thresholds for impulsive sounds: Use whichever results in the largest isopleth for calculating PTS onset. If a non-impulsive sound has the potential of exceeding the peak sound pressure level thresholds associated with impulsive sounds, these thresholds should also be considered.
L_p–denotes sound pressure level period and has a reference value of 1 µPa
L_{pk}, flat–peak sound pressure is flat weighted or unweighted and has a reference value of 1 µPa
L_E - denotes cumulative sound exposure over a 24-hour period and has a reference value of 1 µPa^{2}s
Subscripts indicate the designated marine mammal auditory weighting.

3.1.1. Behavioural response

Southall et al. (2007) extensively reviewed marine mammal behavioural responses to sounds. Their review found that most marine mammals exhibited varying responses between 140 and 180 dB re 1 µPa SPL, but inconsistent results between studies makes choosing a single behavioural threshold difficult. Studies varied in their lack of control groups, imprecise measurements, inconsistent metrics, and that animal responses depended on study context, which included the animal's activity state. To create meaningful quantitative data from the collected information, Southall et al. (2007) proposed a severity scale that increased with increasing sound levels.

NMFS has historically used a relatively simple sound level criterion for potentially disturbing a marine mammal. For impulsive sounds, this threshold is 160 dB re 1 µPa SPL for cetaceans NMFS (NMFS 2014). This threshold has been applied for this report.

3.1.2. Injury and hearing sensitivity changes

There are two categories of auditory threshold shifts or hearing loss: permanent threshold shift (PTS), a physical injury to an animal's hearing organs; and Temporary Threshold Shift (TTS), a temporary reduction in an animal's hearing sensitivity as the result of receptor hair cells in the cochlea becoming fatigued.

To assist in assessing the potential for injuries to marine mammals this report applies the criteria recommended by NMFS (2018), considering both PTS and TTS, to help assess the potential for injuries to marine mammals. Appendix A.2 provides more information about the NMFS (2018) criteria.

3.2. Fish, Turtles, Fish Eggs, and Fish Larvae

In 2006, the Working Group on the Effects of Sound on Fish and Turtles was formed to continue developing noise exposure criteria for fish and turtles, work begun by a panel convened by NOAA two years earlier. The resulting guidelines included specific thresholds for different levels of effects and for different groups of species (Popper et al. 2014). These guidelines defined quantitative thresholds for three types of immediate effects:

- Mortality, including injury leading to death.
- Recoverable injury, including injuries unlikely to result in mortality, such as hair cell damage and minor haematoma.
- TTS.

Masking and behavioural effects can be assessed qualitatively, by assessing relative risk rather than by specific sound level thresholds. These effects are not assessed in this report. Because the presence or absence of a swim bladder has a role in hearing, fish's susceptibility to injury from noise exposure varies depending on the species and the presence and possible role of a swim bladder in hearing. Thus, different thresholds were proposed for fish without a swim bladder (also appropriate for sharks and applied to whale sharks in the absence of other information), fish with a swim bladder not used for hearing, and fish that use their swim bladders for hearing. Turtles, fish eggs, and fish larvae are considered separately.

Table 6 lists relevant effects thresholds from Popper et al. (2014). In general, any adverse effects of seismic sound on fish behaviour depends on the species, the state of the individuals exposed, and other factors. We note that, despite mortality being a possibility for fish exposed to airgun sounds, Popper et al. (2014) do not reference an actual occurrence of this effect. Since the publication of that work, newer studies have further examined the question of possible mortality. Popper et al. (2016) adds further information to the possible levels of impulsive seismic airgun sound to which adult fish can be exposed without immediate mortality. They found that the two fish species in their study, with body masses in the range 200–400 g, exposed to a single-impulse of a maximum received level of either 231 dB re 1 µPa (PK) or 205 dB re 1 $\mu Pa^2 \cdot s$ (SEL), remained alive for 7 days after exposure and that the probability of mortal injury did not differ between exposed and control fish.

The SEL metric integrates noise intensity over some period of exposure. Because the period of integration for regulatory assessments is not well defined for sounds that do not have a clear start or end time, or for very long-lasting exposures, it is required to define a time. Popper et al. (2014) recommend a standard period should be applied, where this is either defined as a justified fixed period or the duration of the activity, however also include caveats about how long the fish will be exposed because they can move (or remain in location) and so can the source. Popper et al. (2014) summarises that in all TTS studies considered, fish that showed TTS recovered to normal hearing levels within 18–24 hours. Due to this, a period of accumulation of 24 hours has been applied in this study for SEL, which is similar to that applied for marine mammals in NMFS (2016, 2018).

In the discussion of the criteria, Popper et al. (2014) discuss the complications in determining a relevant period of mobile seismic surveys, as the received levels at the fish change between impulses due to the mobile source, and that in reality a revised guideline based on the closest PK or the per-pulse SEL might be more useful than one based on accumulated SEL. This is because exposures at the closest point of approach are the primary exposures contributing to a receiver's accumulated level (Gedamke et al. 2011). Additionally, several important factors determine the likelihood and duration a receiver is expected to be in close proximity to a sound source (i.e., overlap in space and time between the source and receiver). For example, accumulation time for fast moving (relative to the receiver) mobile sources is driven primarily by the characteristics of source (i.e., speed, duty cycle; NMFS 2016, 2018).

Table 6. Criteria for seismic noise exposure for fish and turtles, adapted from Popper et al. (2014).

Type of animal	Mortality and Potential mortal injury	Impairment			Behaviour
		Recoverable injury	TTS	Masking	
Fish: No swim bladder (particle motion detection)	>219 dB SEL_{24h} or >213 dB PK	>216 dB SEL_{24h} or >213 dB PK	>>186 dB SEL_{24h}	(N) Low (I) Low (F) Low	(N) High (I) Moderate (F) Low
Fish: Swim bladder not involved in hearing (particle motion detection)	210 dB SEL_{24h} or >207 dB PK	203 dB SEL_{24h} or >207 dB PK	>>186 dB SEL_{24h}	(N) Low (I) Low (F) Low	(N) High (I) Moderate (F) Low
Fish: Swim bladder involved in hearing (primarily pressure detection)	207 dB SEL_{24h} or >207 dB PK	203 dB SEL_{24h} or >207 dB PK	186 dB SEL_{24h}	(N) Low (I) Low (F) Moderate	(N) High (I) High (F) Moderate
Turtles	210 dB SEL_{24h} or > 207 dB PK	(N) High (I) Low (F) Low	(N) High (I) Low (F) Low	(N) Low (I) Low (F) Low	(N) High (I) Moderate (F) Low
Fish eggs and fish larvae	>210 dB SEL_{24h} or >207 dB PK	(N) Moderate (I) Low (F) Low	(N) Moderate (I) Low (F) Low	(N) Low (I) Low (F) Low	(N) Moderate (I) Low (F) Low

Notes: Peak sound level (PK) dB re 1 µPa; SEL_{24h} dB re 1µPa^2·s. All criteria are presented as sound pressure, even for fish without swim bladders, since no data for particle motion exist. Relative risk (high, moderate, or low) is given for animals at three distances from the source defined in relative terms as near (N), intermediate (I), and far (F). >> denotes levels much greater than.

3.2.1. Turtle behavioural response and injury

There is a paucity of data regarding responses of turtles to acoustic exposure, and no studies of hearing loss due to exposure to loud sounds. McCauley et al. (2000) observed the behavioural response of caged turtles—green (*Chelonia mydas*) and loggerhead (*Caretta caretta*)—to an approaching seismic airgun. For received levels above 166 dB re 1 µPa (SPL), the turtles increased their swimming activity and above 175 dB re 1 µPa they began to behave erratically, which was interpreted as an agitated state. The 166 dB re 1 µPa level has been used as the threshold level for a behavioural disturbance response by NMFS and applied in the Arctic Programmatic Environment Impact Statement (PEIS) (NSF 2011). At that time, and in the absence of any data from which to determine the sound levels that could injure an animal, TTS or PTS onset were considered possible at an SPL of 180 dB re 1 µPa (NSF 2011). Some additional data suggest that behavioural responses occur closer to an SPL of 175 dB re 1 µPa, and TTS or PTS at even higher levels (Moein et al. 1995), but the received levels were unknown and the NSF (2011) PEIS maintained the earlier NMFS criteria levels of 166 and 180 dB re 1 µPa (SPL) for behavioural response and injury, respectively. Popper et al. (2014) suggested injury to turtles could occur for sound exposures above 207 dB re 1 µPa (PK) or above 210 dB re 1 µPa^2·s (SEL_{24h}) (Table 6). Sound levels defined by Popper et al. (2014) show that animals are very likely to exhibit a behavioural response when they are near an airgun (tens of metres), a moderate response if they encounter the source at intermediate ranges (hundreds of metres), and a low response if they are far (thousands of meters) from the airgun. Finneran et al. (2017) indicate that the 175 dB re 1 µPa SPL is an appropriate received sound level at which turtles are expected to actively avoid seismic air gun exposures. However, the lower and more conservative NMFS criterion for behavioural disturbance (SPL of 166 dB re 1 µPa) and the Popper et al. (2014) injury criteria were included in this analysis, although the analysis did not consider the ranges where an animal could suffer impairment, as defined by Popper et al. (2014).

3.3. Benthic Invertebrates (Crustaceans and Bivalves)

Research is ongoing into the relationship between sound and its effects on crustaceans, including the relevant metrics for both effect and impact. Available literature suggests particle motion, rather than sound pressure, is a more important factor for crustacean and bivalve hearing. Water depth and seismic source size are related to the particle motion levels at the seafloor, with larger arrays and shallower water being related to higher particle motion levels, more likely relevant to effects on crustaceans and bivalves.

At the seafloor interface, crustaceans and bivalves are subject to particle motion stimuli from several acoustic or acoustically-induced waves. These include the particle motion associated with an impinging sound pressure wave in the water column (the incident, reflected, and transmitted portions), substrate acoustic waves, and interface waves of the Scholte type. However, it is unclear which aspect(s) of these waves is/are most relevant to the animals, either when they normally sense the environment or their physiological responses to loud sounds so there is not enough information to establish similar criteria and thresholds as done for marine mammals and fish. Including recent research, such as Day et al. (2016), current literature does not clearly define an appropriate metric or identify relevant levels (pressure or particle motion) for an assessment. This includes the consideration of what particle motion levels lead to a behavioural response, or mortality. Therefore, at this stage, we cannot propose authoritative thresholds to inform the impact assessment. However, levels can be determined for pressure metrics presented in literature to assist the assessment.

A PK-PK sound level of 202 dB re 1 µPa (Payne et al. 2008) is considered to be associated with no impact, and therefore applied in the assessment. Additionally for context, the PK-PK sound levels determined for crustaceans in Day et al. (2016), 209–212 dB re 1 µPa, are also included

4. Methods

4.1. Acoustic Source Model

The pressure signatures of the individual airguns and the composite 1/3-octave-band point-source equivalent directional levels (i.e., source levels) of three seismic sources (2970, 3000 and 3080 in^3) were modelled with JASCO's Airgun Array Source Model (AASM). Although AASM accounts for notional pressure signatures of each seismic source with respect to the effects of surface-reflected signals on bubble oscillations and inter-bubble interactions, the surface-reflected signal (known as surface ghost) is not included in the far-field source signatures. The acoustic propagation models account for those surface reflections, which are a property of the propagating medium rather than the source.

AASM considers:

- Array layout.
- Volume, tow depth, and firing pressure of each airgun.
- Interactions between different airguns in the array.

The array was modelled over AASM's full frequency range, up to 25 kHz. Appendix B details this model.

4.2. Sound Propagation Models

Three sound propagation models were used to predict the acoustic field around the seismic source for frequencies of 5 Hz to 25 kHz:

- Combined range-dependent parabolic equation and gaussian beam acoustic ray-trace model (MONM-BELLHOP).
- Full Waveform Range-dependent Acoustic Model (FWRAM).
- Wavenumber integration model (VSTACK).

4.3. Parameter Overview

The specifications of the seismic sources and the environmental parameters used in the propagation models are described in detail in Appendix D.

The following seismic sources considered were:

- 2970 in^3 seismic source array consisting of three strings towed at a depth of 7 m, (see Figures D-7 to D-5) with a nominal firing pressure of 2000 psi.
- 3000 in^3 seismic source array consisting of three strings towed at a depth of 6 m, (see Figures D-7 to D-5) with a nominal firing pressure of 2000 psi.
- 3080 in^3 seismic source array consisting of three strings towed at a depth of 7 m, (see Figures D-7 to D-5) with a nominal firing pressure of 2000 psi.

A single sound speed profile for July was considered in the modelling; this was identified as the seasonal period that would provide the greatest propagation. The following four geological regions were identified:

- Gravelly sand (SW shelf), Sites 1–4
- Muddy sand (SW slope), Sites 5 and 6
- Muddy sandy gravel (central shelf), Sites 7–11
- Gravelly muddy sand (NE shelf), Site 12

4.4. Accumulated SEL

During a seismic survey, new sound energy is introduced into the environment with each pulse from the seismic source. While some impact criteria are based on the per-pulse energy released, others, such as the marine mammal and fish SEL criteria used in this report (Sections 3.1 and 3.2) account for the total acoustic energy marine fauna is subjected to over a specified period of time, defined in this report as 24 hours. An accurate assessment of the accumulated sound energy depends not only on the parameters of each seismic pulse impulse, but also on the number of impulses delivered in a period and the relative positions of the impulses.

When there are many seismic pulses, it becomes computationally prohibitive to perform sound propagation modelling for every single event. The distance between the consecutive seismic impulses is small enough, however, that the environmental parameters that influence sound propagation are virtually the same for many impulse points. The acoustic fields can, therefore, be modelled for a subset of seismic pulses and estimated at several adjacent ones. After sound fields from representative impulse locations are calculated, they are adjusted to account for the source position for nearby impulses.

Although estimating the cumulative sound field with the described approach is not as precise as modelling sound propagation at every impulse location, small-scale, site-specific sound propagation features tend to blur and become less relevant when sound fields from adjacent impulses are summed. Larger scale sound propagation features, primarily dependent on water depth, dominate the cumulative field. The accuracy of the present method acceptably reflects those large-scale features, thus providing a meaningful estimate of a wide area SEL field in a computationally feasible framework.

To produce maps of accumulated received sound level distributions and calculate distances to specified sound level thresholds, the maximum-over-depth level and level at the seafloor were calculated at each sampling point within the modelled region. The radial grids of maximum-over-depth and seafloor sound levels for each impulse were then resampled (by linear triangulation) to produce a regular Cartesian grid. The sound field grids from all impulses were summed (Equation A-5) to produce the cumulative sound field grid with cell sizes of 40 m. The contours and threshold ranges were calculated from these flat Cartesian projections of the modelled acoustic fields. The single-impulse SEL fields were computed over model grids 200 × 200 km in range, which encompasses the full area of the cumulative grid (the entire survey area).

The unweighted (fish) and frequency-weighted SEL_{24h} results were rendered as contour maps, including contours that focus on the relevant criteria-based thresholds. Only contours at ranges larger than the nearfield of the seismic source were rendered.

4.5. Geometry and Modelled Regions

To assess sound levels with MONM-BELLHOP, the sound field modelling calculated propagation losses up to distances of 100 km from the source, with a horizontal separation of 10 m between receiver points along the modelled radials. The sound fields were modelled with a horizontal angular resolution of $\Delta\theta = 2.5°$ for a total of N = 144 radial planes. Receiver depths were chosen to span the entire water column over the modelled areas, from 2 m to a maximum of 10,000 m, with step sizes that increased with depth. To supplement the MONM results, high-frequency results for propagation loss were modelled using Bellhop for frequencies from 2.5 to 25 kHz. The MONM and Bellhop results were combined to produce results for the full frequency range of interest.

FWRAM was run to 150 km, but along only four radials (fore and aft endfire and port and starboard broadside) for computational efficiency, from 10 Hz to 2048 Hz in 1 Hz steps. This was done to compute SEL-to-SPL conversions (Appendix D.2). The horizontal range step is dependent on frequency and ranges from 50 m at lower frequencies to 10 m above 800 Hz. Additional single transects from specific modelling sites to the humpback whale receivers (Table 3) were run.

The maximum modelled range for VSTACK was 1000 m and used a step size of 10 m. Received levels were computed for receivers at seafloor.

5. Results

5.1. Acoustic Source Levels and Directivity

AASM (Section 4.1) was used to predict the horizontal and vertical overpressure signatures and corresponding power spectrum levels for the three seismic sources, with results provided in Appendix B.2 along with the horizontal directivity plots.

Tables 7–9 show the PK and per-pulse SEL source levels for each seismic source in the horizontal-plane broadside (perpendicular to the tow direction), endfire (along the tow direction), and vertical directions. The vertical source level that accounts for the "surface ghost" (the out of phase reflected pulse from the water surface) is also presented to make it easier to compare the output of other seismic source models.

Figures B.1 through B.3 show the broadside, endfire, and vertical overpressure signature and corresponding power spectrum levels for each array. The signatures consist of a strong primary peak, related to the initial release of high-pressure air, followed by a series of pulses associated with bubble oscillations. Most energy is produced at frequencies below 500 Hz, although this is different for each array, with noticeable differences between the broadside and endfire signatures. Frequency-dependent peaks and nulls in the spectrum result from interference among airguns in the array and correspond with the volumes and relative locations of the airguns to each other.

The source with the loudest far-field source level specifications is the 3080 in^3 source, therefore, is was selected for consideration in the propagation modelling.

Table 7. Far-field source level specifications for the 2970 in^3 array, for a 7 m tow depth. Source levels are for a point-like acoustic source with equivalent far-field acoustic output in the specified direction. Sound level metrics are per-pulse and unweighted.

Direction	Peak source pressure level ($L_{S,pk}$) (dB re 1 µPa²m²)	Per-pulse source SEL ($L_{S,E}$) (dB 1 µPa²m²s)	
		10–2000 Hz	2000–25000 Hz
Broadside	247.1	223.3	180.0
Endfire	246.5	223.8	183.5
Vertical	255.8	228.8	189.9
Vertical (surface affected source level)	255.8	231.8	192.8

Table 8. Far-field source level specifications for the 3000 in^3 array, for a 6 m tow depth. Source levels are for a point-like acoustic source with equivalent far-field acoustic output in the specified direction. Sound level metrics are per-pulse and unweighted.

Direction	Peak source pressure level ($L_{S,pk}$) (dB re 1 µPa²m²)	Per-pulse source SEL ($L_{S,E}$) (dB 1 µPa²m²s)	
		10–2000 Hz	2000–25000 Hz
Broadside	249.3	224.7	180.8
Endfire	245.8	222.9	181.9
Vertical	255.2	228.2	189.2
Vertical (surface affected source level)	255.2	231.1	192.2

Table 9. Far-field source level specifications for the 3080 in^3 array, for a 7 m tow depth. Source levels are for a point-like acoustic source with equivalent far-field acoustic output in the specified direction. Sound level metrics are per-pulse and unweighted.

Direction	**Peak source pressure level ($L_{S,pk}$) (dB re 1 µPa²m²)**	**Per-pulse source SEL ($L_{S,E}$) (dB 1 µPa²m²s)**	
		10–2000 Hz	2000–25000 Hz
Broadside	249.6	224.8	184.6
Endfire	246.4	223.6	187.2
Vertical	255.9	228.5	194.6
Vertical (surface affected source level)	255.9	231.4	197.6

5.2. Per-pulse Sound Fields

5.2.1. Tabulated results

Per-pulse results for the 3080 in³ seismic source towed at 7 m are presented for SPL, SEL, PK, and PK-PK, including seafloor PK and PK-PK. Tables 10–13 list the estimated ranges for the various applicable maximum-over-depth per-pulse effects criteria and isopleths of interest, and Tables 14 and 15 list the sound levels at the pearl oyster fishery and humpback whale receivers. Tables 16–19 list the estimated ranges for seafloor per-pulse effects criteria and isopleths of interest

5.2.1.1. Entire water column

Table 10. Maximum (R_{max}) and 95% ($R_{95\%}$) horizontal distances (in km) from the 3080 in³ array to modelled maximum-over-depth per-pulse SEL isopleths from the twelve modelled single impulse sites.

Per-pulse SEL (L_E; dB re 1 µPa²·s)	Site 1 (67 m)		Site 2 (98 m)		Site 3 (89 m)		Site 4 (37 m)		Site 5 (451 m)		Site 6 (360 m)	
	R_{max}	$R_{95\%}$	R_{max}	$R_{95\%}$	R_{max}	$R_{95\%}$	R_{max}	$R_{95\%}$	R_{max}	$R_{95\%}$	R_{max}	$R_{95\%}$
190	0.04	0.04	0.04	0.04	0.05	0.04	0.05	0.05	0.05	0.05	0.05	0.04
180	0.27	0.24	0.24	0.21	0.26	0.23	0.23	0.22	0.16	0.14	0.16	0.14
170	0.82	0.72	0.77	0.66	0.74	0.65	0.87	0.77	1.01	0.92	1.00	0.88
160†	2.76	2.37	2.84	2.42	2.92	2.55	2.79	2.29	3.56	3.03	3.89	3.22
150	7.34	6.06	8.10	6.58	7.29	6.25	7.23	5.89	14.57	12.25	15.59	11.90
140	19.73	16.46	19.65	16.24	19.06	15.91	21.56	17.23	43.40	33.82	44.56	36.75
130	54.14	44.02	49.09	41.07	48.41	41.44	76.16	66.42	130.58	100.43	124.36	102.82
Per-pulse SEL (L_E; dB re 1 µPa²·s)	**Site 7 (59 m)**		**Site 8 (45 m)**		**Site 9 (84 m)**		**Site 10 (34 m)**		**Site 11 (70 m)**		**Site 12 (103 m)**	
	R_{max}	$R_{95\%}$	R_{max}	$R_{95\%}$	R_{max}	$R_{95\%}$	R_{max}	$R_{95\%}$	R_{max}	$R_{95\%}$	R_{max}	$R_{95\%}$
190	0.05	0.05	0.05	0.04	0.05	0.05	0.05	0.05	0.05	0.05	0.05	0.05
180	0.34	0.30	0.26	0.23	0.22	0.19	0.26	0.22	0.34	0.29	0.32	0.29
170	1.69	1.38	0.93	0.82	0.85	0.68	1.01	0.83	1.63	1.39	1.60	1.37
160†	4.71	3.82	2.55	2.14	2.94	2.54	3.19	2.42	4.94	3.96	5.88	4.83
150	12.59	10.04	6.36	5.14	7.16	5.97	8.64	6.83	12.32	9.69	14.98	12.54
140	39.97	31.71	16.25	13.08	17.55	13.22	22.54	17.58	29.96	24.70	38.99	32.91
130	92.39	80.91	32.21	25.54	45.51	35.71	62.41	47.18	85.24	63.40	105.30	83.78

† Low power zone assessment criteria DEWHA (2008).

Table 11. Maximum (R_{max}) and 95% ($R_{95\%}$) horizontal distances (in km) from the 3080 in^3 array to modelled maximum-over-depth SPL isopleths from the twelve modelled single impulse sites.

SPL (L_p; dB re 1 µPa)	Site 1 (67 m)		Site 2 (98 m)		Site 3 (89 m)		Site 4 (37 m)		Site 5 (451 m)		Site 6 (360 m)	
	R_{max}	$R_{95\%}$	R_{max}	$R_{95\%}$	R_{max}	$R_{95\%}$	R_{max}	$R_{95\%}$	R_{max}	$R_{95\%}$	R_{max}	$R_{95\%}$
200	0.04	0.04	0.04	0.04	0.04	0.04	0.05	0.05	0.05	0.05	0.04	0.04
190	0.23	0.20	0.18	0.15	0.21	0.18	0.22	0.20	0.15	0.13	0.15	0.13
180	0.73	0.62	0.67	0.57	0.68	0.58	0.80	0.70	0.48	0.40	0.88	0.79
170	2.60	2.13	2.36	2.08	2.79	2.19	2.59	2.10	2.82	2.31	3.06	2.59
166†	4.07	3.25	3.98	3.36	3.79	3.40	3.81	3.08	4.29	3.69	4.53	3.83
160‡	6.73	5.57	7.22	5.96	6.73	5.81	6.55	5.41	7.74	6.51	8.04	6.69
150	17.96	14.88	17.64	14.67	17.06	14.52	18.85	15.29	24.32	19.46	23.90	18.83
140	49.41	40.75	44.19	37.79	44.96	38.80	69.50	60.78	112.80	66.18	120.30	65.62
130	101.45	76.56	79.64	66.57	93.77	72.85	139.36*	112.61*	141.39*	109.96*	139.61*	112.51*
SPL (L_p; dB re 1 µPa)	**Site 7 (59 m)**		**Site 8 (45 m)**		**Site 9 (84 m)**		**Site 10 (34 m)**		**Site 11 (70 m)**		**Site 12 (103 m)**	
	R_{max}	$R_{95\%}$	R_{max}	$R_{95\%}$	R_{max}	$R_{95\%}$	R_{max}	$R_{95\%}$	R_{max}	$R_{95\%}$	R_{max}	$R_{95\%}$
200	0.05	0.05	0.05	0.05	0.05	0.05	0.05	0.05	0.05	0.05	0.05	0.05
190	0.31	0.27	0.24	0.21	0.19	0.15	0.23	0.21	0.30	0.26	0.31	0.28
180	1.35	1.17	0.81	0.70	0.68	0.58	0.91	0.74	1.35	1.15	1.24	1.09
170	3.77	3.15	2.19	1.91	2.35	2.06	2.50	1.99	4.01	3.29	4.09	3.56
166†	5.98	4.73	3.09	2.65	3.74	3.07	4.16	3.07	6.13	4.76	6.09	5.10
160‡	10.84	8.62	5.52	4.35	6.80	5.16	7.11	5.70	10.32	8.19	11.19	9.14
150	33.85	27.13	14.58	11.51	14.77	11.80	20.37	16.23	27.45	22.64	28.25	24.19
140	90.49	75.93	29.85	23.96	40.71	32.01	55.04	42.43	75.51	57.72	78.18	62.97
130	112.26	94.57	61.14	45.10	87.13	69.86	93.07	75.72	114.92*	96.09	131.72*	102.65*

* Radii extend beyond modelling boundary.
† Threshold for turtle behavioural response to impulsive noise (NSF 2011).
‡ Marine mammal behavioural threshold for impulsive sound sources (NMFS 2014)

Table 12. Maximum (R_{max}) horizontal distances (km) from the 3080 in^3 array to modelled maximum-over-depth peak pressure level (PK) thresholds based on the NOAA Technical Guidance (NMFS 2018) for marine mammals, and Popper et al. (2014) for fish and turtles, at four of the modelling sites (Table 2).

Hearing group	PK threshold (L_{pk}; dB re 1 µPa)	Distance R_{max} (km)			
		Site 1 (67 m)	Site 5 (451 m)	Site 7 (59 m)	Site 12 (103 m)
Low-frequency cetaceans (PTS)	219	0.03	0.03	0.03	0.03
Low-frequency cetaceans (TTS)	213	0.06	0.06	0.06	0.06
Mid-frequency cetaceans (PTS)	230	< 0.02	< 0.02	< 0.02	< 0.02
Mid-frequency cetaceans (TTS)	224	0.02	0.02	0.02	0.02
High-frequency cetaceans (PTS)	202	0.27	0.22	0.39	0.44
High-frequency cetaceans (TTS)	196	0.64	0.43	0.67	0.8
Sirenians (PTS)	226	0.02	NA	0.02	0.02
Sirenians (TTS)	220	0.03	NA	0.03	0.03
Fish: No swim bladder (also applied to sharks)	213	0.06	0.06	0.06	0.06
Fish: Swim bladder not involved in hearing, Swim bladder involved in hearing Turtles, fish eggs, and larvae	207	0.12	0.12	0.22	0.12

Table 13. Maximum (R_{max}) horizontal distances (in km) from the 3080 in^3 array to modelled maximum-over-depth 178 dB re 1µPa PK-PK , assessed along the three FWRAM modelling transects (maximum presented) at four of the modelling sites (Table 2).

PK-PK (L_{pk-pk}; dB re 1 µPa)	Distance R_{max} (km)			
	Site 1 (67 m)	Site 5 (451 m)	Site 7 (59 m)	Site 12 (103 m)
178	7.94	12.23	10.71	9.56

Table 14. Received maximum-over-depth per-pulse SEL and SPL at pearl oyster fishery receivers (Table 4) from the closest modelling sites.

Pearl oyster fishery receiver	Relevant modelling site	Location relevance	Distance (km)	Location	Received SEL (L_E; dB re 1 µPa²·s)	Received SPL (L_p; dB re 1 µPa)
A – Compass Rose fishing ground	1	Closest fishing ground	100.7	18° 56' 51.1990" S, 121° 05' 11.6198" E	95.6	119.4
B – Port Smith farm lease	1	Closest lease	74.5	18° 21' 06.1200" S, 121° 42' 06.1200" E	101.9	121.1
C – North Coulomb Pt farm lease	4	Closest lease	56.0	17° 14' 18.2400" S, 122° 05' 02.7600" E	101.1	110.1
D – Lacepede Channel fishing ground	4	Closest fishing ground	63.6	16° 58' 48.7447" S, 122° 09' 54.4718" E	97.6	106.6
E - Pearl Transport Exempt Area / Kuri Bay farm leases	11	Closest lease	90.8	15° 15' 52.9045" S, 124° 20' 32.5257" E	113	121.9

Table 15. Received SPL, LF-weighted SPL and per-pulse SEL at humpback whale resting/calving receivers (Table 3) from the closest modelling sites.

Receiver location	Relevant modelling site	Distance (km)	Received SPL (L_p; dB re 1 µPa)	Received LF-weighted ($L_{p,LF}$; dB re 1 µPa)	Received SEL (L_E; dB re 1 µPa²·s)
Camden Sound	11	93.8	120.5	118.2	113.2
	12	142.9	120.3	120.2	111.4
Tasmanian Shoal	7	79.0	134.6	120.1	126.2
	11	69.1	120.6	120.2	111.6
Pender Bay	4	125.4	107.6	107.6	98.6
	7	93.1	123.2	122.9	114.2
Gourdon Bay	1	75.1	118.0	117.8	109.0
	4	129.5	120.5	120.3	111.5

5.2.1.2. Seafloor

Table 16. Maximum (R_{max}) horizontal distances (in m) from the 3080 in^3 array to modelled seafloor PK for representative depths in WA-532-P.

Hearing group/animal type	PK threshold (L_{pk}; dB re 1 µPa)	Distance R_{max} (m)				
		30 m	40 m	50 m	60 m	70 m
Sound levels for sponges and corals†	226	12	7	—	—	—
Fish: No swim bladder (also applied to sharks)	213	89	98	105	114	88
Fish: Swim bladder not involved in hearing, Swim bladder involved in hearing Turtles, fish eggs, and larvae	207	185	154	164	185	178

†(Heyward et al. 2018)
A dash indicates the level is not reached.

Table 17. Maximum (R_{max}) horizontal distances (in m) from the 3080 in^3 array to modelled seafloor PK for representative depths in WA-533-P

Hearing group/animal type	PK threshold (L_{pk}; dB re 1 µPa)	Distance R_{max} (m)		
		45 m	55 m	65 m
Sound levels for sponges and corals†	226	1	—	—
Fish: No swim bladder (also applied to sharks)	213	95	82	71
Fish: Swim bladder not involved in hearing, Swim bladder involved in hearing Turtles, fish eggs, and larvae	207	168	185	205

† Heyward et al. (2018)
A dash indicates the level is not reached.

Table 18. Maximum (R_{max}) horizontal distances (in m) from the 3080 in^3 array to modelled seafloor PK from five single-impulse modelling sites (Table 2).

Hearing group/animal type	PK threshold (L_{pk}; dB re 1 µPa)	Distance R_{max} (m)				
		Site 1 (67 m)	Site 4 (37 m)	Site 7 (59 m)	Site 11 (70 m)	Site 12 (103 m)
Sound levels for sponges and corals†	226	—	7	—	—	—
Fish: No swim bladder (also applied to sharks)	213	71	100	114	88	54
Fish: Swim bladder not involved in hearing, Swim bladder involved in hearing Turtles, fish eggs, and larvae	207	205	163	185	178	230

† Heyward et al. (2018)
A dash indicates the level is not reached.

Table 19. Maximum (R_{max}) horizontal distances (in m) from the 3080 in^3 array to modelled seafloor PK-PK from five modelling sites (Table 2). Results included in relation to benthic invertebrates (Section 3.3).

PK-PK (L_{pk-pk}; dB re 1 µPa)	Distance R_{max} (m)				
	Site 1 (67 m)	Site 4 (37 m)	Site 7 (59 m)	Site 11 (70 m)	Site 12 (103 m)
213	190	161	181	177	212
212	210	169	190	189	241
211	228	178	199	203	266
210	243	186	215	215	289
209	257	195	304	231	310
202	559	461	536	536	666

5.2.2. Sound field maps and graphs

5.2.2.1. Sound level contour maps

Maps of the estimated sound fields, threshold contours, and isopleths of interest for the per-pulse SEL and SPL sound fields have been presented at all modelling sites, with representative sites (the six standalone single impulse sites, Table 2), shown in Figures 5–16, and the additional six sites included in the accumulated SEL scenarios shown in Appendix E.1, Figures E-1 to E-12.

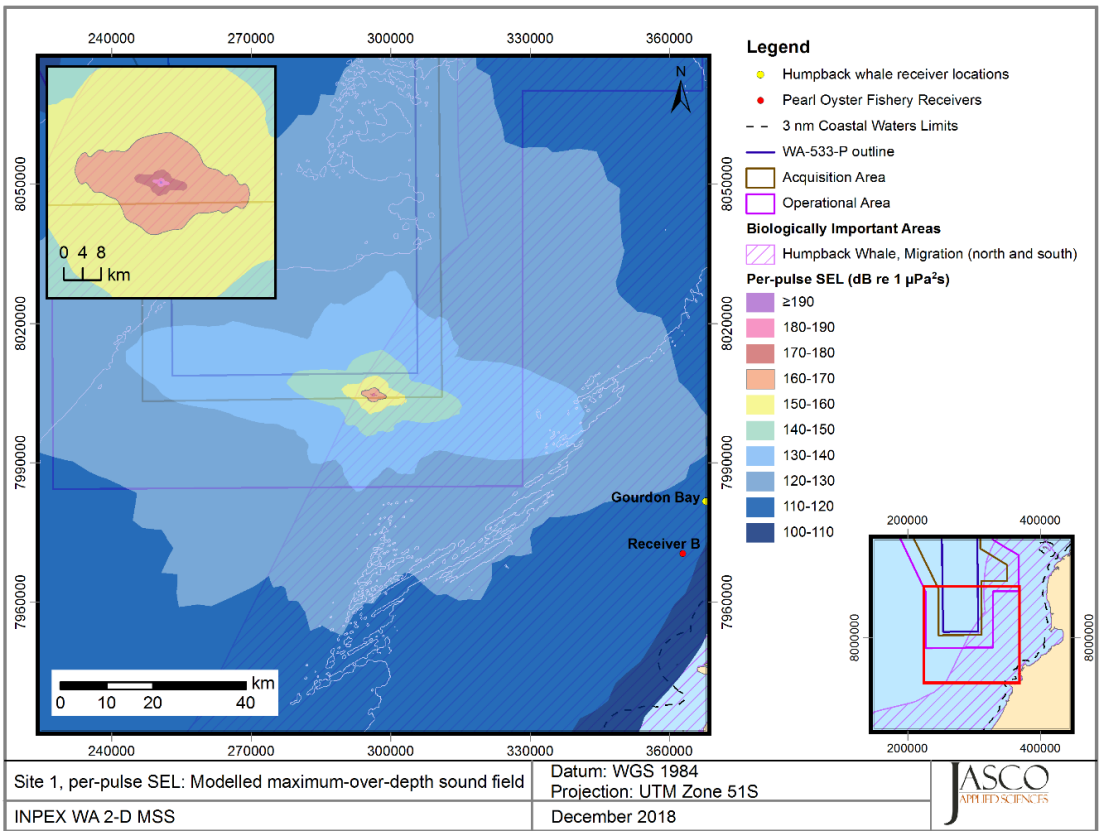

Figure 5. *Site 1 (WA-533-P), per-pulse SEL*: Sound level contour map showing unweighted maximum-over-depth results.

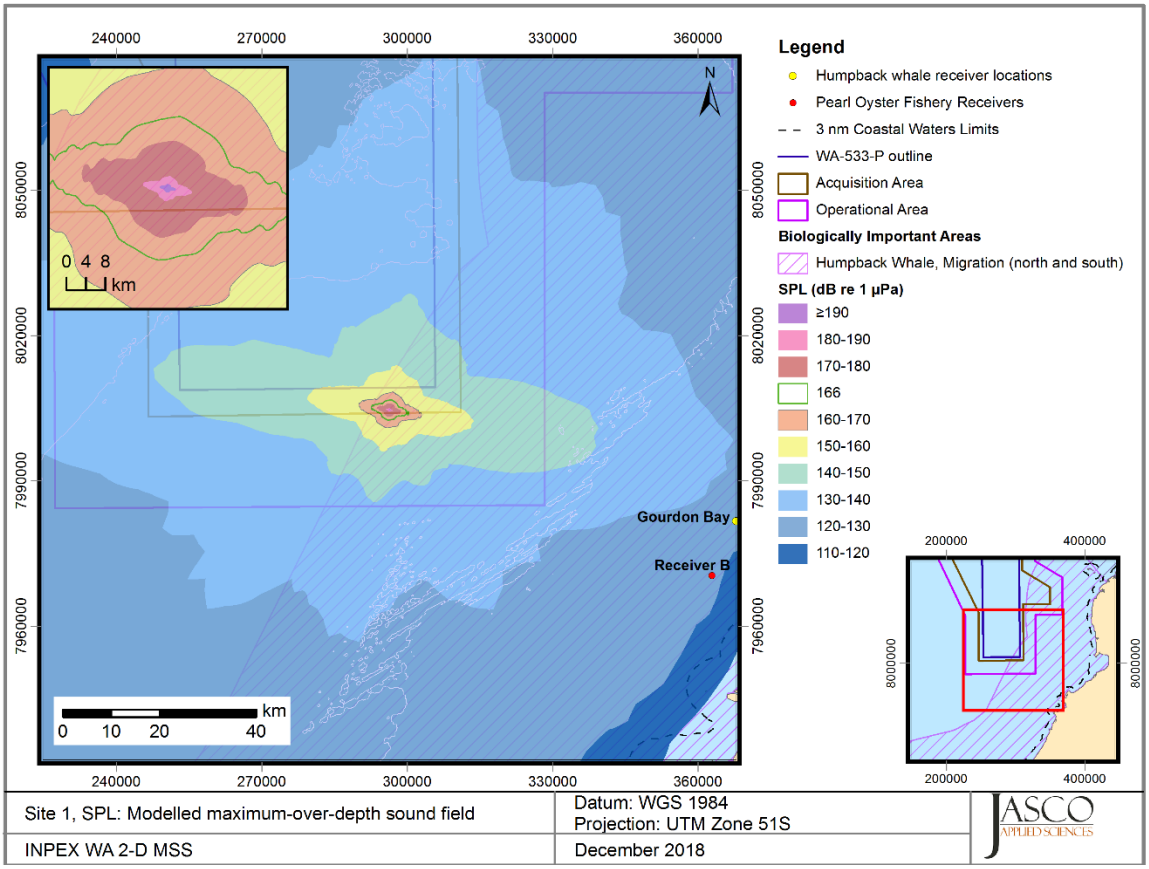

Figure 6. *Site 1 (WA-533-P), SPL*: Sound level contour map showing unweighted maximum-over-depth results.

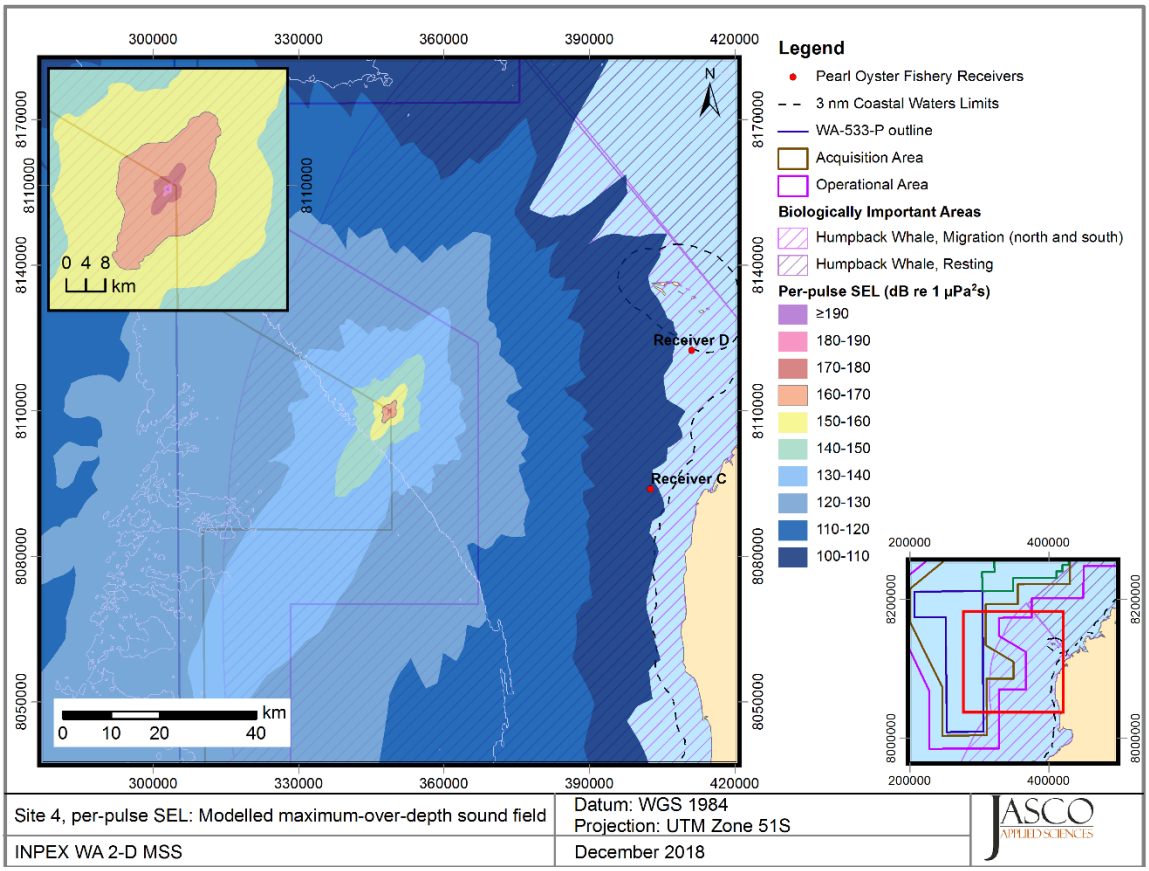

Figure 7. *Site 4 (WA-533-P), per-pulse SEL*: Sound level contour map showing unweighted maximum-over-depth results.

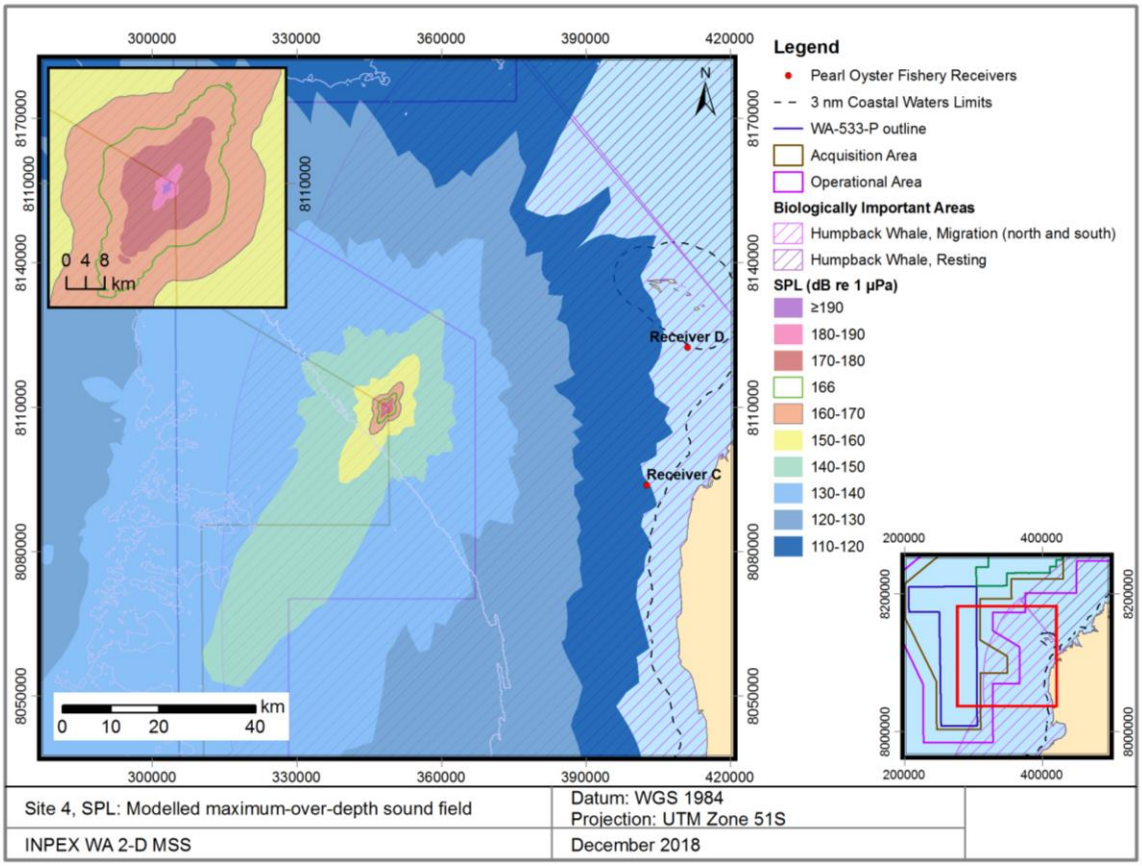

Figure 8. *Site 4 (WA-533-P), SPL*: Sound level contour map showing unweighted maximum-over-depth results.

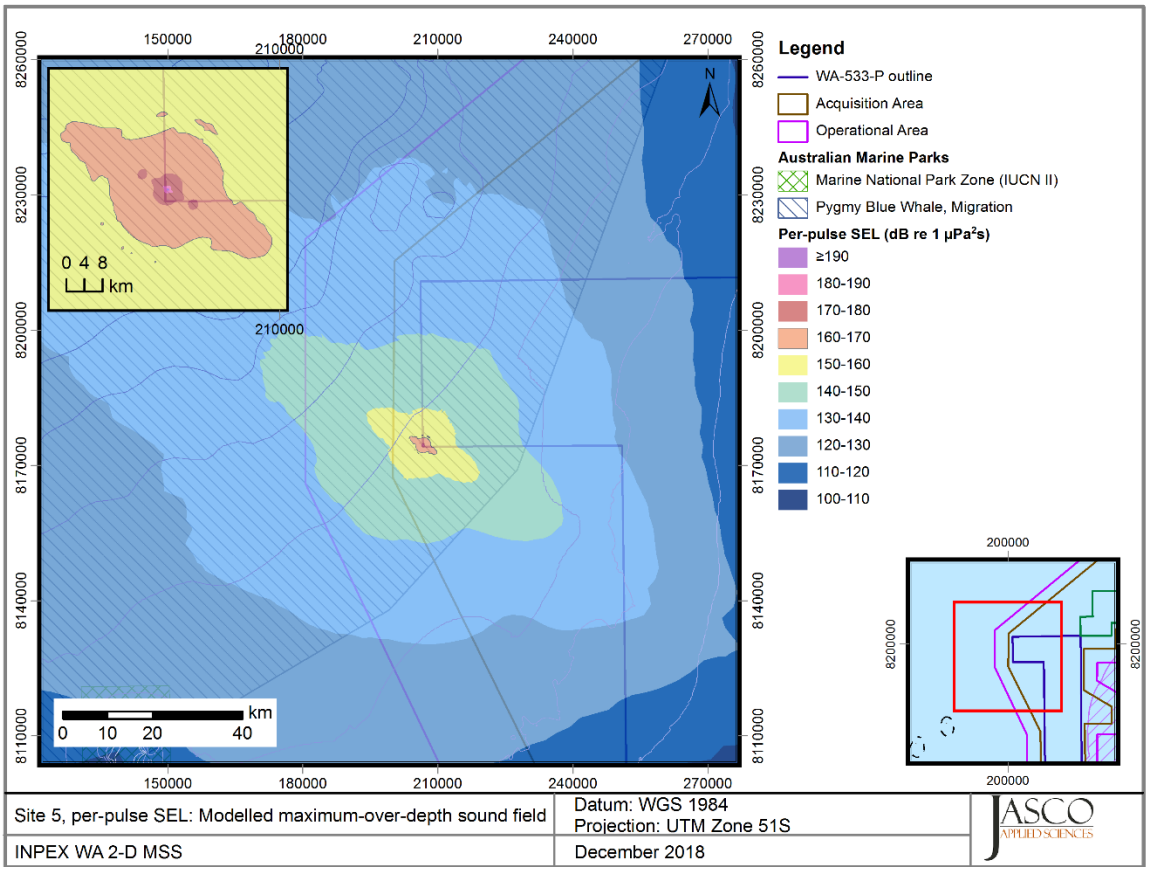

Figure 9. *Site 5 (WA-533-P), per-pulse SEL*: Sound level contour map showing unweighted maximum-over-depth results.

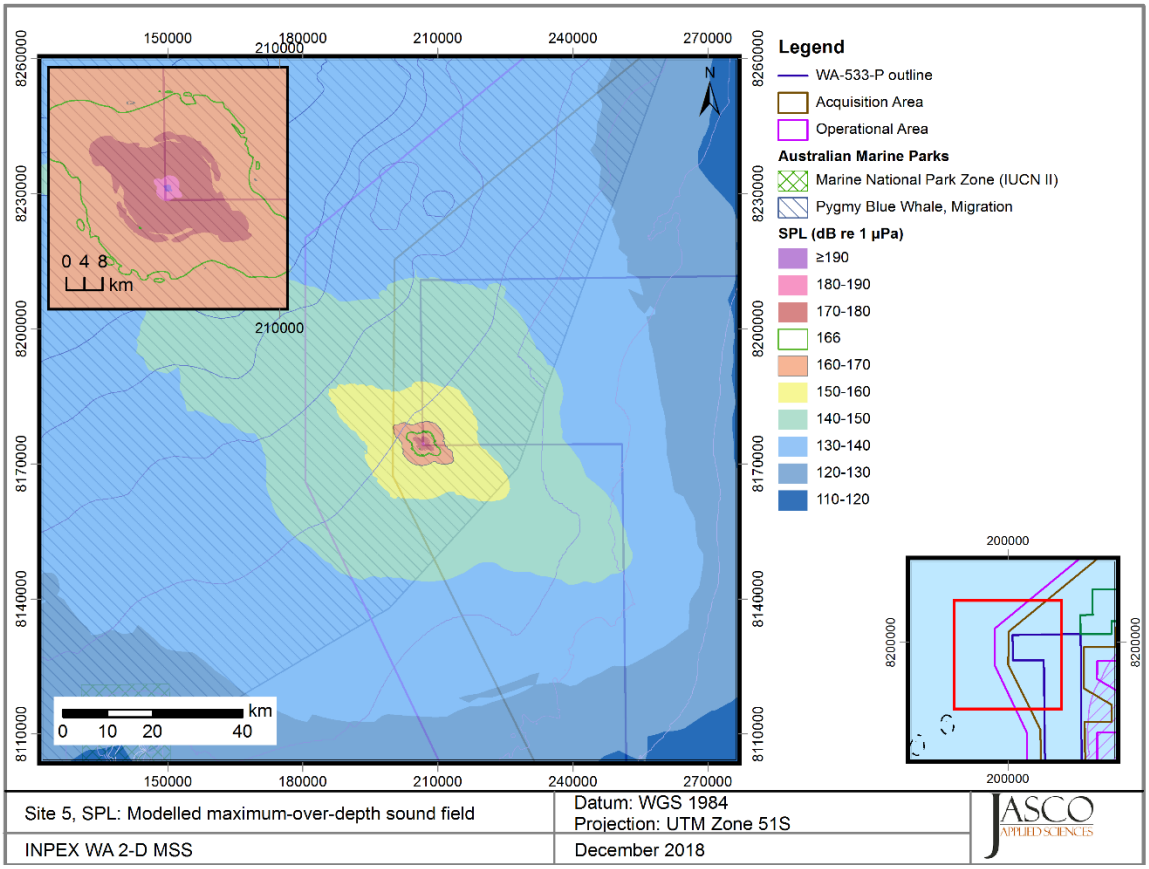

Figure 10. *Site 5 (WA-532-P), SPL*: Sound level contour map showing unweighted maximum-over-depth results.

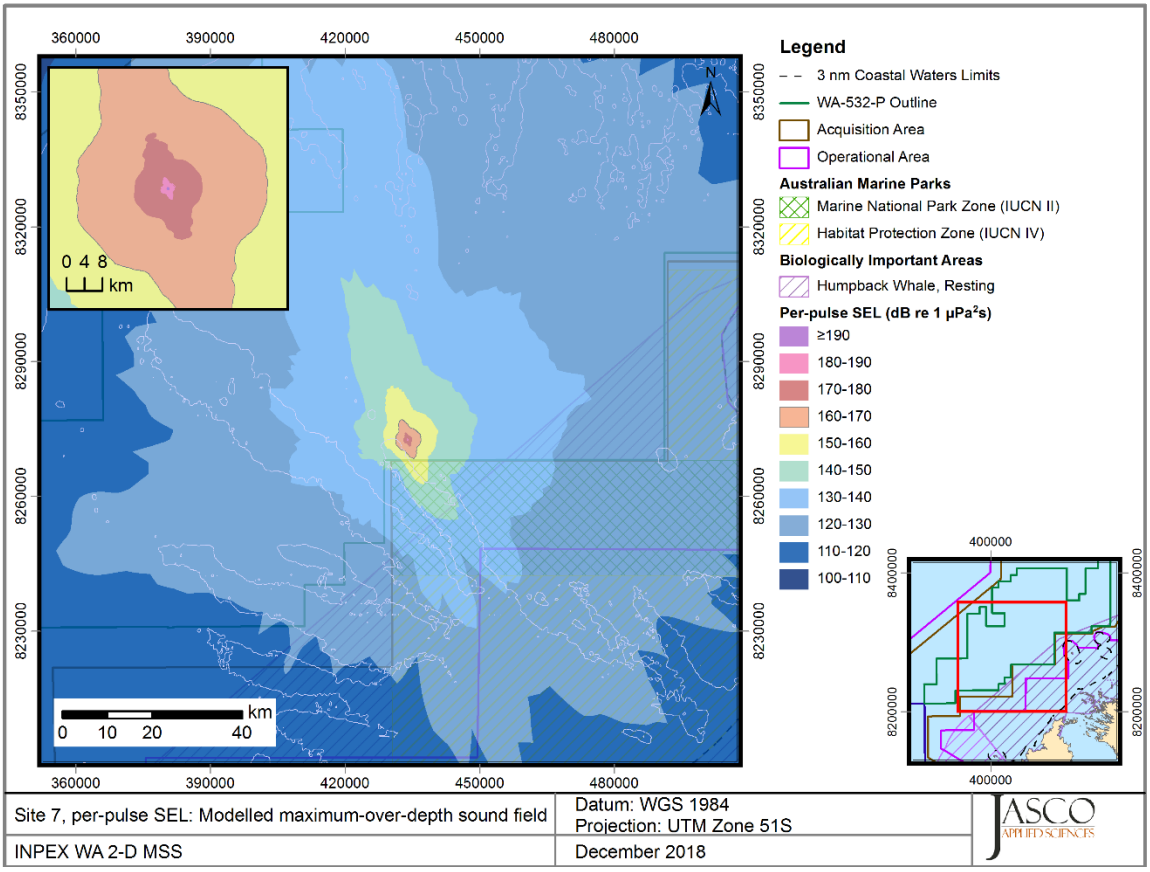

Figure 11. *Site 7 (WA-532-P), per-pulse SEL*: Sound level contour map showing unweighted maximum-over-depth results.

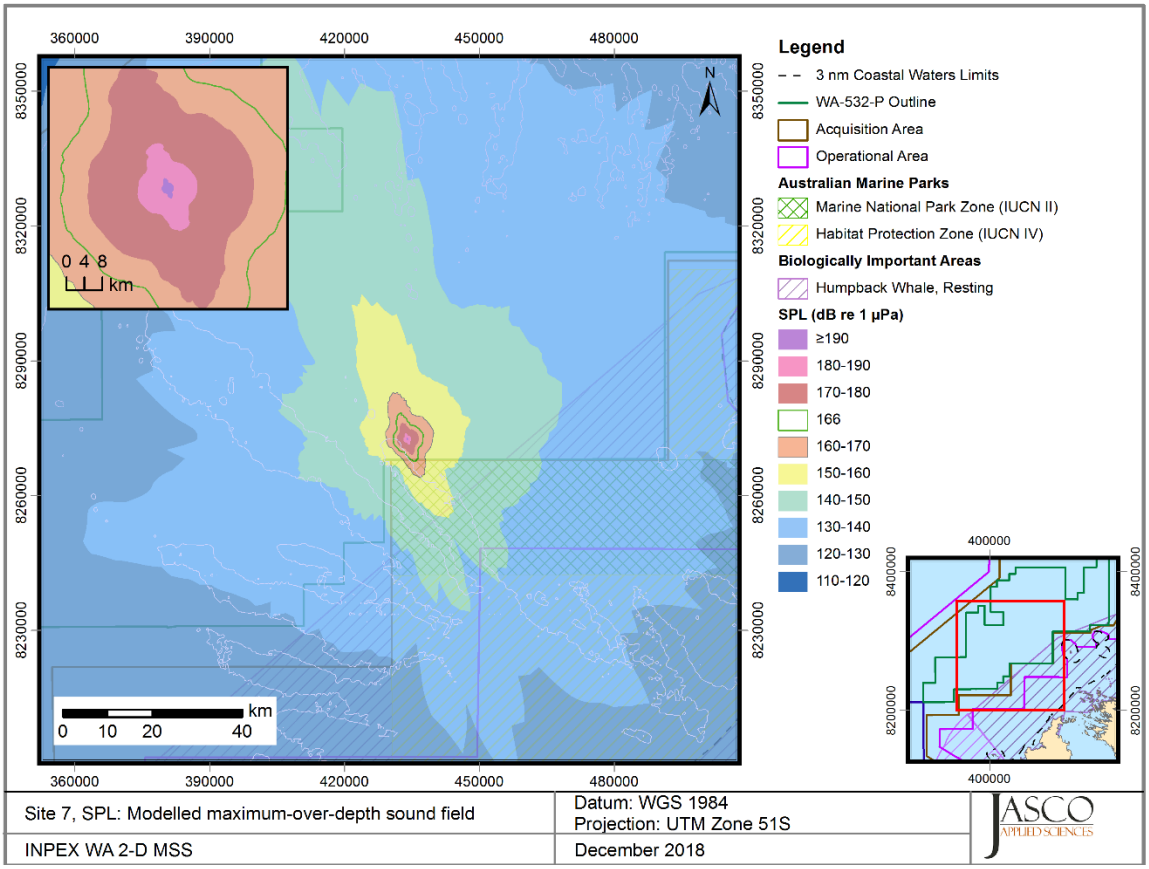

Figure 12. *Site 7 (WA-532-P), SPL*: Sound level contour map showing unweighted maximum-over-depth results.

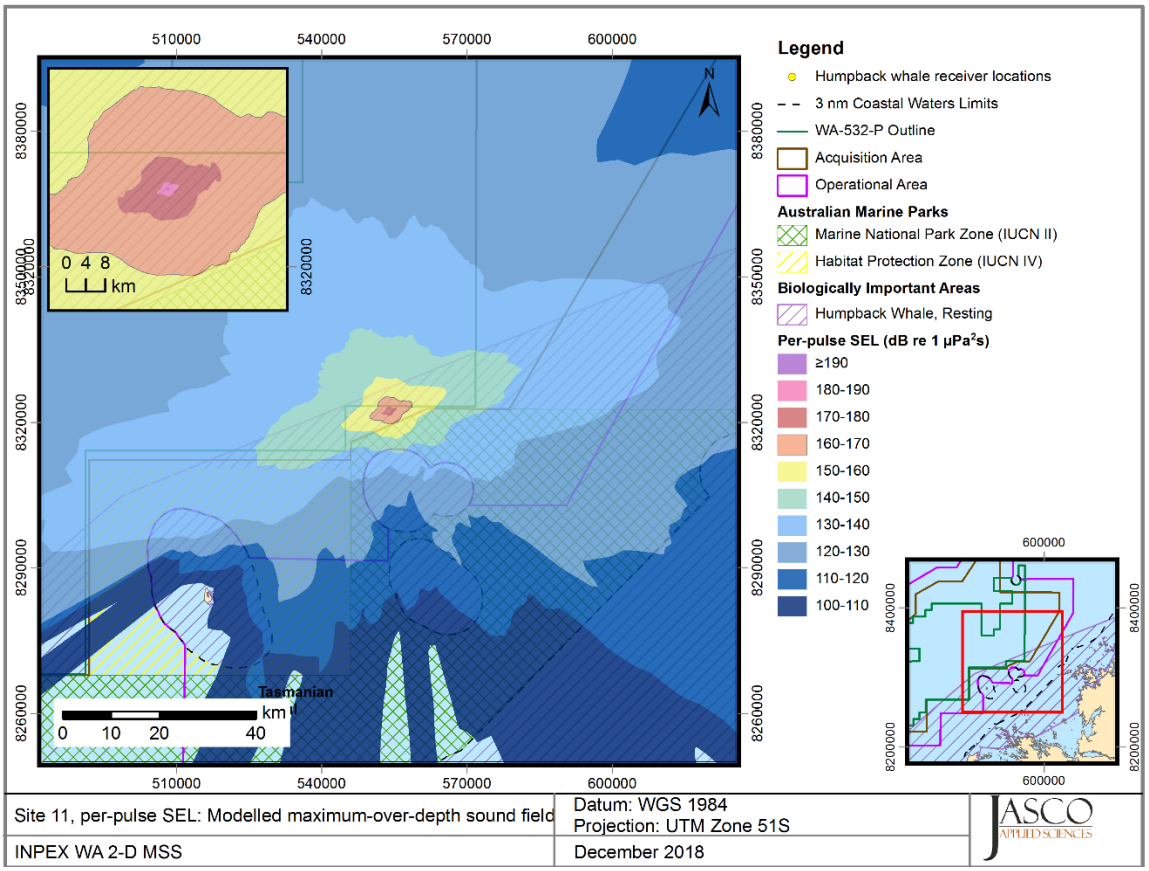

Figure 13. *Site 11 (WA-532-P), per-pulse SEL*: Sound level contour map showing unweighted maximum-over-depth results.

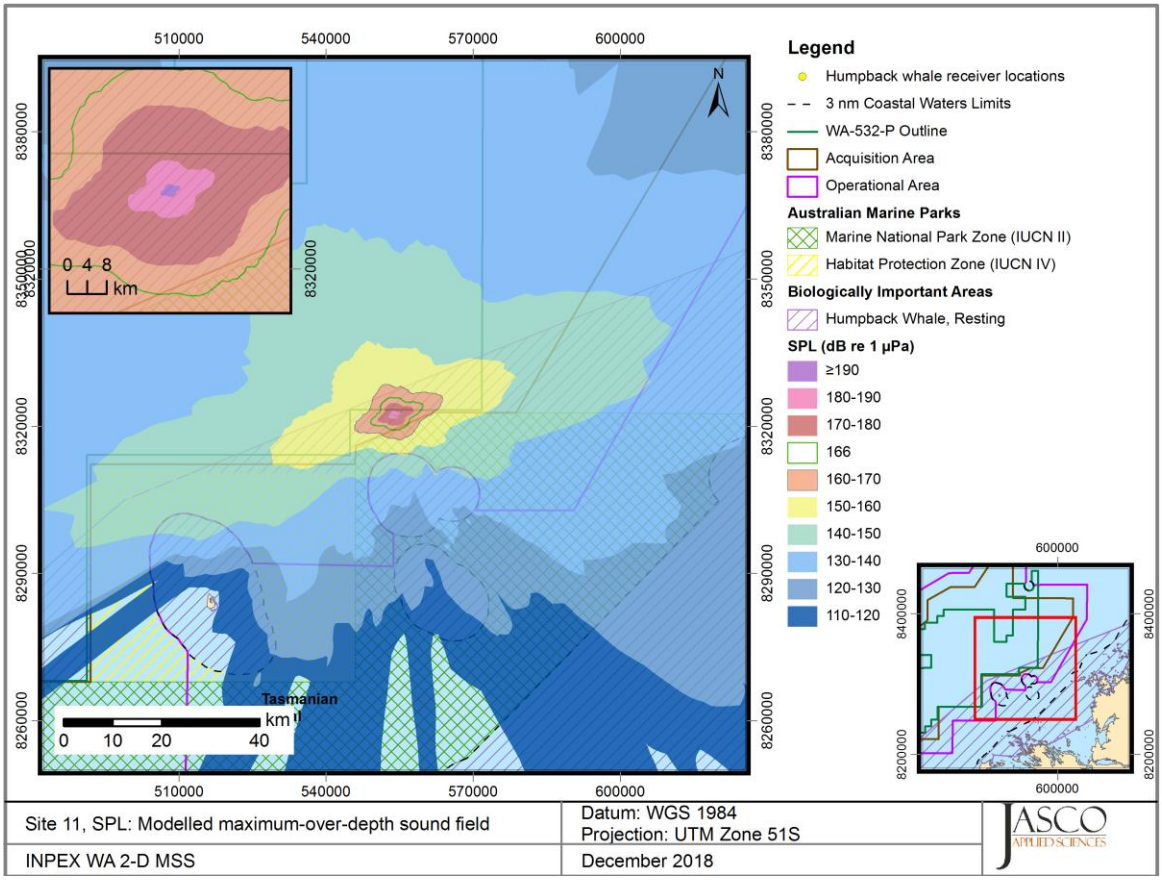

Figure 14. *Site 11 (WA-532-P), SPL*: Sound level contour map showing unweighted maximum-over-depth results.

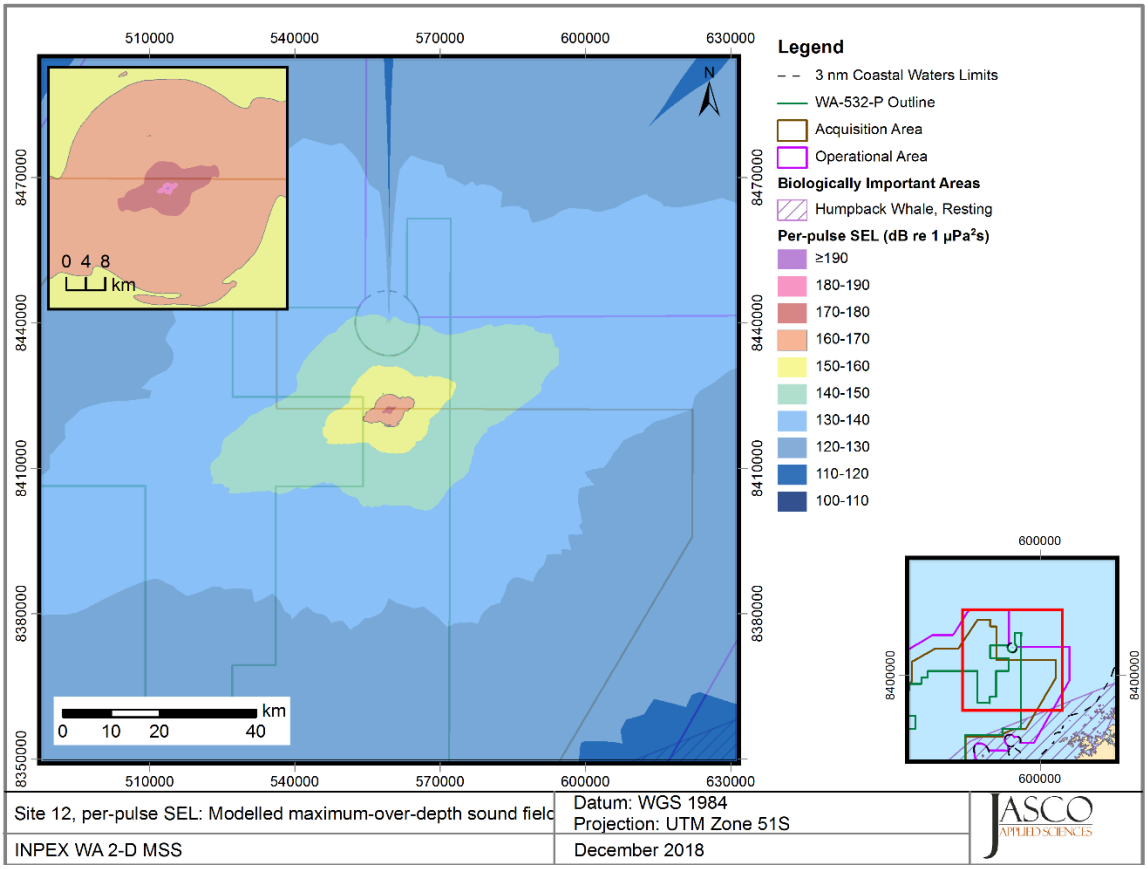

Figure 15. *Site 12 (WA-532-P), per-pulse SEL*: Sound level contour map showing unweighted maximum-over-depth results.

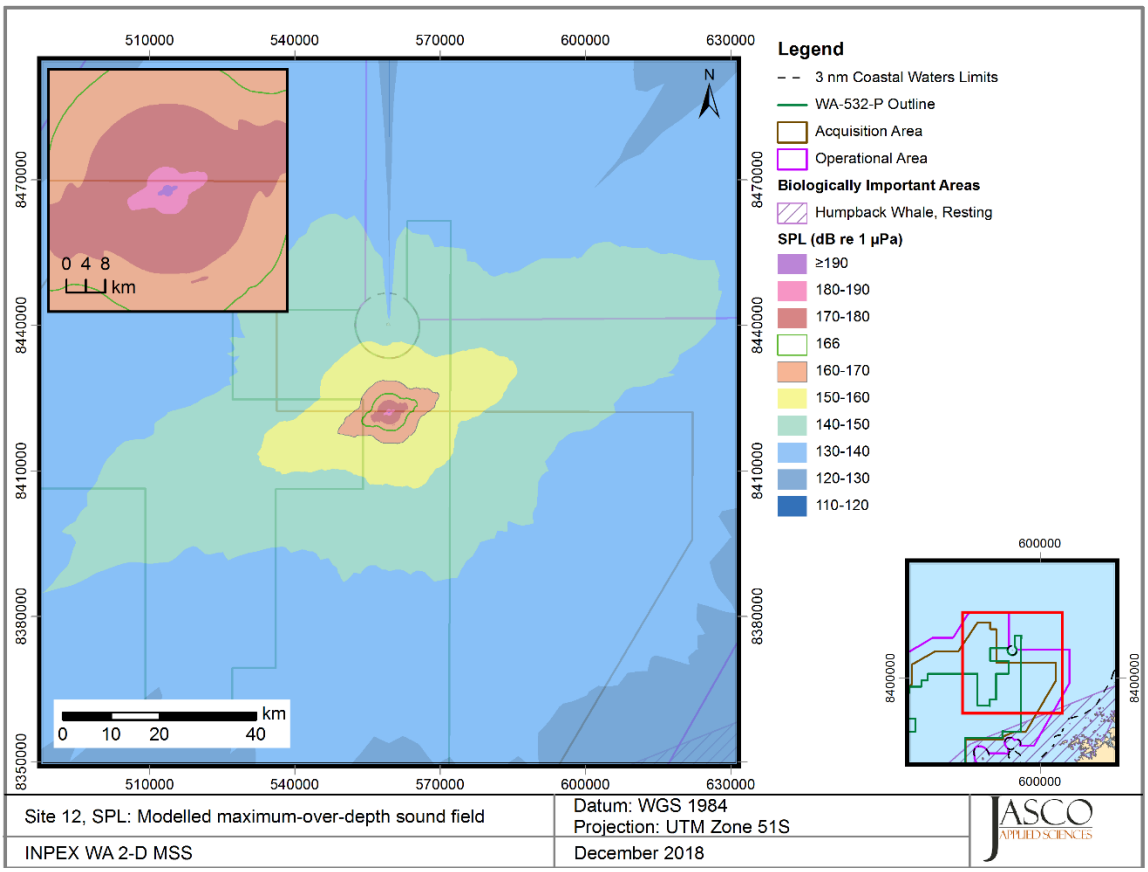

Figure 16. *Site 12 (WA-532-P), SPL*: Sound level contour map showing unweighted maximum-over-depth results.

5.2.2.2. Vertical slices of modelled sound fields

Vertical slices of the per-pulse SEL sound fields for the 3080 in^3 airgun array are shown in Figures 17–22, while vertical slices of the SPL sound fields are shown in Appendix E.2, Figures E-13 to E-18.

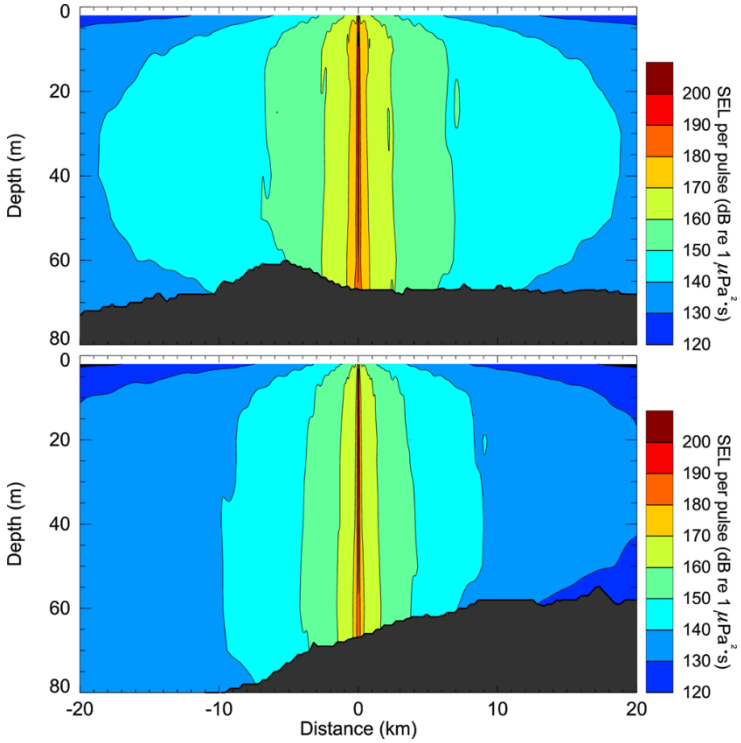

Figure 17. *Site 1 (WA-533-P), per-pulse SEL*: Vertical slice of the predicted per-pulse SEL for the 3080 in^3 array. Levels are shown along the broadside (top) and endfire (bottom) directions.

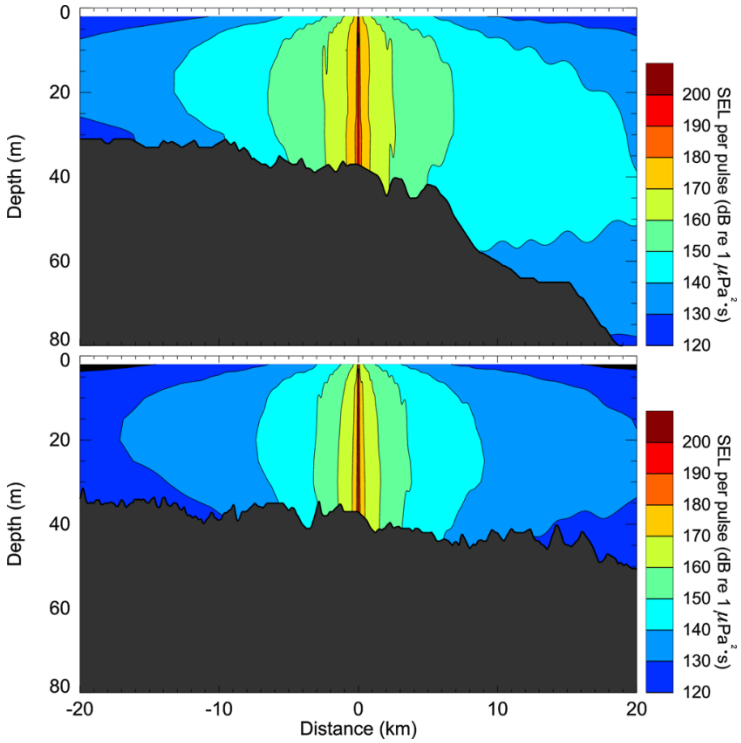

Figure 18. *Site 4 (WA-533-P), per-pulse SEL*: Vertical slice of the predicted per-pulse SEL for the 3080 in^3 array. Levels are shown along the broadside (top) and endfire (bottom) directions.

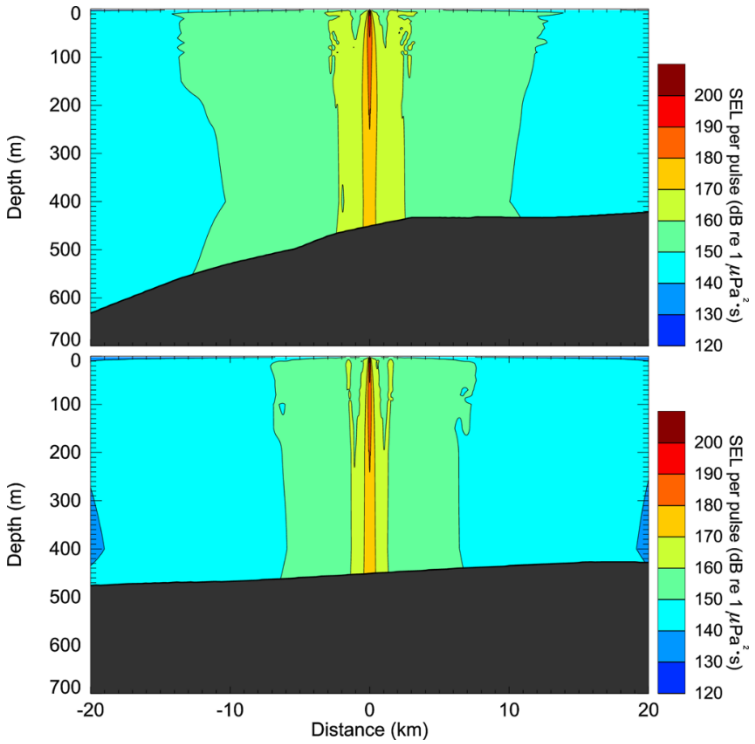

Figure 19. *Site 5 (WA-533-P), per-pulse SEL*: Vertical slice of the predicted per-pulse SEL for the 3080 in^3 array. Levels are shown along the broadside (top) and endfire (bottom) directions.

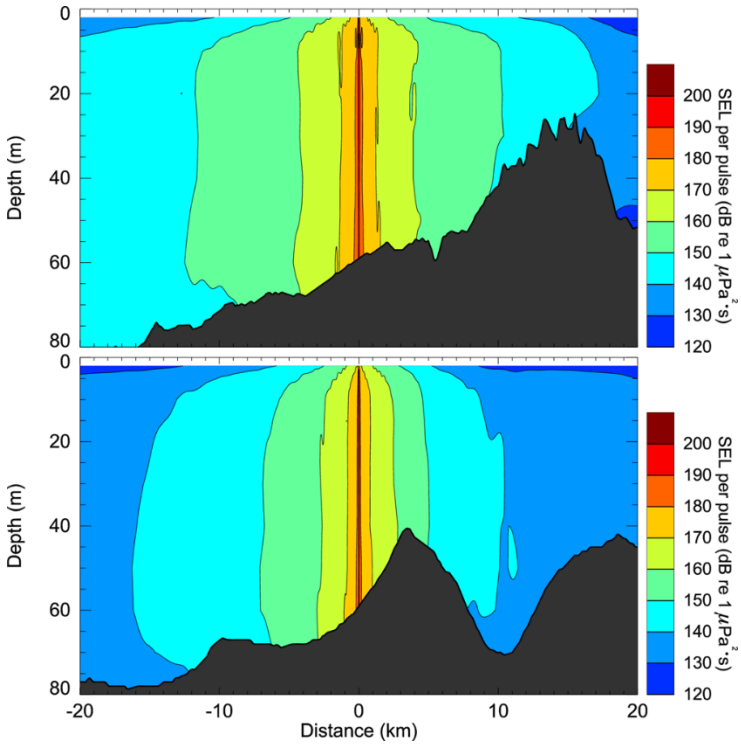

Figure 20. *Site 7 (WA-532-P), per-pulse SEL*: Vertical slice of the predicted per-pulse SEL for the 3080 in^3 array. Levels are shown along the broadside (top) and endfire (bottom) directions.

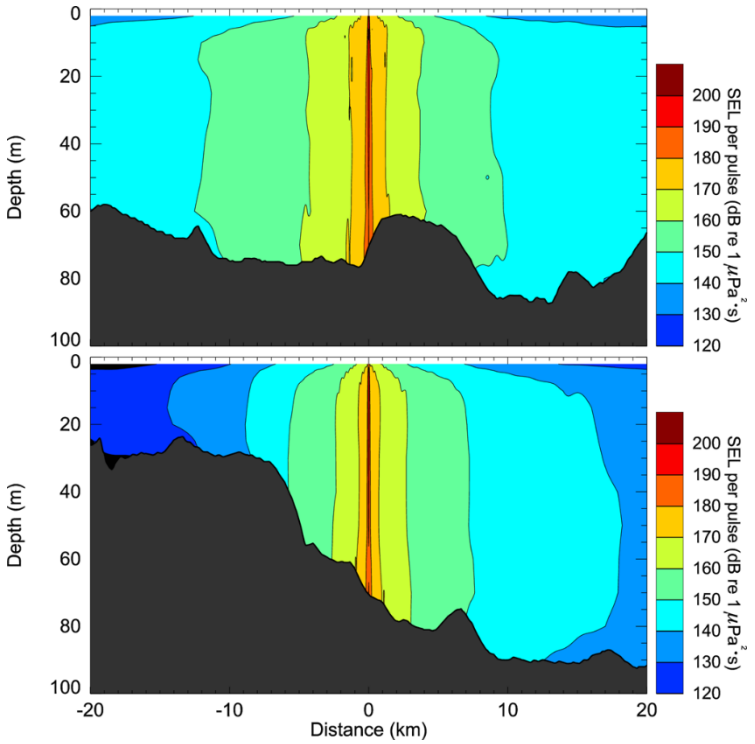

Figure 21. *Site 11 (WA-532-P), per-pulse SEL*: Vertical slice of the predicted per-pulse SEL for the 3080 in^3 array. Levels are shown along the broadside (top) and endfire (bottom) directions.

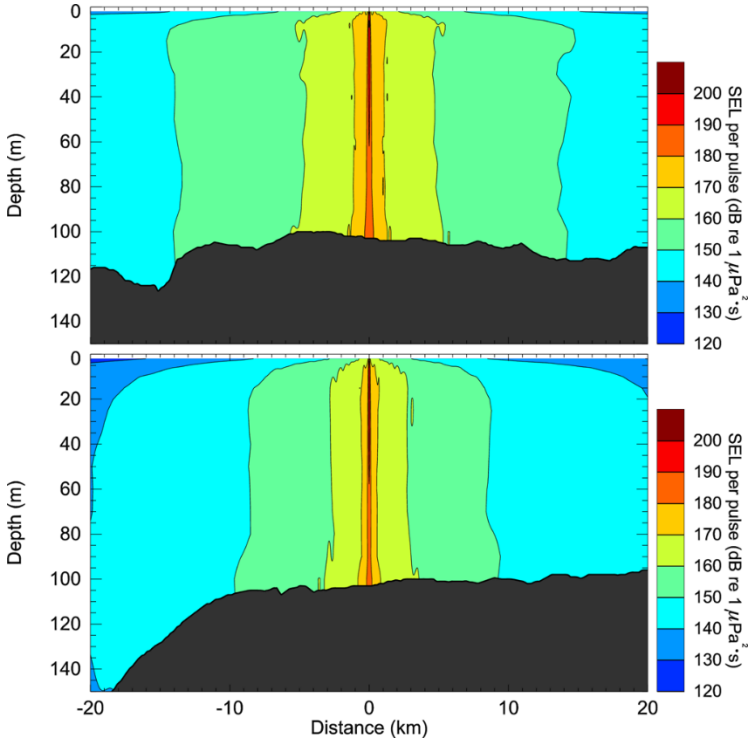

Figure 22. *Site 12 (WA-532-P), per-pulse SEL*: Vertical slice of the predicted per-pulse SEL for the 3080 in^3 array. Levels are shown along the broadside (top) and endfire (bottom) directions.

5.3. Multiple Pulse Sound Fields

The SEL_{24h} results for the proposed survey are presented for three possible operational scenarios within the Acquisition Area, described in Section 2. Tables 20–25 show the estimated ranges to the appropriate cumulative exposure criterion contour for the various marine fauna groups considered, and the corresponding ensonified areas. The ranges in this section are the perpendicular distance from the survey line to the relevant isopleth.

5.3.1. Scenario 1

Table 20. *Scenario 1*: Maximum-over-depth distances to SEL_{24h} based marine mammal PTS and TTS thresholds (NMFS 2018).

Hearing group	PTS		
	Threshold for SEL_{24h} ($L_{E,24h}$; dB re 1 µPa²·s)	R_{max} (km)	Area (km²)
Low-frequency cetaceans	183	0.70	213.05
Mid-frequency cetaceans	185	—	—
High-frequency cetaceans	155	—	—
Hearing group	**TTS**		
	Threshold for SEL_{24h} ($L_{E,24h}$; dB re 1 µPa²·s)	R_{max} (km)	Area (km²)
Low-frequency cetaceans	168	17.92	3470.09
Mid-frequency cetaceans	170	—	—
High-frequency cetaceans	140	0.34	100.50

A dash indicates the threshold is not reached.

Table 21. *Scenario 1*: Distances to SEL_{24h} based fish and turtle criteria.

Marine fauna group	Threshold for SEL_{24h} ($L_{E,24h}$; dB re 1 µPa²·s)	Maximum-over-depth		At seafloor	
		R_{max} (km)	Area (km²)	R_{max} (km)	Area (km²)
Mortality and potential mortal injury					
I	219	0	0	—	—
II, Turtles, fish eggs and fish larvae	210	0	0	—	—
III	207	0.03	3.59	—	—
Fish recoverable injury					
I	216	0	0	—	—
II, III	203	0.03	3.62	—	—
Fish TTS					
I, II, III	186	1.58	540.0	1.58	496.6

A dash denotes a value below the minimum resolution of the modelling.
Fish I–No swim bladder; Fish II–Swim bladder not involved with hearing; Fish III–Swim bladder involved with hearing.

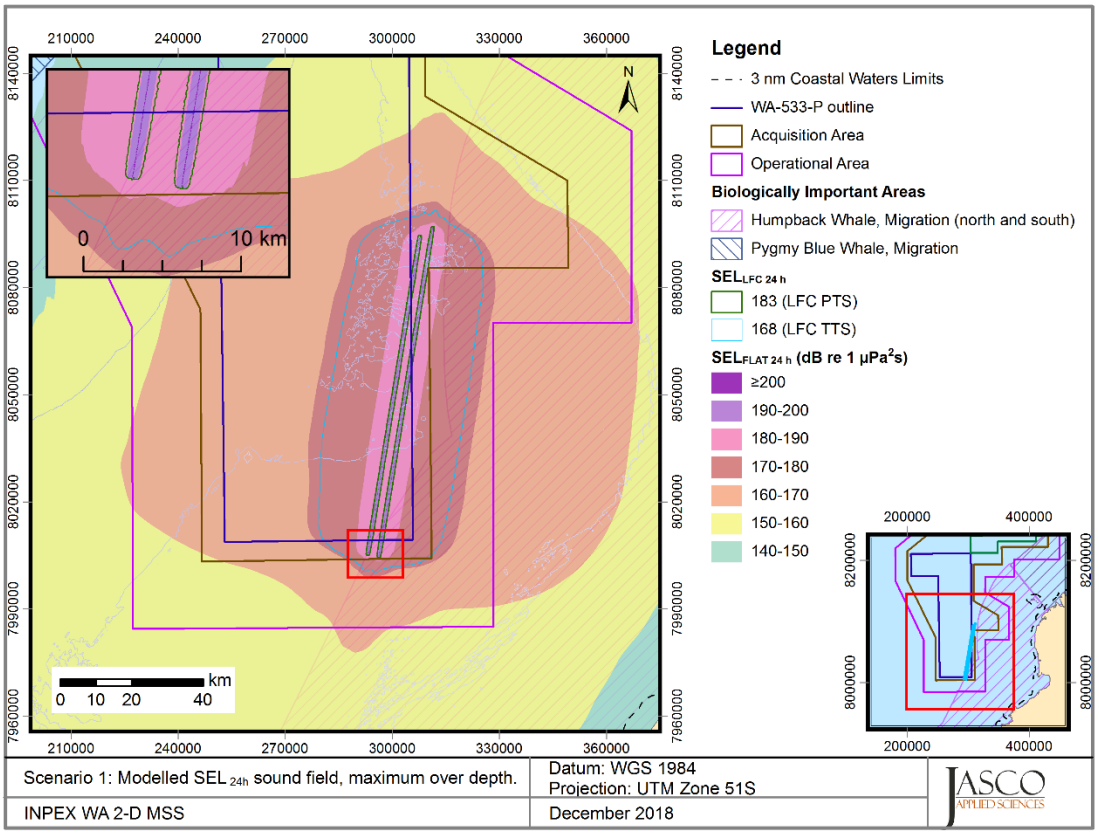

Figure 23. *Scenario 1*: Sound level contour map showing maximum-over-depth SEL_{24h} results.

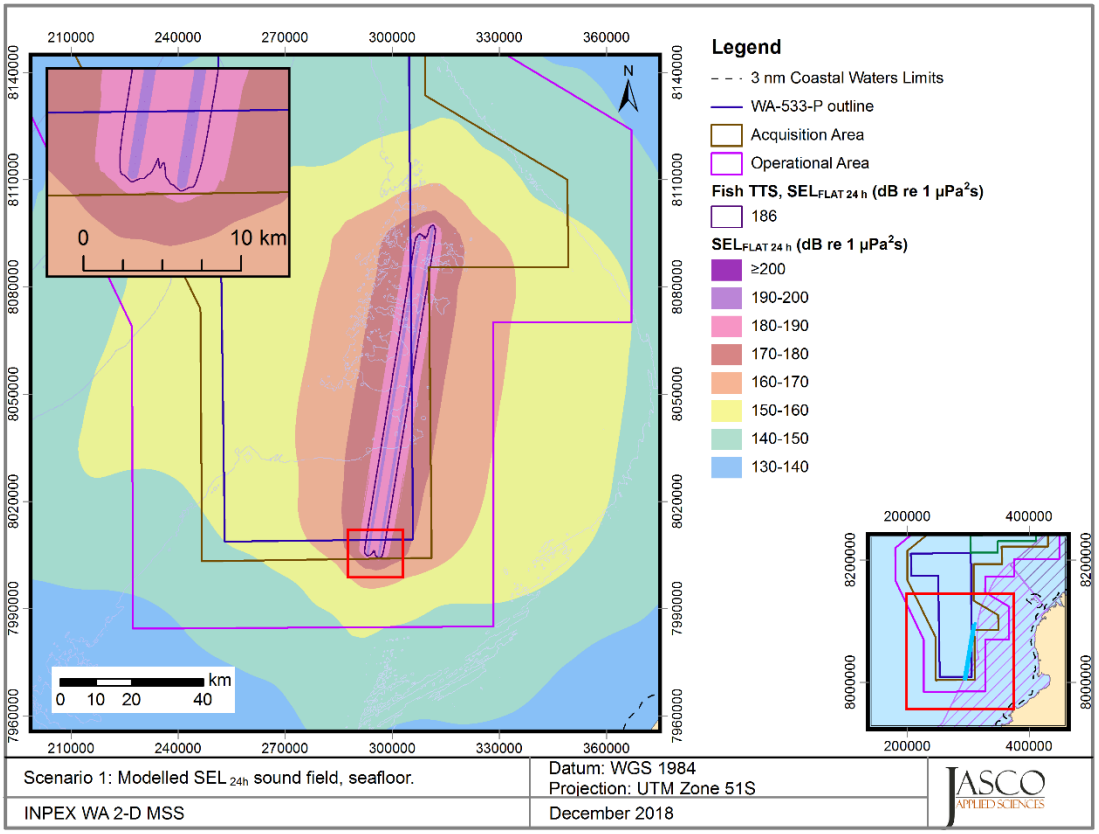

Figure 24. *Scenario 1*: Sound level contour map showing seafloor SEL_{24h} results.

5.3.2. Scenario 2

Table 22. *Scenario 2*: Maximum-over-depth distances to SEL_{24h} based marine mammal PTS and TTS thresholds (NMFS 2018).

Hearing group	PTS		
	Threshold for SEL_{24h} ($L_{E,24h}$; dB re 1 µPa²·s)	R_{max} (km)	Area (km²)
Low-frequency cetaceans	183	1.35	195.57
Mid-frequency cetaceans	185	—	—
High-frequency cetaceans	155	0.03	1.37
Hearing group	**TTS**		
	Threshold for SEL_{24h} ($L_{E,24h}$; dB re 1 µPa²·s)	R_{max} (km)	Area (km²)
Low-frequency cetaceans	168	60.16	8228.74
Mid-frequency cetaceans	170	—	—
High-frequency cetaceans	140	0.19	51.28

A dash indicates the threshold is not reached.

Table 23. *Scenario 2*: Distances to SEL_{24h} based fish and turtle criteria.

Marine fauna group	Threshold for SEL_{24h} ($L_{E,24h}$; dB re 1 µPa²·s)	Maximum-over-depth	
		R_{max} (km)	*Area* (km²)
Mortality and potential mortal injury			
I	219	0.03	1.37
II, Turtles, fish eggs and fish larvae	210	0.03	1.37
III	207	0.03	1.37
Fish recoverable injury			
I	216	0.03	1.37
II, III	203	0.04	3.62
Fish TTS			
I, II, III	186	4.94	1109

A dash denotes a value below the minimum resolution of the modelling.
Fish I–No swim bladder; Fish II–Swim bladder not involved with hearing; Fish III–Swim bladder involved with hearing.

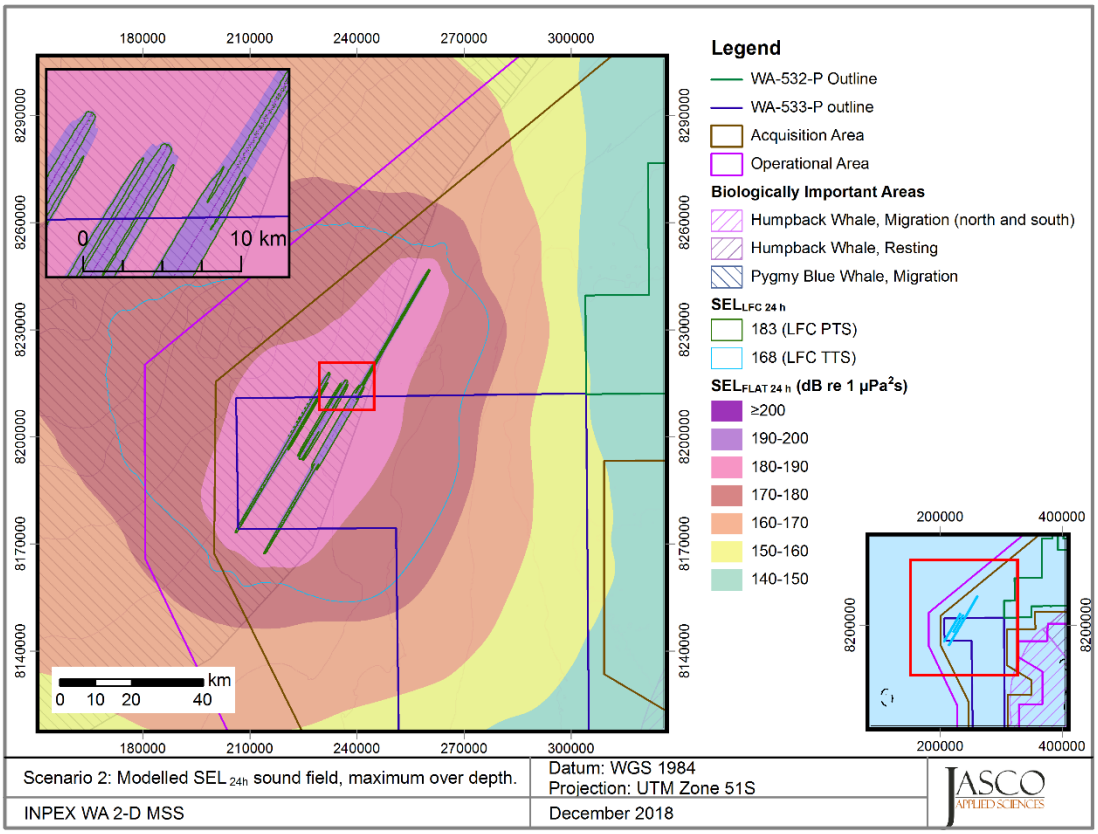

Figure 25. *Scenario 2*: Sound level contour map showing maximum-over-depth SEL_{24h} results.

5.3.3. Scenario 3

Table 24. *Scenario 3*: Maximum-over-depth distances to SEL_{24h} based marine mammal PTS and TTS thresholds (NMFS 2018).

Hearing group	PTS		
	Threshold for SEL_{24h} ($L_{E,24h}$; dB re 1 µPa²·s)	R_{max} (km)	Area (km²)
Low-frequency cetaceans	183	2.13	387.22
Mid-frequency cetaceans	185	—	—
High-frequency cetaceans	155	—	—
Sirenians	190	—	—
Hearing group	**TTS**		
	Threshold for SEL_{24h} ($L_{E,24h}$; dB re 1 µPa²·s)	R_{max} (km)	Area (km²)
Low-frequency cetaceans	168	37.22	4003.93
Mid-frequency cetaceans	170	—	—
High-frequency cetaceans	140	1.63	186.60
Sirenians	175	—	—

A dash indicates the threshold is not reached.

Table 25. *Scenario 3*: Distances to SEL_{24h} based fish and turtle criteria.

Marine fauna group	Threshold for SEL_{24h} ($L_{E,24h}$; dB re 1 µPa²·s)	Maximum-over-depth		At seafloor	
		R_{max} (km)	*Area* (km²)	R_{max} (km)	*Area* (km²)
Mortality and potential mortal injury					
I	219	—	—	—	—
II, Turtles, fish eggs and fish larvae	210	—	—	—	—
III	207	—	—	—	—
Fish recoverable injury					
I	216	—	—	—	—
II, III	203	0.04	2.67	0.02	0.07
Fish TTS					
I, II, III	186	3.50	697.9	2.92	657.8

A dash denotes a value below the minimum resolution of the modelling.
Fish I–No swim bladder; Fish II–Swim bladder not involved with hearing; Fish III–Swim bladder involved with hearing.

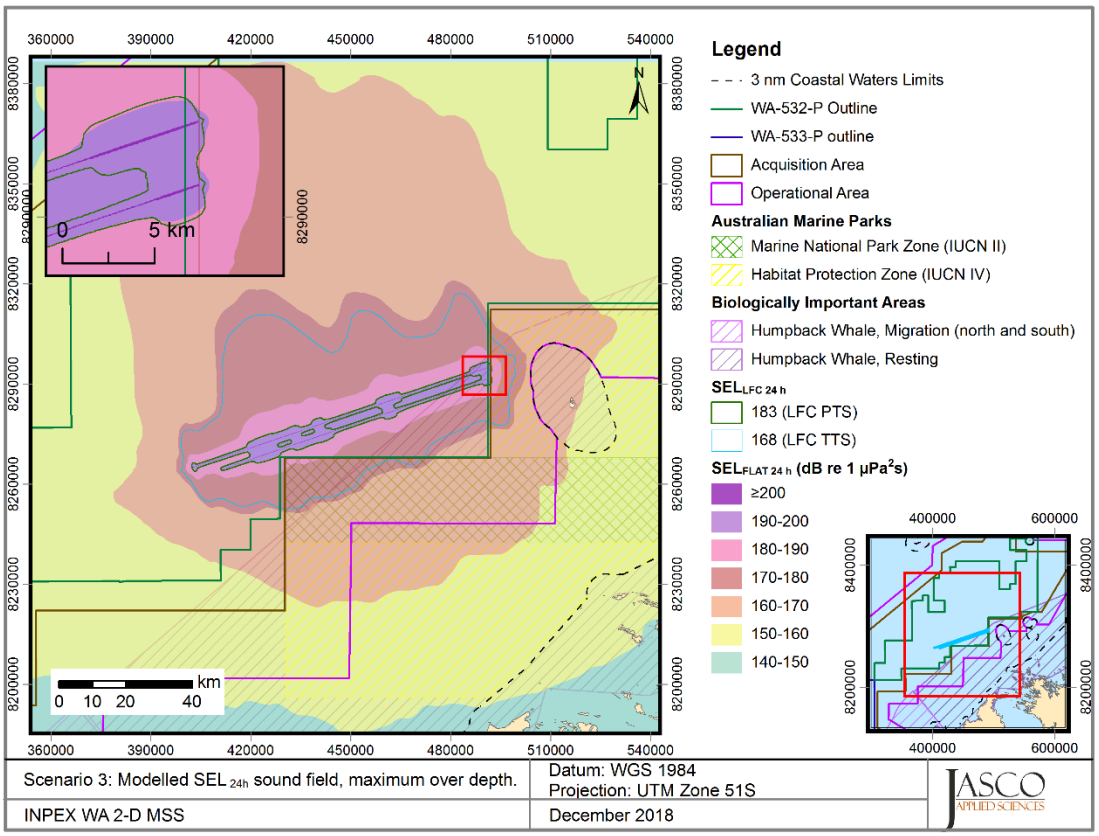

Figure 26. *Scenario 3*: Sound level contour map showing maximum-over-depth SEL_{24h} results.

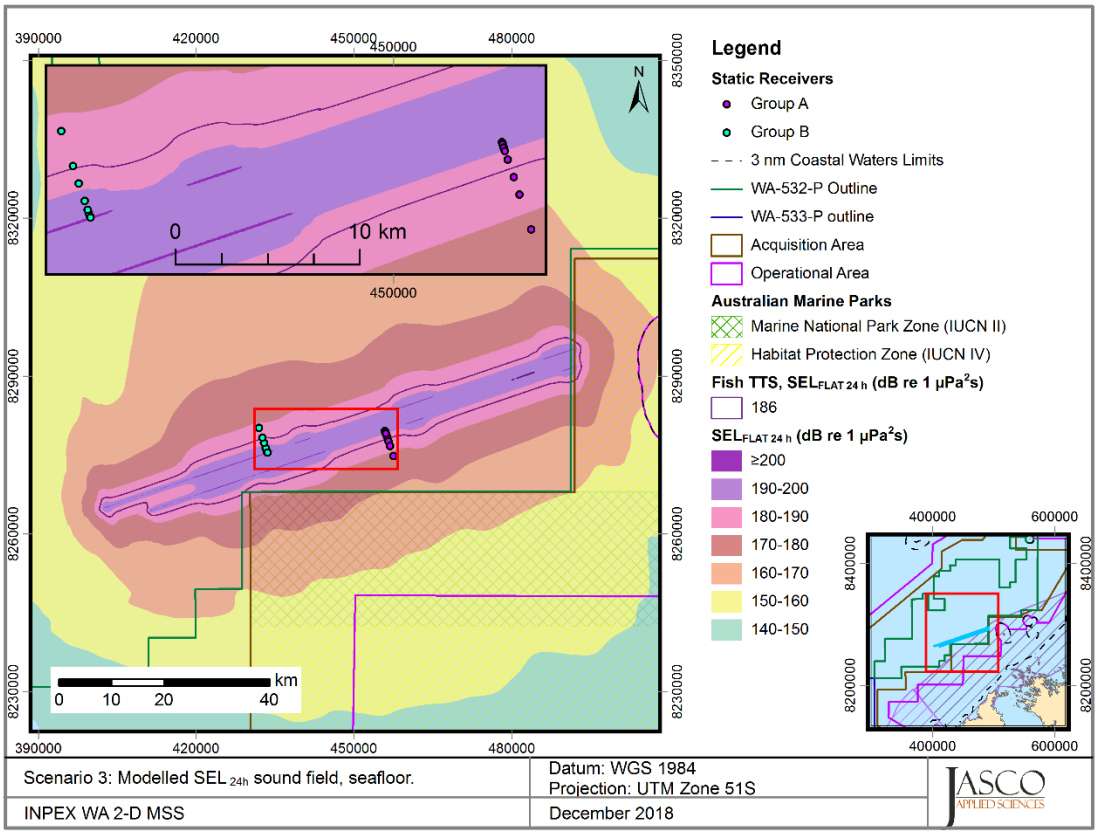

Figure 27. *Scenario 3*: Sound level contour map showing seafloor SEL_{24h} results.

5.3.3.1. Sound levels at static receivers

Sound exposure levels were modelled at static receivers located at eight offset distances (50, 100, 300, 500, 1000, 2000, 3000, and 5000 m) from the closest survey line for each survey line within Scenario 3 (Section 2, Figure 4), with Group A being associated with the southern line and Group B the northern line. The per-pulse and accumulated SEL were plotted as a function of time on a common graph. The results are presented in Figure 32 for seafloor sound levels.

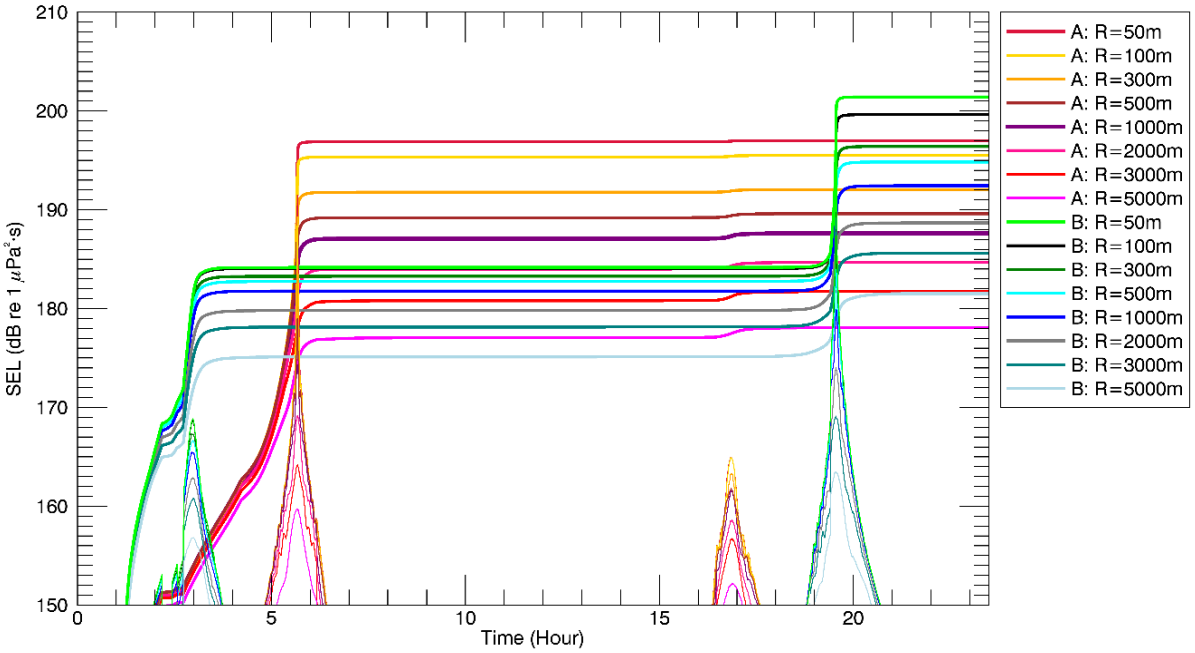

Figure 28. *Scenario 3*: Per-pulse unweighted SEL (thin lines) and accumulated unweighted SEL (thick lines) for nine receivers (denoted by R) located at the seafloor at increasing distance from the survey lines. Gaps in the per-pulse curves correspond to vessel turns.

6. Discussion

6.1. Overview and Source Levels

This modelling study predicted underwater sound levels associated with the planned INPEX WA 2-D MSS. The underwater sound field was modelled for a 3080 in^3 seismic source (Appendix B) with a water column sound speed profile for July. An analysis of seasonal sound speed profiles (Appendix D.3.2) indicated that this month was the most conducive to sound propagation, and as such it was selected to ensure a conservative estimation of distances to received sound level thresholds over the entire survey period. The modelling also accounted for site-specific bathymetric variations (Appendix D.3.1) and local geoacoustic properties (Appendix D.3.3).

Most acoustic energy from the seismic sources is output at lower frequencies, in the tens to hundreds of Hertz. Although there was little difference between the three considered sources in the broadband source levels in the endfire, broadside and vertical directions, the 3080 in^3 source was slightly louder. It also has a more pronounced broadside directivity for 1/3-octave-bands between approximately 100 Hz to about 400 Hz (Appendix B.2), which leads to a noticeable axial bulge in the modelled acoustic footprints. For the modelling sites in shallow water, the low-frequency components associated with the highest spectral levels for the source attenuated rapidly compared to those at higher frequencies.

The overall broadband (10–25000 Hz) unweighted per-pulse SEL source level of the 3080 in^3 array operating at 7 m depth was 224.8 dB 1 μPa^2m^2s in the broadside direction and 223.6 dB 1 μPa^2m^2s in the endfire direction. The peak pressure level in the same directions was 249.6 and 246.4 dB re 1 μPa^2m^2, respectively. These results are presented in Table 9.

6.2. Per-Pulse Sound Fields

At all sites, the distance to isopleths was longer in the broadside direction compared to the endfire direction, which is apparent in all footprint maps in Section 5.2.2 and Appendix E.1. The array directionality coupled with the bathymetry had a considerable effect on propagation at longer distances, with significantly larger lobes of sound energy extending into the deeper waters at some modelling sites (e.g. Sites 4 (Figure 7) and 7 (Figure 11)). The vertical slice plots (Section 5.2.2.2 and Appendix E.2) assist in demonstrating the rate of change of the bathymetry over distance and the influence on the sound field, with the endfire results for Site 11 (Figure 21) showing strong attenuation in the upslope direction compared to the downslope.

The per-pulse modelling sites encompassed water depths from 45 to 451 m across four geological profiles, with some sites close to shallower areas such as shoals. The distances to isopleths across the 12 modelled sites reflects this environmental variability, with the distances to isopleths for lower sound levels (below 140 dB re 1 $\mu Pa^2 \cdot s$) being longest at the deepest sites (Sites 5 and 6), and shortest at the shallowest site (Site 8). Distances to higher sound levels are greater for Sites 11 and 12, in permit WA-532-P, likely influenced by the different geology in the northern regions of the Acquisition Area.

The distances to PK based potential injury criteria (Section 3.2) for fish at the seafloor do not always decrease with increasing depth (Tables 16–18), a phenomenon related to a complex pattern of destructive surface reflection and constructive critical angle bottom reflections that singularly affect sound propagation in shallow water; the distances could be longer for depths even slightly shallower or deeper.

6.3. Multiple Pulse Sound Fields

The accumulated SEL over 24 hours of seismic operation was modelled considering three realistic acquisition patterns or scenarios within the Acquisition Area but across the two permits. The model predicted the accumulation of sound energy, considering the change in location and the azimuth of the source at each pulse point, which were used to assess possible injury in marine mammals and the

SEL_{24h} based fish and turtle criteria. The results were presented both as maps of the accumulated exposure levels and as tables of ranges to threshold levels and areas exposed above given effects criteria (Section 5.3).

Sound exposure levels were also modelled at static receivers located at various offset distances from the closest survey line in Scenario 3 (Figures 4 and 28). This provides a sense for the accumulation of acoustic energy as the seismic source acquires multiple lines over a 24-hour period. The sampling locations were chosen so they sampled the sound fields early and late in the 24-hour period. The resulting time histories of accumulated SEL show that generally the single nearest pass of the seismic source to a receiver will account for most of the exposure over the 24-hour period. However, depending upon previous exposure within the period, the levels at the receivers close to the track lines late in the period could be higher than those at similarly distances early in the period.

SEL_{24h} is a cumulative metric that reflects the dosimetric impact of noise levels within 24 h, based on the assumption that an animal is consistently exposed to such noise levels at a fixed position. The radii that correspond to SEL_{24h} typically represent an unlikely worst-case scenario for SEL-based exposure since, more realistically, marine fauna (mammals or fish) would not stay in the same location or at the same range for 24 hours. Therefore, a reported radius of SEL_{24h} criteria does not mean that any animal travelling within this radius of the source will be injured, but rather that it could be injured if it remained in that range for 24 hours. The reported radii represent the perpendicular distance from to the closest survey line to the relevant isopleth.

6.4. Summary

The findings of the study pertaining each of the metrics and criteria for various marine species of interest are summarised below with references to the result location.

Marine mammal injury and behaviour

- The maximum distance where the NMFS (2014) marine mammal behavioural response criterion of 160 dB re 1 µPa (SPL) could be exceeded varied between 5.52 and 11.19 km (Site 8, 45 m and Site 12, 103 m, permit WA-532-P), Table 11.
- The maximum received SPL, LF-weighted SPL and per-pulse SEL at any of the four locations relevant to calving and resting humpback whales were received at Tasmanian Shoal considering a modelled site 79 km away. The respective levels were 134.6 (L_p; dB re 1 µPa), 120 ($L_{p,LF}$; dB re 1 µPa) and 126.2 (L_E; dB re 1 µPa²·s) (Table 15).
- The results for the criteria applied for marine mammal Permanent Threshold Shift (PTS), NMFS (2018), consider both metrics within the criteria (PK and SEL_{24h}). The longest distance associated with either metric is required to be applied. The table below summarise the maximum distances for PTS, along with the relevant metric and the location of the results within this report.
- The furthest distance from the array that high-frequency cetaceans could experience PTS was 440 m at Site 12 (103 m, permit WA-532-P), a site in a different location to any of the 24-hour SEL scenarios (Table 12).

Table 26. Summary of maximum marine mammal PTS onset distances for SEL_{24h} modelled scenarios (Tables 12, 20, 22 and 24)

Relevant hearing group	Metric associated with longest distance to PTS onset	R_{max} (km)		
		Scenario 1 (WA-533-P)	Scenario 2 (WA-533-P Deep)	Scenario 3 (WA-532-P)
Low-frequency cetaceans†	SEL_{24h}	0.7	1.35	2.13
Mid-frequency cetaceans†	PK	< 0.02	< 0.02	< 0.02
High-frequency cetaceans	PK	0.27	0.22	0.39
Sirenians	PK	NA	NA	0.02

† The model does not account for shutdowns.

- SEL_{24h} is a cumulative metric that reflects the dosimetric impact of noise levels within 24 hours based on the assumption that an animal is consistently exposed to such noise levels at a fixed position. The corresponding 24-h SEL radii for low-frequency cetaceans were larger than those for peak pressure criteria, but they represent an unlikely worst-case scenario. More realistically, marine mammals (and fish) would not stay in the same location or at the same range for 24 hours. Therefore, a reported radius for 24-h SEL criteria does not mean that marine fauna travelling within this radius of the source will be injured, but rather that an animal could be exposed to the sound level associated with injury (either PTS or TTS) if it remained in that range for 24 hours.

Turtle Behaviour

- The maximum distance where the United States NMFS criterion (NSF 2011) for behavioural effects in turtles of 166 dB re 1 µPa (SPL) could be exceeded varied between 3.09 and 6.13 km (Site 8, 45 m and Site 11, 70 m, permit WA-532-P), Table 11.

Fish, turtle injury, fish eggs, and fish larvae

- The modelling study assessed the seafloor and water column ranges for quantitative criteria based on Popper et al. (2014) and considering both PK and SEL_{24h} metrics associated with mortality and potential mortal injury and impairment in:
  - Fish without a swim bladder (also appropriate for sharks in the absence of other information)
  - Fish with a swim bladder that do not use it for hearing
  - Fish that use their swim bladders for hearing
  - Turtles
  - Fish eggs and fish larvae
- Water column receptors, assessed at four modelling sites:
  - The maximum distance to sound levels associated with mortality and potential mortal injury on most the sensitive fish groups are associated with the PK metric, and range from 120 m (Sites 1, 5 and 12) to 220 m (Site 7). For fish without a swim bladder, the distance is 60 m at all four sites (Table 12).
- Seafloor receptors, assessed at five modelling sites, along with sites representative of different depths and geoacoustic parameters, three in WA-533-P and five in WA-532-P (depths from 30 to 103 m) (Tables 16–18):
  - The maximum distance to sound levels associated with mortality and potential mortal injury in fish, turtles, fish eggs and fish larvae is associated with the PK metric in all cases.
  - The maximum distance for the most sensitive fish groups (associated with a PK threshold of 207 dB re 1 µPa) varies between 154 and 185 m.

  - The maximum distance for the less sensitive fish groups (associated with a PK threshold of 213 dB re 1 µPa) varies between 54 and 114 m.

- Considering the three 24-hour SEL scenarios, and based on Popper et al. (2014), the SEL_{24h} metric criteria for potential TTS could be exceeded within the following distances:
  - 1.58 km of the array at both the seafloor for maximum-over-depth during Scenario 1 (Table 21),
  - 4.94 km for maximum-over-depth during Scenario 2 (Table 23),
  - within 2.92 km at the seafloor and 3.5 km for maximum-over-depth during Scenario 3 (Table 25).

Crustaceans and Bivalves, Sponges and Coral, and Plankton

To assist with assessing the potential effects on these receptors, the following have been determined:

- The maximum received SPL and per-pulse SEL at any of the five locations relevant to the pearl oyster fishery were received at the closest lease to modelling Site 1, 74.5 km away. The respective levels were 101.9 (L_p; dB re 1 µPa) and 121.1 (L_E; dB re 1 µPa²·s) (Table 14).
- Crustaceans: The sound level of 202 dB re 1 µPa PK-PK from Payne et al. (2008) was considered; it was reached at ranges between 461 and 666 m depending on the modelled site, with range generally increasing with bottom depth (Table 19).
- Sponges and coral: The PK sound level at the seafloor directly underneath the seismic source was estimated at all modelling sites considered for seafloor fish receptors, and compared to the sound level of 226 dB re 1 µPa PK for sponges and corals (Heyward et al. 2018); it was found to reach or just exceed the criterion only at sites with a water depth less than 45 m, with the maximum distance being < 12 m (30 m depth), Tables 16–18.
- Plankton: The distance to the sound level of 178 dB re 1 µPa PK-PK from McCauley et al. (2017) was estimated at all modelling sites through full-waveform modelling using FWRAM; the results ranged from 7.94 km to 12.23 km, Table 13.

Glossary

1/3-octave-band
Non-overlapping passbands that are one-third of an octave wide (where an octave is a doubling of frequency). Three adjacent 1/3-octave-bands comprise a one octave-band. One-third-octave-bands become wider with increasing frequency. Also see octave.

attenuation
The gradual loss of acoustic energy from absorption and scattering as sound propagates through a medium.

auditory weighting function (frequency-weighting function)
Auditory weighting functions account for marine mammal hearing sensitivity. They are applied to sound measurements to emphasise frequencies that an animal hears well and de-emphasise frequencies they hear less well or not at all (Southall et al. 2007, Finneran and Jenkins 2012, NOAA 2013).

azimuth
A horizontal angle relative to a reference direction, which is often magnetic north or the direction of travel. In navigation it is also called bearing.

bandwidth
The range of frequencies over which a sound occurs. Broadband refers to a source that produces sound over a broad range of frequencies (e.g., seismic airguns, vessels) whereas narrowband sources produce sounds over a narrow frequency range (e.g., sonar) (ANSI/ASA S1.13-2005 R2010).

bar
Unit of pressure equal to 100 kPa, which is approximately equal to the atmospheric pressure on Earth at sea level. 1 bar is equal to 10^{6} Pa or 10^{11} µPa.

broadside direction
Perpendicular to the travel direction of a source. Compare to endfire direction.

cetacean
Any animal in the order Cetacea. These are aquatic, mostly marine mammals and include whales, dolphins, and porpoises.

compressional wave
A mechanical vibration wave in which the direction of particle motion is parallel to the direction of propagation. Also called primary wave or P-wave.

decibel (dB)
One-tenth of a bel. Unit of level when the base of the logarithm is the tenth root of ten, and the quantities concerned are proportional to power (ANSI S1.1-1994 R2004).

endfire direction
Parallel to the travel direction of a source. Also see broadside direction.

frequency
The rate of oscillation of a periodic function measured in cycles-per-unit-time. The reciprocal of the period. Unit: hertz (Hz). Symbol: *f*. 1 Hz is equal to 1 cycle per second.

functional hearing group
Grouping of marine mammal species with similar estimated hearing ranges. Southall et al. (2007) proposed the following functional hearing groups: low-, mid-, and high-frequency cetaceans, pinnipeds in water, and pinnipeds in air.

geoacoustic
Relating to the acoustic properties of the seafloor.

hearing threshold
The sound pressure level that is barely audible for a given individual in the absence of significant background noise during a specific percentage of experimental trials.

hertz (Hz)
A unit of frequency defined as one cycle per second.

high-frequency (HF) cetacean
The functional hearing group that represents odontocetes specialised for using high frequencies.

impulsive sound
Sound that is typically brief and intermittent with rapid (within a few seconds) rise time and decay back to ambient levels (NOAA 2013, ANSI S12.7-1986 R2006). For example, seismic airguns and impact pile driving.

low-frequency (LF)cetacean
The functional hearing group that represents mysticetes (baleen whales).

maximum-over-depth
The maximum value over all modelled depths above the sea floor.

mid-frequency (MF) cetacean
The functional hearing group that represents some odontocetes (dolphins, toothed whales, beaked whales, and bottlenose whales).

mysticete
Mysticeti, a suborder of cetaceans, use their baleen plates, rather than teeth, to filter food from water. They are not known to echolocate but use sound for communication. Members of this group include rorquals (Balaenopteridae), right whales (Balaenidae), and the grey whale (*Eschrichtius robustus*).

non-impulsive sound
Sound that is broadband, narrowband or tonal, brief or prolonged, continuous or intermittent, and typically does not have a high peak pressure with rapid rise time (typically only small fluctuations in decibel level) that impulsive signals have (ANSI/ASA S3.20-1995 R2008). Marine vessels, aircraft, machinery, construction, and vibratory pile driving are examples.

octave
The interval between a sound and another sound with double or half the frequency. For example, one octave above 200 Hz is 400 Hz, and one octave below 200 Hz is 100 Hz.

odontocete
The presence of teeth, rather than baleen, characterises these whales. Members of the Odontoceti are a suborder of cetaceans, a group comprised of whales, dolphins, and porpoises. The toothed whales' skulls are mostly asymmetric, an adaptation for their echolocation. This group includes sperm whales, killer whales, belugas, narwhals, dolphins, and porpoises.

parabolic equation method
A computationally-efficient solution to the acoustic wave equation that is used to model transmission loss. The parabolic equation approximation omits effects of back-scattered sound, simplifying the computation of transmission loss. The effect of back-scattered sound is negligible for most ocean-acoustic propagation problems.

peak sound pressure level (PK)
The maximum instantaneous sound pressure level, in a stated frequency band, within a stated period. Also called zero-to-peak sound pressure level. Unit: dB re 1 µPa

permanent threshold shift (PTS)
A permanent loss of hearing sensitivity caused by excessive noise exposure. PTS is considered auditory injury.

pinniped
A common term used to describe all three groups that form the superfamily Pinnipedia: phocids (true seals or earless seals), otariids (eared seals or fur seals and sea lions), and walrus.

point source
A source that radiates sound as if from a single point (ANSI S1.1-1994 R2004).

power spectrum density
The acoustic signal power per unit frequency as measured at a single frequency. Unit: $\mu Pa^2/Hz$, or $\mu Pa^2 \cdot s$.

power spectrum density level
The decibel level ($10\log_{10}$) of the power spectrum density, usually presented in 1 Hz bins. Unit: dB re 1 $\mu Pa^2/Hz$.

pressure, acoustic
The deviation from the ambient hydrostatic pressure caused by a sound wave. Also called overpressure. Unit: pascal (Pa). Symbol: *p*.

pulsed sound
Discrete sounds with durations less than a few seconds. Sounds with longer durations are called continuous sounds.

received level
The sound level measured at a receiver.

signature
Pressure signal generated by a source.

sound
A time-varying pressure disturbance generated by mechanical vibration waves travelling through a fluid medium such as air or water.

sound exposure
Time integral of squared, instantaneous frequency-weighted sound pressure over a stated time interval or event. Unit: pascal-squared second ($Pa^2 \cdot s$) (ANSI S1.1-1994 R2004).

sound exposure level (SEL)
A measure related to the sound energy in one or more pulses. Unit: dB re 1 $\mu Pa^2 \cdot s$.

sound field
Region containing sound waves (ANSI S1.1-1994 R2004).

sound pressure level (SPL)
The decibel ratio of the time-mean-square sound pressure, in a stated frequency band, to the square of the reference sound pressure (ANSI S1.1-1994 R2004).

For sound in water, the reference sound pressure is one micropascal (p_0 = 1 µPa) and the unit for SPL is dB re 1 µPa:

$$\mathrm{SPL} = 10\log_{10}\left(p^2 / p_0^2\right) = 20\log_{10}\left(p / p_0\right)$$

Unless otherwise stated, SPL refers to the root-mean-square sound pressure level Unit: dB re 1 µPa.

sound speed profile
The speed of sound in the water column as a function of depth below the water surface.

source level (SL)
The sound pressure level or sound exposure level measured 1 metre from a theoretical point source that radiates the same total sound power as the actual source. Unit: dB re 1 μPa^2m^2 or dB 1 μPa^2m^2s.

spectrum
An acoustic signal represented in terms of its power (or energy) distribution versus frequency.

temporary threshold shift (TTS)
Temporary loss of hearing sensitivity caused by excessive noise exposure.

transmission loss (TL)
Also called propagation loss, this refers to the decibel reduction in sound level between two stated points that results from sound spreading away from an acoustic source subject to the influence of the surrounding environment.

wavelength
Distance over which a wave completes one oscillation cycle. Unit: meter (m). Symbol: λ.

Literature Cited

[DEWHA] Department of the Environment Water Heritage and the Arts. 2008. *EPBC Act Policy Statement 2.1 - Interaction Between Offshore Seismic Exploration and Whales*. *In*: Australian Government. Department of the Environment, W., Heritage and the Arts. 14 pp. http://www.environment.gov.au/resource/epbc-act-policy-statement-21-interaction-between-offshore-seismic-exploration-and-whales.

[HESS] High Energy Seismic Survey. 1999. *High Energy Seismic Survey Review Process and Interim Operational Guidelines for Marine Surveys Offshore Southern California*. Prepared for the California State Lands Commission and the United States Minerals Management Service Pacific Outer Continental Shelf Region by the High Energy Seismic Survey Team, Camarillo, CA. 98 pp.

[ISO] International Organization for Standardization. 2017. *ISO/DIS 18405.2:2017. Underwater acoustics—Terminology*. Geneva. https://www.iso.org/standard/62406.html.

[NMFS] National Marine Fisheries Service. 1998. *Acoustic Criteria Workshop*. Dr. Roger Gentry and Dr. Jeanette Thomas Co-Chairs.

[NMFS] National Marine Fisheries Service. 2014. *Marine Mammals: Interim Sound Threshold Guidance* (webpage). National Marine Fisheries Service, National Oceanic and Atmospheric Administration, U.S. Department of Commerce. http://www.westcoast.fisheries.noaa.gov/protected_species/marine_mammals/threshold_guidance.html.

[NMFS] National Marine Fisheries Service. 2016. *Technical Guidance for Assessing the Effects of Anthropogenic Sound on Marine Mammal Hearing: Underwater Acoustic Thresholds for Onset of Permanent and Temporary Threshold Shifts*. U.S. Department of Commerce, NOAA. NOAA Technical Memorandum NMFS-OPR-55. 178 pp.

[NMFS] National Marine Fisheries Service. 2018. *2018 Revision to: Technical Guidance for Assessing the Effects of Anthropogenic Sound on Marine Mammal Hearing (Version 2.0): Underwater Thresholds for Onset of Permanent and Temporary Threshold Shifts*. U.S. Department of Commerce, NOAA. NOAA Technical Memorandum NMFS-OPR-59. 167 pp. https://www.fisheries.noaa.gov/webdam/download/75962998.

[NOAA] National Oceanic and Atmospheric Administration. 2013. *Draft guidance for assessing the effects of anthropogenic sound on marine mammals: Acoustic threshold levels for onset of permanent and temporary threshold shifts*, December 2013, Silver Spring, MA: NMFS Office of Protected Resources, p. 76. http://www.nmfs.noaa.gov/pr/acoustics/draft_acoustic_guidance_2013.pdf.

[NOAA] National Oceanic and Atmospheric Administration. 2015. *Draft guidance for assessing the effects of anthropogenic sound on marine mammal hearing: Underwater acoustic threshold levels for onset of permanent and temporary threshold shifts*, July 2015, 180 pp. Silver Spring, Maryland: NMFS Office of Protected Resources. http://www.nmfs.noaa.gov/pr/acoustics/draft%20acoustic%20guidance%20July%202015.pdf.

[NOAA] National Oceanic and Atmospheric Administration. 2016. *Document Containing Proposed Changes to the NOAA Draft Guidance for Assessing the Effects of Anthropogenic Sound on Marine Mammal Hearing: Underwater Acoustic Threshold Levels for Onset of Permanent and Temporary Threshold Shifts*, p. 24. http://www.nmfs.noaa.gov/pr/acoustics/draft_guidance_march_2016_.pdf.

[NSF] National Science Foundation (U.S.), U.S. Geological Survey, and [NOAA] National Oceanic and Atmospheric Administration (U.S.). 2011. *Final Programmatic Environmental Impact Statement/Overseas. Environmental Impact Statement for Marine Seismic Research Funded*

by the National Science Foundation or Conducted by the U.S. Geological Survey. National Science Foundation, Arlington, VA.

[ONR] Office of Naval Research. 1998. *ONR Workshop on the Effect of Anthropogenic Noise in the Marine Environment*. Dr. R. Gisiner Chair.

Aerts, L., M. Blees, S. Blackwell, C. Greene, K. Kim, D.E. Hannay, and M. Austin. 2008. *Marine mammal monitoring and mitigation during BP Liberty OBC seismic survey in Foggy Island Bay, Beaufort Sea, July-August 2008: 90-day report*. Document Number LGL Report P1011-1. Report by LGL Alaska Research Associates Inc., LGL Ltd., Greeneridge Sciences Inc. and JASCO Applied Sciences for BP Exploration Alaska. 199 pp. http://www.nmfs.noaa.gov/pr/pdfs/permits/bp_liberty_monitoring.pdf.

ANSI S12.7-1986. R2006. *American National Standard Methods for Measurements of Impulsive Noise*. American National Standards Institute, New York.

ANSI S1.1-1994. R2004. *American National Standard Acoustical Terminology*. American National Standards Institute, New York.

ANSI/ASA S1.13-2005. R2010. *American National Standard Measurement of Sound Pressure Levels in Air*. American National Standards Institute and Acoustical Society of America, New York.

ANSI/ASA S3.20-1995. R2008. *American National Standard Bioacoustical Terminology*. American National Standards Institute and Acoustical Society of America, New York.

Austin, M. and G. Warner. 2012. *Sound Source Acoustic Measurements for Apache's 2012 Cook Inlet Seismic Survey*. Version 2.0. Technical report for Fairweather LLC and Apache Corporation by JASCO Applied Sciences Ltd.

Austin, M. and L. Bailey. 2013. *Sound Source Verification: TGS Chukchi Sea Seismic Survey Program 2013*. Document Number 00706, Version 1.0. Technical report by JASCO Applied Sciences for TGS-NOPEC Geophysical Company, .

Austin, M., A. McCrodan, C. O'Neill, Z. Li, and A.O. MacGillivray. 2013. *Marine mammal monitoring and mitigation during exploratory drilling by Shell in the Alaskan Chukchi and Beaufort Seas, July–November 2012: 90-Day Report*. *In*: Funk, D.W., C.M. Reiser, and W.R. Koski (eds.). Underwater Sound Measurements. LGL Rep. P1272D–1. Report from LGL Alaska Research Associates Inc. and JASCO Applied Sciences, for Shell Offshore Inc., National Marine Fisheries Service (US), and U.S. Fish and Wildlife Service. 266 pp plus appendices.

Austin, M. 2014. Underwater noise emissions from drillships in the Arctic. *Underwater Acoustics 2014*. Rhodes, Greece.

Austin, M. and Z. Li. 2016. *Marine Mammal Monitoring and Mitigation During Exploratory Drilling by Shell in the Alaskan Chukchi Sea, July–October 2015: Draft 90-day report*. *In*: Ireland, D.S. and L.N. Bisson (eds.). Underwater Sound Measurements. LGL Rep. P1363D. Report from LGL Alaska Research Associates Inc., LGL Ltd., and JASCO Applied Sciences Ltd. For Shell Gulf of Mexico Inc, National Marine Fisheries Service, and U.S. Fish and Wildlife Service. 188 pp + appendices pp.

Austin, M.A., H. Yurk, and R. Mills. 2015. *Acoustic Measurements and Animal Exclusion Zone Distance Verification for Furie's 2015 Kitchen Light Pile Driving Operations in Cook Inlet*. Version 2.0. Technical report for Jacobs LLC and Furie Alaska by JASCO Applied Sciences.

Baker, C., A. Potter, M. Tran, and A.D. Heap. 2008. *Sedimentology and Geomorphology of the Northwest Marine Region*. Geoscience Australia Record 2008/07, Canberra, Australia. 220 pp.

Buckingham, M.J. 2005. Compressional and shear wave properties of marine sediments: Comparisons between theory and data. *Journal of the Acoustical Society of America* 117(1): 137-152. http://dx.doi.org/10.1121/1.1810231.

Carnes, M.R. 2009. *Description and Evaluation of GDEM-V 3.0*. Document Number NRL Memorandum Report 7330-09-9165. U.S. Naval Research Laboratory, Stennis Space Center, MS. 21 pp.

Collins, M.D. 1993. A split-step Padé solution for the parabolic equation method. *Journal of the Acoustical Society of America* 93(4): 1736-1742. https://doi.org/10.1121/1.406739.

Collins, M.D., R.J. Cederberg, D.B. King, and S. Chin-Bing. 1996. Comparison of algorithms for solving parabolic wave equations. *Journal of the Acoustical Society of America* 100(1): 178-182. https://doi.org/10.1121/1.415921.

Coppens, A.B. 1981. Simple equations for the speed of sound in Neptunian waters. *Journal of the Acoustical Society of America* 69(3): 862-863. http://dx.doi.org/10.1121/1.385486.

Day, R.D., R.D. McCauley, Q.P. Fitzgibbon, and J.M. Semmens. 2016. Seismic air gun exposure during early-stage embryonic development does not negatively affect spiny lobster *Jasus edwardsii larvae* (Decapoda:Palinuridae). *Scientific Reports* 6: 1-9. http://dx.doi.org/10.1038/srep22723.

Dragoset, W.H. 1984. A comprehensive method for evaluating the design of airguns and airgun arrays. *Proceedings, 16th Annual Offshore Technology Conference* Volume 3, 7-9 May 1984. OTC 4747, Houston, TX. pp 75–84.

Ellison, W.T. and P.J. Stein. 1999. *SURTASS LFA High Frequency Marine Mammal Monitoring (HF/M3) Sonar: Sustem Description and Test & Evaluation*. Under U.S. Navy Contract N66604-98-D-5725.

Finneran, J.J. and C.E. Schlundt. 2010. Frequency-dependent and longitudinal changes in noise-induced hearing loss in a bottlenose dolphin (*Tursiops truncatus*). *Journal of the Acoustical Society of America* 128(2): 567-570. https://doi.org/10.1121/1.3458814.

Finneran, J.J. and A.K. Jenkins. 2012. *Criteria and thresholds for U.S. Navy acoustic and explosive effects analysis*. SPAWAR Systems Center Pacific, San Diego, CA.

Finneran, J.J. 2015. *Auditory weighting functions and TTS/PTS exposure functions for cetaceans and marine carnivores*. Technical report by SSC Pacific, San Diego, CA.

Finneran, J.J. 2016. *Auditory weighting functions and TTS/PTS exposure functions for marine mammals exposed to underwater noise*. Technical Report for Space and Naval Warfare Systems Center Pacific, San Diego, CA. 49 pp. http://www.dtic.mil/dtic/tr/fulltext/u2/1026445.pdf.

Fisher, F.H. and V.P. Simmons. 1977. Sound absorption in sea water. *Journal of the Acoustical Society of America* 62(3): 558-564. https://doi.org/10.1121/1.381574.

Funk, D., D.E. Hannay, D. Ireland, R. Rodrigues, and W. Koski (eds.). 2008. *Marine mammal monitoring and mitigation during open water seismic exploration by Shell Offshore Inc. in the Chukchi and Beaufort Seas, July–November 2007: 90-day report*. LGL Report P969-1. Prepared by LGL Alaska Research Associates Inc., LGL Ltd., and JASCO Research Ltd. for Shell Offshore Inc., National Marine Fisheries Service (U.S.), and U.S. Fish and Wildlife Service. 218 pp.

Gedamke, J., N. Gales, and S. Frydman. 2011. Assessing risk of baleen whale hearing loss from seismic surveys: The effect of uncertainty and individual variation. *Journal of the Acoustical Society of America* 129(1): 496-506. https://doi.org/10.1121/1.3493445.

Hannay, D.E. and R.G. Racca. 2005. *Acoustic Model Validation*. Document Number 0000-S-90-04-T-7006-00-E, Revision 02. Technical report by JASCO Research Ltd. for Sakhalin Energy Investment Company Ltd. 34 pp.

Heyward, A., J. Colquhoun, E. Cripps, D. McCorry, M. Stowar, B. Radford, K. Miller, I. Miller, and C. Battershill. 2018. No evidence of damage to the soft tissue or skeletal integrity of mesophotic corals exposed to a 3D marine seismic survey. *Marine Pollution Bulletin* 129(1): 8-13. https://doi.org/10.1016/j.marpolbul.2018.01.057.

Ireland, D.S., R. Rodrigues, D. Funk, W. Koski, and D.E. Hannay. 2009. *Marine mammal monitoring and mitigation during open water seismic exploration by Shell Offshore Inc. in the Chukchi and Beaufort Seas, July–October 2008: 90-Day Report*. Document Number LGL Report P1049-1. 277 pp.

Landro, M. 1992. Modeling of GI gun signatures. *Geophysical Prospecting* 40: 721–747. https://doi.org/10.1111/j.1365-2478.1992.tb00549.x

Laws, R.M., L. Hatton, and M. Haartsen. 1990. Computer modeling of clustered airguns. *First Break* 8(9): 331–338.

Lucke, K., U. Siebert, P. Lepper, A., and M.-A. Blanchet. 2009. Temporary shift in masked hearing thresholds in a harbor porpoise (*Phocoena phocoena*) after exposure to seismic airgun stimuli. *Journal of the Acoustical Society of America* 125(6): 4060-4070. https://asa.scitation.org/doi/10.1121/1.3117443.

Lurton, X. 2002. *An Introduction to Underwater Acoustics: Principles and Applications*. Springer, Chichester, UK. 347 pp.

MacGillivray, A.O. and N.R. Chapman. 2012. Modeling underwater sound propagation from an airgun array using the parabolic equation method. *Canadian Acoustics* 40(1): 19-25. http://jcaa.caa-aca.ca/index.php/jcaa/article/view/2502.

MacGillivray, A.O. 2018. Underwater noise from pile driving of conductor casing at a deep-water oil platform. *Journal of the Acoustical Society of America* 143(1): 450-459. https://doi.org/10.1121/1.5021554.

Martin, B., K. Broker, M.-N.R. Matthews, J. MacDonnell, and L. Bailey. 2015. *Comparison of measured and modeled air-gun array sound levels in Baffin Bay, West Greenland. OceanNoise 2015*, 11-15 May, Barcelona, Spain.

Martin, B., J.T. MacDonnell, and K. Bröker. 2017a. Cumulative sound exposure levels—Insights from seismic survey measurements. *Journal of the Acoustical Society of America* 141(5): 3603-3603. https://asa.scitation.org/doi/10.1121/1.4987709.

Martin, S.B. and A.N. Popper. 2016. Short- and long-term monitoring of underwater sound levels in the Hudson River (New York, USA). *Journal of the Acoustical Society of America* 139(4): 1886-1897. http://dx.doi.org/10.1121/1.4944876.

Martin, S.B., M.-N.R. Matthews, J.T. MacDonnell, and K. Bröker. 2017b. Characteristics of seismic survey pulses and the ambient soundscape in Baffin Bay and Melville Bay, West Greenland. *Journal of the Acoustical Society of America* 142(6): 3331-3346. https://doi.org/10.1121/1.5014049.

Matthews, M.-N.R. and A.O. MacGillivray. 2013. Comparing modeled and measured sound levels from a seismic survey in the Canadian Beaufort Sea. *Proceedings of Meetings on Acoustics* 19(1): 1-8. https://doi.org/10.1121/1.4800553

Mattsson, A. and M. Jenkerson. 2008. *Single Airgun and Cluster Measurement Project*. *Joint Industry Programme (JIP) on Exploration and Production Sound and Marine Life Proramme Review*, October 28-30. International Association of Oil and Gas Producers, Houston, TX.

McCauley, R.D., J. Fewtrell, A.J. Duncan, C. Jenner, M.-N. Jenner, J.D. Penrose, R.I.T. Prince, A. Adihyta, J. Murdoch, et al. 2000. Marine seismic surveys: A study of environmental implications. *Australian Petroleum Production Exploration Association (APPEA) Journal* 40(1): 692-708. https://doi.org/10.1071/AJ99048.

McCauley, R.D., R.D. Day, K.M. Swadling, Q.P. Fitzgibbon, R.A. Watson, and J.M. Semmens. 2017. Widely used marine seismic survey air gun operations negatively impact zooplankton. *Nature Ecology & Evolution* 1: 1-8. http://dx.doi.org/10.1038/s41559-017-0195.

McCrodan, A., C. McPherson, and D.E. Hannay. 2011. *Sound Source Characterization (SSC) Measurements for Apache's 2011 Cook Inlet 2D Technology Test*. Version 3.0. Technical report for Fairweather LLC and Apache Corporation by JASCO Applied Sciences. 51 pp.

McPherson, C.R. and G. Warner. 2012. *Sound Sources Characterization for the 2012 Simpson Lagoon OBC Seismic Survey 90-Day Report*. Document Number 00443, Version 2.0. Technical report by JASCO Applied Sciences for BP Exploration (Alaska) Inc. http://www.nmfs.noaa.gov/pr/pdfs/permits/bp_openwater_90dayreport_appendices.pdf.

McPherson, C.R., K. Lucke, B. Gaudet, B.S. Martin, and C.J. Whitt. 2018. *Pelican 3-D Seismic Survey Sound Source Characterisation*. Report Number 001583. Version 1.0. Technical report by JASCO Applied Sciences for RPS Energy Services Pty Ltd.

McPherson, C.R. and B. Martin. 2018. *Characterisation of Polarcus 2380 in^3 Airgun Array*. Document Number 001599, Version 1.0. Technical report by JASCO Applied Sciences for Polarcus Asia Pacific Pte Ltd.

Moein, S.E., J.A. Musick, J.A. Keinath, D.E. Barnard, M.L. Lenhardt, and R. George. 1995. *Evaluation of Seismic Sources for Repelling Sea Turtles from Hopper Dredges, in Sea Turtle Research Program: Summary Report*. *In*: Hales, L.Z. (ed.). Report from U.S. Army Engineer Division, South Atlantic, Atlanta GA, and U.S. Naval Submarine Base, Kings Bay GA. Technical Report CERC-95. 90 pp.

Nedwell, J.R. and A.W. Turnpenny. 1998. The use of a generic frequency weighting scale in estimating environmental effect. *Workshop on Seismics and Marine Mammals*. 23–25 Jun 1998, London, U.K.

Nedwell, J.R., A.W.H. Turnpenny, J. Lovell, S.J. Parvin, R. Workman, and J.A.L. Spinks. 2007. *A validation of the dB$_{ht}$ as a measure of the behavioural and auditory effects of underwater noise*. Document Number 534R1231 Report prepared by Subacoustech Ltd. for the UK Department of Business, Enterprise and Regulatory Reform under Project No. RDCZ/011/0004. http://www.subacoustech.com/wp-content/uploads/534R1231.pdf.

O'Neill, C., D. Leary, and A. McCrodan. 2010. Sound Source Verification. (Chapter 3) *In* Blees, M.K., K.G. Hartin, D.S. Ireland, and D.E. Hannay (eds.). *Marine mammal monitoring and mitigation during open water seismic exploration by Statoil USA E&P Inc. in the Chukchi Sea, August-October 2010: 90-day report*. LGL Report P1119. Prepared by LGL Alaska Research Associates Inc., LGL Ltd., and JASCO Applied Sciences Ltd. for Statoil USA E&P Inc., National Marine Fisheries Service (U.S.), and U.S. Fish and Wildlife Service. pp 1-34.

Payne, J.F., C. Andrews, L. Fancey, D. White, and J. Christian. 2008. *Potential Effects of Seismic Energy on Fish and Shellfish: An Update since 2003*. Report Number 2008/060. Canadian Science Advisory Secretariat. 22 pp.

Payne, R. and D. Webb. 1971. Orientation by means of long range acoustic signaling in baleen whales. *Annals of the New York Academy of Sciences* 188: 110-142. https://doi.org/10.1111/j.1749-6632.1971.tb13093.x.

Popper, A.N., A.D. Hawkins, R.R. Fay, D.A. Mann, S. Bartol, T.J. Carlson, S. Coombs, W.T. Ellison, R.L. Gentry, et al. 2014. *Sound Exposure Guidelines for Fishes and Sea Turtles: A Technical Report prepared by ANSI-Accredited Standards Committee S3/SC1 and registered with*

ANSI. ASA S3/SC1.4 TR-2014. SpringerBriefs in Oceanography. ASA Press and Springer. https://doi.org/10.1007/978-3-319-06659-2.

Popper, A.N., T.J. Carlson, J.A. Gross, A.D. Hawkins, D.G. Zeddies, L. Powell, and J. Young. 2016. Effects of seismic air guns on pallid sturgeon and paddlefish. *In* Popper, A.N. and A.D. Hawkins (eds.). *The Effects of Noise on Aquatic Life II*. Volume 875. Springer, New York. pp 871-878. https://doi.org/10.1007/978-1-4939-2981-8_107.

Porter, M.B. and Y.-C. Liu. 1994. Finite-element ray tracing. *In*: Lee, D. and M.H. Schultz (eds.). *Proceedings of the International Conference on Theoretical and Computational Acoustics*. Volume 2. World Scientific Publishing Co. pp 947-956.

Racca, R.G., A. Rutenko, K. Bröker, and M. Austin. 2012a. A line in the water - design and enactment of a closed loop, model based sound level boundary estimation strategy for mitigation of behavioural impacts from a seismic survey. *11th European Conference on Underwater Acoustics 2012*. Volume 34(3), Edinburgh, United Kingdom.

Racca, R.G., A. Rutenko, K. Bröker, and G. Gailey. 2012b. *Model based sound level estimation and in-field adjustment for real-time mitigation of behavioural impacts from a seismic survey and post-event evaluation of sound exposure for individual whales*. *Acoustics 2012 Fremantle: Acoustics, Development and the Environment*, Fremantle, Australia. http://www.acoustics.asn.au/conference_proceedings/AAS2012/papers/p92.pdf.

Racca, R.G., M. Austin, A. Rutenko, and K. Bröker. 2015. Monitoring the gray whale sound exposure mitigation zone and estimating acoustic transmission during a 4-D seismic survey, Sakhalin Island, Russia. *Endangered Species Research* 29(2): 131-146. https://doi.org/10.3354/esr00703.

Southall, B.L., A.E. Bowles, W.T. Ellison, J.J. Finneran, R.L. Gentry, C.R. Greene, Jr., D. Kastak, D.R. Ketten, J.H. Miller, et al. 2007. Marine Mammal Noise Exposure Criteria: Initial Scientific Recommendations. *Aquatic Mammals* 33(4): 411-521. https://doi.org/10.1080/09524622.2008.9753846.

Teague, W.J., M.J. Carron, and P.J. Hogan. 1990. A comparison between the Generalized Digital Environmental Model and Levitus climatologies. *Journal of Geophysical Research* 95(C5): 7167-7183.

Tougaard, J., A.J. Wright, and P.T. Madsen. 2015. Cetacean noise criteria revisited in the light of proposed exposure limits for harbour porpoises. *Marine Pollution Bulletin* 90(1): 196-208. https://doi.org/10.1016/j.marpolbul.2014.10.051.

Warner, G., C. Erbe, and D.E. Hannay. 2010. Underwater Sound Measurements. (Chapter 3) *In* Reiser, C.M., D.W. Funk, R. Rodrigues, and D. Hannay (eds.). *Marine Mammal Monitoring and Mitigation during Open Water Shallow Hazards and Site Clearance Surveys by Shell Offshore Inc. in the Alaskan Chukchi Sea, July-October 2009: 90-Day Report*. LGL Report P1112-1. Report by LGL Alaska Research Associates Inc. and JASCO Applied Sciences for Shell Offshore Inc., National Marine Fisheries Service (U.S.), and U.S. Fish and Wildlife Service. pp 1-54.

Warner, G.A., M. Austin, and A.O. MacGillivray. 2017. Hydroacoustic measurements and modeling of pile driving operations in Ketchikan, Alaska. *Journal of the Acoustical Society of America* 141(5): 3992. https://doi.org/10.1121/1.4989141.

Whiteway, T. 2009. *Australian Bathymetry and Topography Grid, June 2009*. GeoScience Australia, Canberra. http://dx.doi.org/10.4225/25/53D99B6581B9A.

Wood, J., B.L. Southall, and D.J. Tollit. 2012. *PG&E offshore 3-D Seismic Survey Project Environmental Impact Report–Marine Mammal Technical Draft Report*. SMRU Ltd. 121 pp. https://www.coastal.ca.gov/energy/seismic/mm-technical-report-EIR.pdf.

Zhang, Z.Y. and C.T. Tindle. 1995. Improved equivalent fluid approximations for a low shear speed ocean bottom. *Journal of the Acoustical Society of America* 98(6): 3391-3396. https://doi.org/10.1121/1.413789.

Ziolkowski, A. 1970. A method for calculating the output pressure waveform from an air gun. *Geophysical Journal of the Royal Astronomical Society* 21(2): 137-161. https://doi.org/10.1111/j.1365-246X.1970.tb01773.x.

Zykov, M.M. and J.T. MacDonnell. 2013. *Sound Source Characterizations for the Collaborative Baseline Survey Offshore Massachusetts Final Report: Side Scan Sonar, Sub-Bottom Profiler, and the R/V Small Research Vessel experimental*. Document Number 00413, Version 2.0. Technical report by JASCO Applied Sciences for Fugro GeoServices, Inc. and the (US) Bureau of Ocean Energy Management.

Appendix A. Acoustic Metrics

A.1. Pressure Related Acoustic Metrics

Underwater sound pressure amplitude is measured in decibels (dB) relative to a fixed reference pressure of p_0 = 1 µPa. Because the perceived loudness of sound, especially impulsive noise such as from seismic airguns, pile driving, and sonar, is not generally proportional to the instantaneous acoustic pressure, several sound level metrics are commonly used to evaluate noise and its effects on marine life. We provide specific definitions of relevant metrics used in the accompanying report. Where possible we follow the ANSI and ISO standard definitions and symbols for sound metrics, but these standards are not always consistent.

The zero-to-peak sound pressure level (PK; L_{pk}; $L_{p,pk}$; dB re 1 µPa), is the maximum instantaneous sound pressure level in a stated frequency band attained by an acoustic pressure signal, $p(t)$:

$$L_{p,pk} = 20\log_{10}\left[\frac{\max\left(\left|p(t)\right|\right)}{p_0}\right] \quad \text{(A-1)}$$

PK is often included as a criterion for assessing whether a sound is potentially injurious; however, because it does not account for the duration of a noise event, it is generally a poor indicator of perceived loudness.

The peak-to-peak sound pressure level (PK-PK; $L_{pk\text{-}pk}$; $L_{p,pk\text{-}pk}$; dB re 1 µPa) is the difference between the maximum and minimum instantaneous sound pressure levels in a stated frequency band attained by an impulsive sound, $p(t)$:

$$L_{p,pk-pk} = 10\log_{10}\left\{\frac{\left[\max\left(p(t)\right) - \min\left(p(t)\right)\right]^2}{p_0^2}\right\} \quad \text{(A-2)}$$

The sound pressure level (SPL; L_p; dB re 1 µPa) is the rms pressure level in a stated frequency band over a specified time window (T, s) containing the acoustic event of interest. It is important to note that SPL always refers to a rms pressure level and therefore not instantaneous pressure:

$$L_p = 10\log_{10}\left(\frac{1}{T}\int_T p^2(t)dt \Big/ p_0^2\right) \quad \text{(A-3)}$$

The SPL represents a nominal effective continuous sound over the duration of an acoustic event, such as the emission of one acoustic pulse, a marine mammal vocalization, the passage of a vessel, or over a fixed duration. Because the window length, T, is the divisor, events with similar sound exposure level (SEL) but more spread out in time have a lower SPL. A fixed window length of 0.125 s (critical duration defined by Tougaard et al. (2015)) is used in this study for impulsive sounds.

The sound exposure level (SEL; L_E; $L_{E,p}$; dB re 1 µPa^2·s) is a measure related to the acoustic energy contained in one or more acoustic events (N). The SEL for a single event is computed from the time-integral of the squared pressure over the full event duration (T):

$$L_E = 10\log_{10}\left(\int_T p^2(t)dt \Big/ T_0 p_0^2\right) \quad \text{(A-4)}$$

where T_0 is a reference time interval of 1 s. The SEL continues to increase with time when non-zero pressure signals are present. It therefore can be construed as a dose-type measurement, so the integration time used must be carefully considered in terms of relevance for impact to the exposed recipients.

SEL can be calculated over periods with multiple acoustic events or over a fixed duration. For a fixed duration, the square pressure is integrated over the duration of interest. For multiple events, the SEL can be computed by summing (in linear units) the SEL of the *N* individual events:

$$L_{E,N} = 10\log_{10}\left(\sum_{i=1}^{N} 10^{\frac{L_{E,i}}{10}}\right). \qquad \text{(A-5)}$$

If applied, the frequency weighting of an acoustic event should be specified, as in the case of weighted SEL (e.g., $L_{E,LFC,24h}$; Appendix A.3). The use of fast, slow, or impulse exponential-time-averaging or other time-related characteristics should else be specified.

A.2. Marine Mammal Impact Criteria

It has been long recognised that marine mammals can be adversely affected by underwater anthropogenic noise. For example, Payne and Webb (1971) suggested that communication distances of fin whales are reduced by shipping sounds. Subsequently, similar concerns arose regarding effects of other underwater noise sources and the possibility that impulsive sources—primarily airguns used in seismic surveys—could cause auditory injury. This led to a series of workshops held in the late 1990s, conducted to address acoustic mitigation requirements for seismic surveys and other underwater noise sources (NMFS 1998, ONR 1998, Nedwell and Turnpenny 1998, HESS 1999, Ellison and Stein 1999). In the years since these early workshops, a variety of thresholds have been proposed for both injury and disturbance. The following sections summarize the recent development of thresholds; however, this field remains an active research topic.

A.2.1. Injury

In recognition of shortcomings of the SPL-only based injury criteria, in 2005 NMFS sponsored the Noise Criteria Group to review literature on marine mammal hearing to propose new noise exposure criteria. Some members of this expert group published a landmark paper (Southall et al. 2007) that suggested assessment methods similar to those applied for humans. The resulting recommendations introduced dual acoustic injury criteria for impulsive sounds that included peak pressure level thresholds and SEL_{24h} thresholds, where the subscripted 24h refers to the accumulation period for calculating SEL. The peak pressure level criterion is not frequency weighted whereas the SEL_{24h} is frequency weighted according to one of four marine mammal species hearing groups: low-, mid- and high-frequency cetaceans (LF, MF, and HF cetaceans, respectively) and Pinnipeds in Water (PINN). These weighting functions are referred to as M-weighting filters (analogous to the A-weighting filter for human; Appendix A.3). The SEL_{24h} thresholds were obtained by extrapolating measurements of onset levels of Temporary Threshold Shift (TTS) in belugas by the amount of TTS required to produce Permanent Threshold Shift (PTS) in chinchillas. The Southall et al. (2007) recommendations do not specify an exchange rate, which suggests that the thresholds are the same regardless of the duration of exposure (i.e., it implies a 3 dB exchange rate).

Wood et al. (2012) refined Southall et al.'s (2007) thresholds, suggesting lower injury values for LF and HF cetaceans while retaining the filter shapes. Their revised thresholds were based on TTS-onset levels in harbour porpoises from Lucke et al. (2009), which led to a revised impulsive sound PTS threshold for HF cetaceans of 179 dB re 1 $\mu Pa^2 \cdot s$. Because there were no data available for baleen whales, Wood et al. (2012) based their recommendations for LF cetaceans on results obtained from MF cetacean studies. In particular they referenced Finneran and Schlundt (2010) research, which found mid-frequency cetaceans are more sensitive to non-impulsive sound exposure than Southall et al. (2007) assumed. Wood et al. (2012) thus recommended a more conservative TTS-onset level for LF cetaceans of 192 dB re 1 $\mu Pa^2 \cdot s$.

As of 2017, an optimal approach is not apparent. There is consensus in the research community that an SEL-based method is preferable either separately or in addition to an SPL-based approach to assess the potential for injuries. In August 2016, after substantial public and expert input into three draft versions and based largely on the above-mentioned literature (NOAA 2013, 2015, 2016), NMFS finalised technical guidance for assessing the effect of anthropogenic sound on marine mammal hearing (NMFS 2016). The guidance describes injury criteria with new thresholds and frequency

weighting functions for the five hearing groups described by Finneran and Jenkins (2012). The latest revision to this work was published in 2018; only the PK criteria defined in NMFS (2018) are applied in this report.

A.3. Marine Mammal Frequency Weighting

The potential for noise to affect animals depends on how well the animals can hear it. Noises are less likely to disturb or injure an animal if they are at frequencies that the animal cannot hear well. An exception occurs when the sound pressure is so high that it can physically injure an animal by non-auditory means (i.e., barotrauma). For sound levels below such extremes, the importance of sound components at particular frequencies can be scaled by frequency weighting relevant to an animal's sensitivity to those frequencies (Nedwell and Turnpenny 1998, Nedwell et al. 2007).

A.3.1. Marine mammal frequency weighting functions

In 2015, a U.S. Navy technical report by Finneran (2015) recommended new auditory weighting functions. The overall shape of the auditory weighting functions is similar to human A-weighting functions, which follows the sensitivity of the human ear at low sound levels. The new frequency-weighting function is expressed as:

$$G(f) = K + 10\log_{10}\left[\left(\frac{(f/f_{lo})^{2a}}{\left[1+(f/f_{lo})^{2}\right]^{a}\left[1+(f/f_{hi})^{2}\right]^{b}}\right)\right] \quad \text{(A-6)}$$

Finneran (2015) proposed five functional hearing groups for marine mammals in water: low-, mid-, and high-frequency cetaceans, phocid pinnipeds, and otariid pinnipeds. The parameters for these frequency-weighting functions were further modified the following year (Finneran 2016) and were adopted in NOAA's technical guidance that assesses noise impacts on marine mammals (NMFS 2016, NMFS 2018). Table A-1 lists the frequency-weighting parameters for each hearing group; Figure A-1 shows the resulting frequency-weighting curves.

Table A-1. Parameters for the auditory weighting functions recommended by NMFS (2018).

Hearing group	a	b	f_{lo} (Hz)	f_{hi} (kHz)	K (dB)
Low-frequency cetaceans (baleen whales)	1.0	2	200	19,000	0.13
Mid-frequency cetaceans (dolphins, plus toothed, beaked, and bottlenose whales)	1.6	2	8,800	110,000	1.20
High-frequency cetaceans (true porpoises, *Kogia*, river dolphins, cephalorhynchid, *Lagenorhynchus cruciger* and *L. australis*)	1.8	2	12,000	140,000	1.36
Phocid pinnipeds in water (true seals)	1.0	2	1,900	30,000	0.75
Otariid pinnipeds in water (sea lions and fur seals)	2.0	2	940	25,000	0.64
Sirenians (dugongs and manatees)	1.8	2	4,300	25,000	2.62

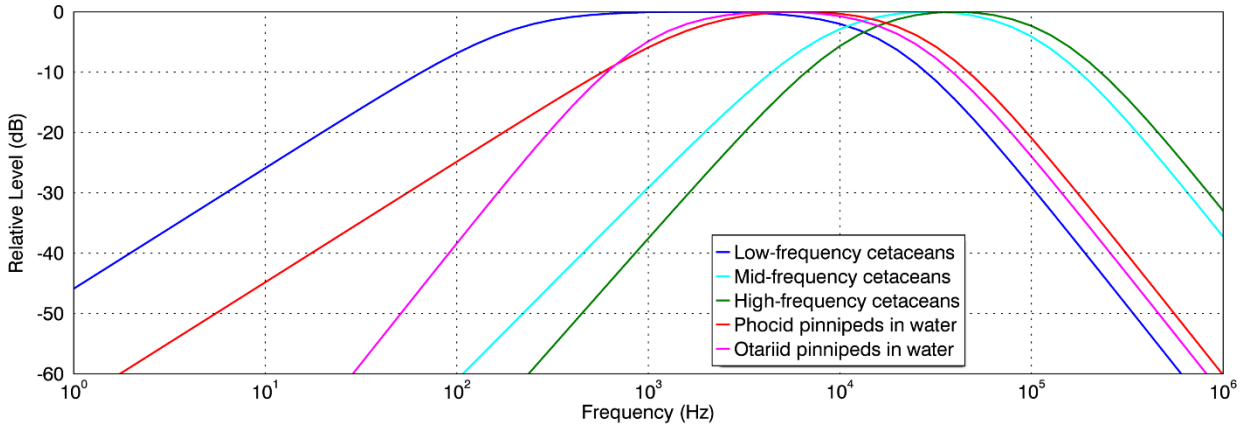

Figure A-1. Auditory weighting functions for functional marine mammal hearing groups (excluding sirenians) as recommended by NMFS (2018).

Appendix B. Acoustic Source Model

B.1. Airgun Array Source Model

The source levels and directivity of the seismic source were predicted with JASCO's Airgun Array Source Model (AASM). AASM includes low- and high-frequency modules for predicting different components of the seismic source spectrum. The low-frequency module is based on the physics of oscillation and radiation of airgun bubbles, as originally described by Ziolkowski (1970), that solves the set of parallel differential equations that govern bubble oscillations. Physical effects accounted for in the simulation include pressure interactions between airguns, port throttling, bubble damping, and generator-injector (GI) gun behaviour discussed by Dragoset (1984), Laws et al. (1990), and Landro (1992). A global optimisation algorithm tunes free parameters in the model to a large library of airgun source signatures.

While airgun signatures are highly repeatable at the low frequencies, which are used for seismic imaging, their sound emissions have a large random component at higher frequencies that cannot be predicted using a deterministic model. Therefore, AASM uses a stochastic simulation to predict the high-frequency (800−25,000 Hz) sound emissions of individual airguns, using a data-driven multiple-regression model. The multiple-regression model is based on a statistical analysis of a large collection of high quality seismic source signature data recently obtained from the Joint Industry Program (JIP) on Sound and Marine Life (Mattsson and Jenkerson 2008). The stochastic model uses a Monte-Carlo simulation to simulate the random component of the high-frequency spectrum of each airgun in an array. The mean high-frequency spectra from the stochastic model augment the low-frequency signatures from the physical model, allowing AASM to predict airgun source levels at frequencies up to 25,000 Hz.

AASM produces a set of "notional" signatures for each array element based on:

- Array layout
- Volume, tow depth, and firing pressure of each airgun
- Interactions between different airguns in the array

These notional signatures are the pressure waveforms of the individual airguns at a standard reference distance of 1 m; they account for the interactions with the other airguns in the array. The signatures are summed with the appropriate phase delays to obtain the far-field source signature of the entire array in all directions. This far-field array signature is filtered into 1/3-octave-bands to compute the source levels of the array as a function of frequency band and azimuthal angle in the horizontal plane (at the source depth), after which it is considered a directional point source in the far field.

A seismic array consists of many sources and the point source assumption is invalid in the near field where the array elements add incoherently. The maximum extent of the near field of an array (R_{nf}) is:

$$R_{nf} < \frac{l^2}{4\lambda} \tag{B-1}$$

where λ is the sound wavelength and l is the longest dimension of the array (Lurton 2002, §5.2.4). For example, a seismic source length of l = 21 m yields a near-field range of 147 m at 2 kHz and 7 m at 100 Hz. Beyond this R_{nf} range, the array is assumed to radiate like a directional point source and is treated as such for propagation modelling.

The interactions between individual elements of the array create directionality in the overall acoustic emission. Generally, this directionality is prominent mainly at frequencies in the mid-range between tens of hertz to several hundred hertz. At lower frequencies, with acoustic wavelengths much larger than the inter-airgun separation distances, the directionality is small. At higher frequencies, the pattern of lobes is too finely spaced to be resolved and the effective directivity is less.

B.2. Array Source Levels and Directivity

Figures B-1 through B-3 shows the broadside (perpendicular to the tow direction), endfire (parallel to the tow direction), and vertical overpressure signature and corresponding power spectrum levels for the 2970, 3000 and 3080 in^3 arrays.

Horizontal 1/3-octave-band source levels are shown as a function of band centre frequency and azimuth (Figures B-4 through B-6); directivity in the sound field is most noticeable at mid-frequencies as described in the model detail in Appendix B.1.

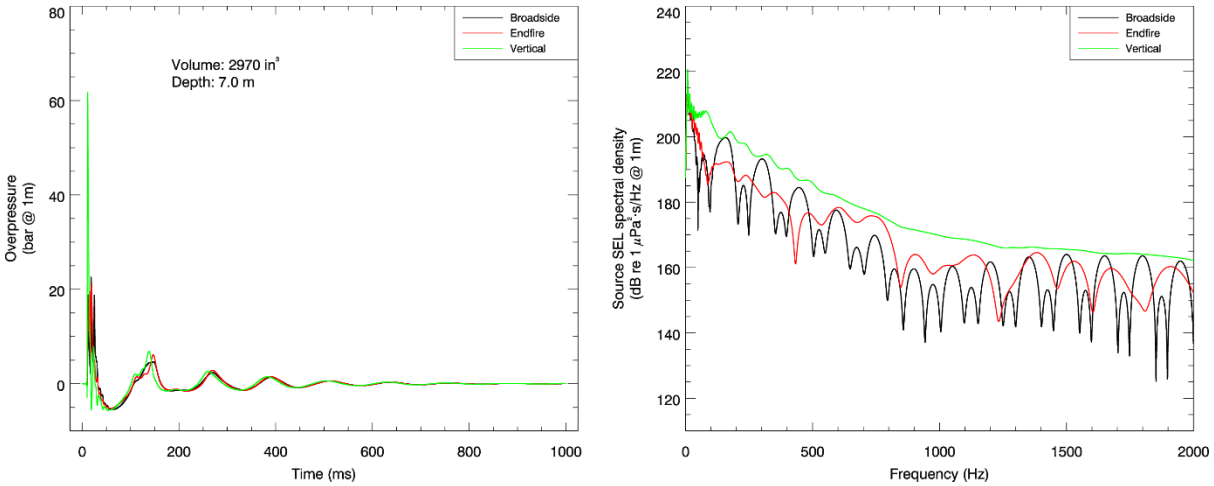

Figure B-1. Predicted source level details for the 2970 in^3 array at a 7 m towed depth. (Left) the overpressure signature and (right) the power spectrum for in-plane horizontal (broadside), perpendicular (endfire), and vertical directions.

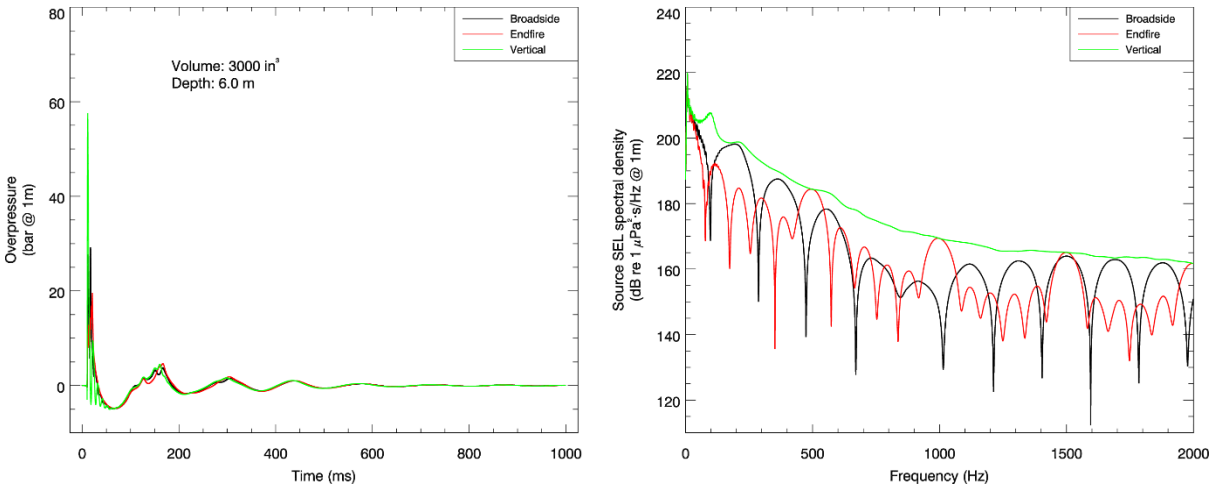

Figure B-2. Predicted source level details for the 3000 in^3 array at a 6 m towed depth. (Left) the overpressure signature and (right) the power spectrum for in-plane horizontal (broadside), perpendicular (endfire), and vertical directions.

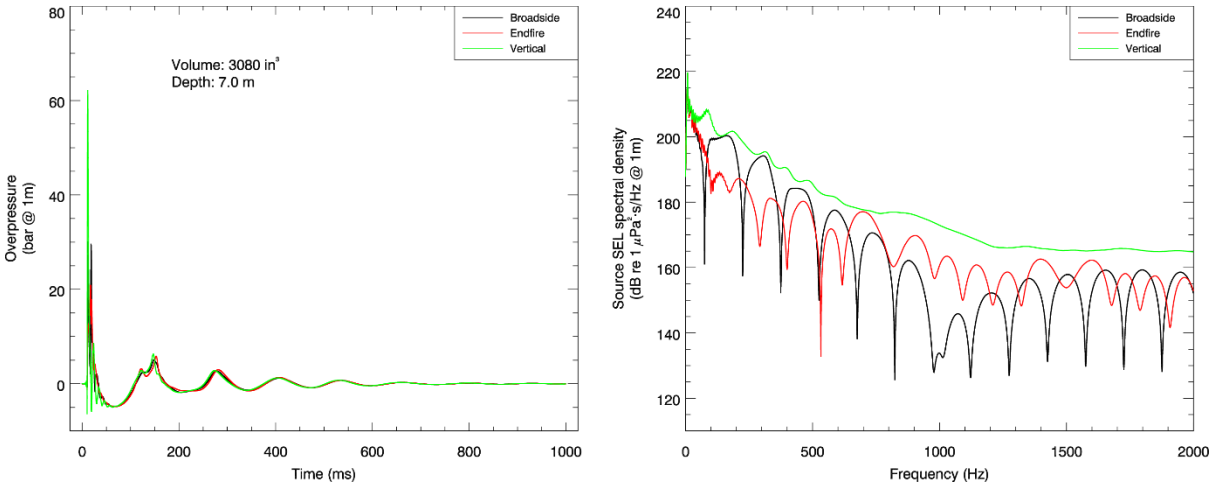

Figure B-3. Predicted source level details for the 3080 in^3 array at a 7 m towed depth. (Left) the overpressure signature and (right) the power spectrum for in-plane horizontal (broadside), perpendicular (endfire), and vertical directions.

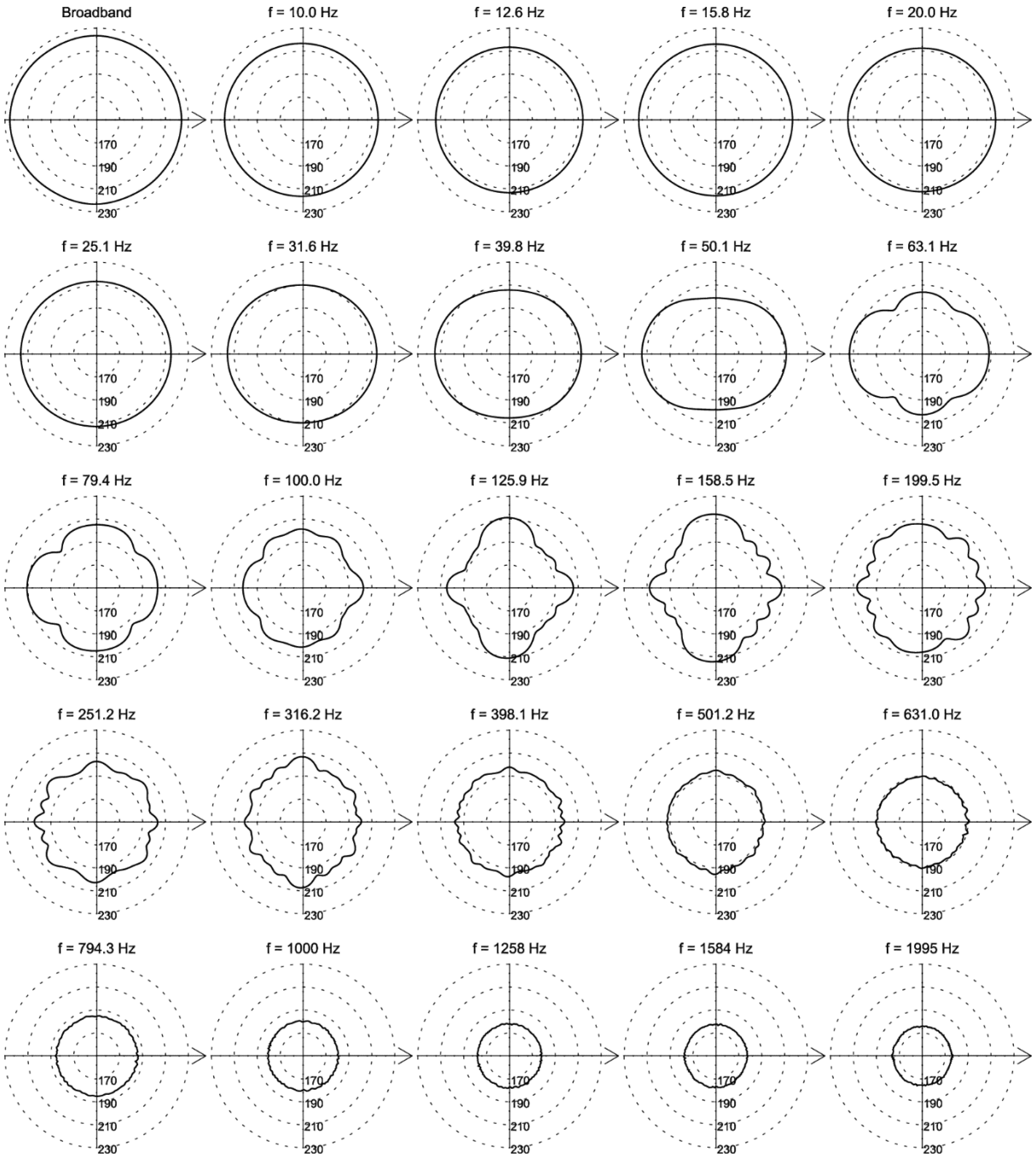

Figure B-4. Directionality of the predicted horizontal source levels for the 2970 in^3 seismic source array, 10 Hz to 2 kHz. Source levels (in dB re 1 $\mu Pa^2 \cdot s\ m^2$) are shown as a function of azimuth for the centre frequencies of the 1/3-octave-bands modelled; frequencies are shown above the plots. The perpendicular direction to the frame is to the right. Tow depth is 7 m (see Figure B-1).

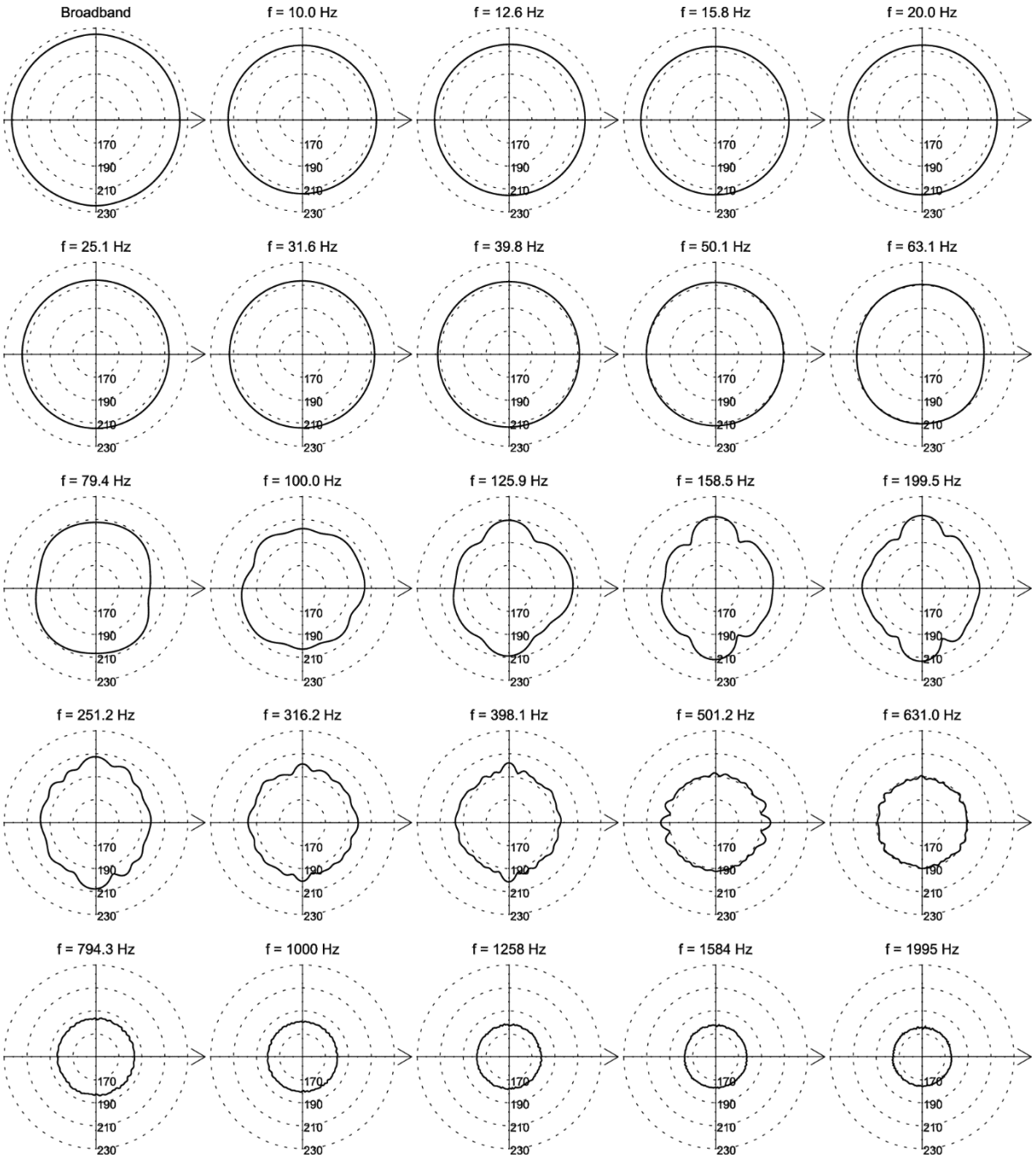

Figure B-5. Directionality of the predicted horizontal source levels for the 3000 in^3 seismic source array, 10 Hz to 2 kHz. Source levels (in dB re 1 $\mu Pa^2 \cdot s\ m^2$) are shown as a function of azimuth for the centre frequencies of the 1/3-octave-bands modelled; frequencies are shown above the plots. The perpendicular direction to the frame is to the right. Tow depth is 7 m (see Figure B-2).

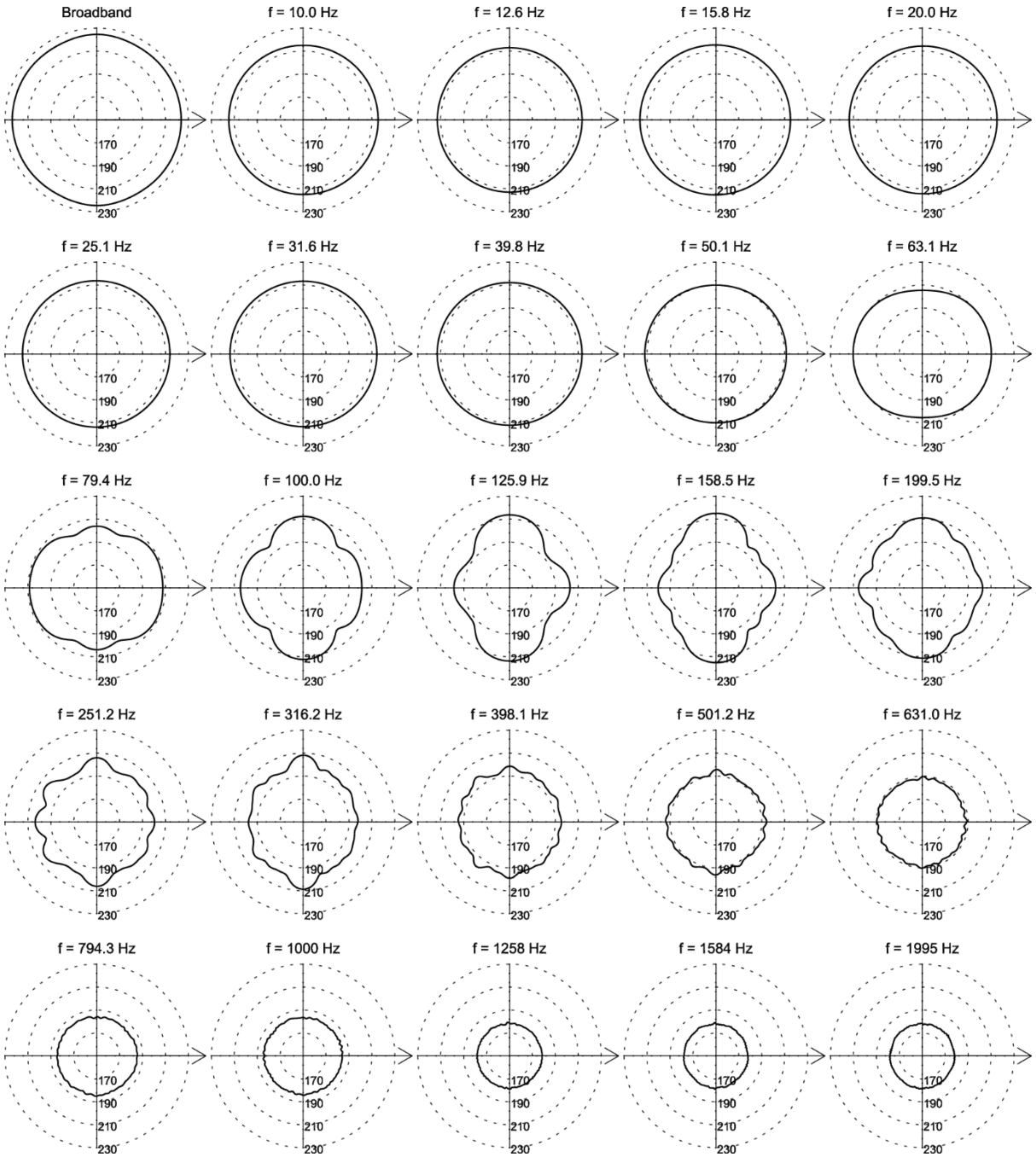

Figure B-6. Directionality of the predicted horizontal source levels for the 3080 in^3 seismic source array, 10 Hz to 2 kHz. Source levels (in dB re 1 µPa^2·s m^2) are shown as a function of azimuth for the centre frequencies of the 1/3-octave-bands modelled; frequencies are shown above the plots. The perpendicular direction to the frame is to the right. Tow depth is 7 m (see Figure B-3).

Appendix C. Sound Propagation Models

C.1. MONM-BELLHOP

Long-range sound fields were computed using JASCO's Marine Operations Noise Model (MONM). Compared to VSTACK, MONM less accurately predicts steep-angle propagation for environments with higher shear speed but is well suited for effective longer-range estimation. This model computes sound propagation at frequencies of 10 Hz to 1.25 kHz via a wide-angle parabolic equation solution to the acoustic wave equation (Collins 1993) based on a version of the U.S. Naval Research Laboratory's Range-dependent Acoustic Model (RAM), which has been modified to account for a solid seabed (Zhang and Tindle 1995). MONM computes sound propagation at frequencies > 1.25 kHz via the BELLHOP Gaussian beam acoustic ray-trace model (Porter and Liu 1994).

The parabolic equation method has been extensively benchmarked and is widely employed in the underwater acoustics community (Collins et al. 1996). MONM accounts for the additional reflection loss at the seabed, which results from partial conversion of incident compressional waves to shear waves at the seabed and sub-bottom interfaces, and it includes wave attenuations in all layers. MONM incorporates the following site-specific environmental properties: a bathymetric grid of the modelled area, underwater sound speed as a function of depth, and a geoacoustic profile based on the overall stratified composition of the seafloor.

This version of MONM accounts for sound attenuation due to energy absorption through ion relaxation and viscosity of water in addition to acoustic attenuation due to reflection at the medium boundaries and internal layers (Fisher and Simmons 1977). The former type of sound attenuation is significant for frequencies higher than 5 kHz and cannot be neglected without noticeably affecting the model results.

MONM computes acoustic fields in three dimensions by modelling transmission loss within two-dimensional (2-D) vertical planes aligned along radials covering a 360° swath from the source, an approach commonly referred to as N×2-D. These vertical radial planes are separated by an angular step size of $\Delta\theta$, yielding N = 360°/$\Delta\theta$ number of planes (Figure C-1).

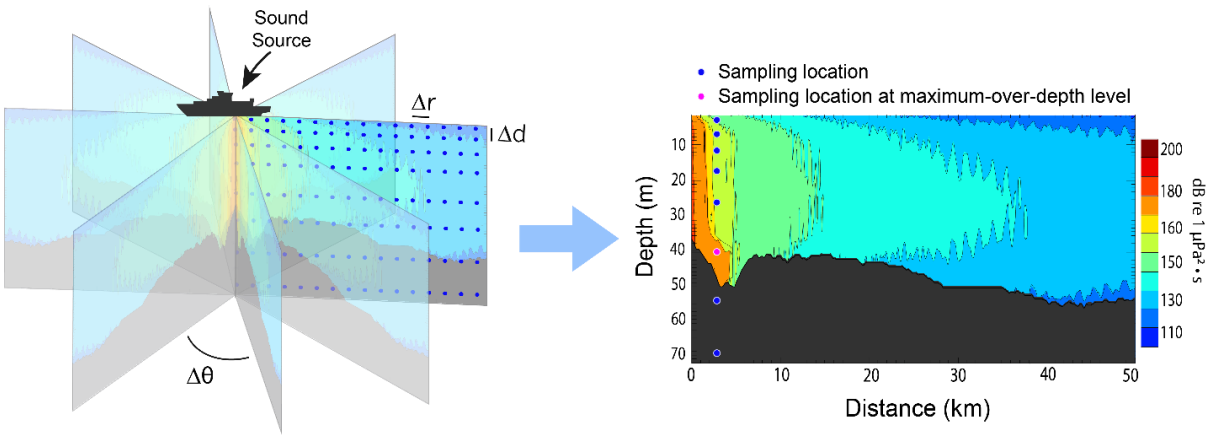

Figure C-1. The N×2-D and maximum-over-depth modelling approach used by MONM.

MONM treats frequency dependence by computing acoustic transmission loss at the centre frequencies of 1/3-octave-bands. Sufficiently many 1/3-octave-bands, starting at 10 Hz, are modelled to include most of the acoustic energy emitted by the source. At each centre frequency, the transmission loss is modelled within each of the N vertical planes as a function of depth and range from the source. The 1/3-octave-band received per-pulse SEL are computed by subtracting the band transmission loss values from the directional source level in that frequency band. Composite broadband received per-pulse SEL are then computed by summing the received 1/3-octave-band levels.

The received per-pulse SEL sound field within each vertical radial plane is sampled at various ranges from the source, generally with a fixed radial step size. At each sampling range along the surface, the sound field is sampled at various depths, with the step size between samples increasing with depth

below the surface. The step sizes are chosen to provide increased coverage near the depth of the source and at depths of interest in terms of the sound speed profile. For areas with deep water, sampling is not performed at depths beyond those reachable by marine mammals. The received per-pulse SEL at a surface sampling location is taken as the maximum value that occurs over all samples within the water column, i.e., the maximum-over-depth received per-pulse SEL. These maximum-over-depth per-pulse SEL are presented as colour contours around the source.

An inherent variability in measured sound levels is caused by temporal variability in the environment and the variability in the signature of repeated acoustic impulses (sample sound source verification results is presented in Figure C-2). While MONM's predictions correspond to the averaged received levels, cautionary estimates of the threshold radii are obtained by shifting the best fit line (solid line, Figure C-2) upward so that the trend line encompasses 90% of all the data (dashed line, Figure C-2).

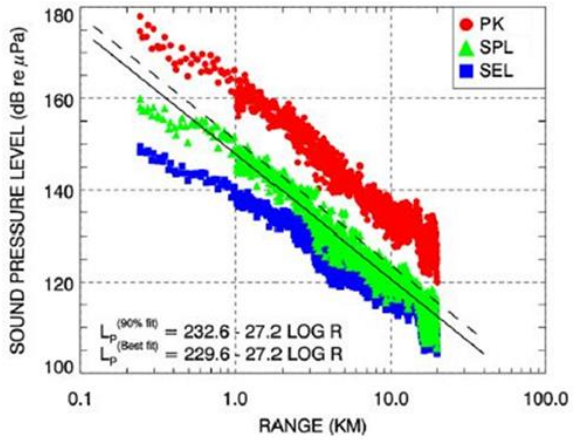

Figure C-2. PK and SPL and per-pulse SEL versus range from a 20 in^3 seismic source. Solid line is the least squares best fit to SPL. Dashed line is the best fit line increased by 3.0 dB to exceed 90% of all SPL values (90th percentile fit) (Ireland et al. 2009, Figure 10).

C.2. Full Waveform Range-dependent Acoustic Model: FWRAM

For impulsive sounds from the seismic source, time-domain representations of the pressure waves generated in the water are required to calculate SPL and PK. Furthermore, the seismic source must be represented as a distributed source to accurately characterise vertical directivity effects in the near-field zone. For this study, synthetic pressure waveforms were computed using FWRAM, which is a time-domain acoustic model based on the same wide-angle parabolic equation (PE) algorithm as MONM. FWRAM computes synthetic pressure waveforms versus range and depth for range-varying marine acoustic environments, and it takes the same environmental inputs as MONM (bathymetry, water sound speed profile, and seafloor geoacoustic profile). Unlike MONM, FWRAM computes pressure waveforms via Fourier synthesis of the modelled acoustic transfer function in closely spaced frequency bands. FWRAM employs the array starter method to accurately model sound propagation from a spatially distributed source (MacGillivray and Chapman 2012).

Besides providing direct calculations of the PK and SPL, the synthetic waveforms from FWRAM can also be used to convert the SEL values from MONM to SPL.

C.3. Wavenumber Integration Model

Sound pressure levels near the seismic source were modelled using JASCO's VSTACK wavenumber integration model. VSTACK computes synthetic pressure waveforms versus depth and range for arbitrarily layered, range-independent acoustic environments using the wavenumber integration approach to solve the exact (range-independent) acoustic wave equation. This model is valid over the full angular range of the wave equation and can fully account for the elasto-acoustic properties of the sub-bottom. Wavenumber integration methods are extensively used in the field of underwater acoustics and seismology where they are often referred to as reflectivity methods or discrete

wavenumber methods. VSTACK computes sound propagation in arbitrarily stratified water and seabed layers by decomposing the outgoing field into a continuum of outward-propagating plane cylindrical waves. Seabed reflectivity in the model is dependent on the seabed layer properties: compressional and shear wave speeds, attenuation coefficients, and layer densities. The output of the model can be post-processed to yield estimates of the SEL, SPL, and PK.

VSTACK accurately predicts steep-angle propagation in the proximity of the source, but it is computationally slow at predicting sound pressures at large distances due to the need for smaller wavenumber steps with increasing distance. Additionally, VSTACK assumes range-invariant bathymetry with a horizontally stratified medium (i.e., a range-independent environment) which is azimuthally symmetric about the source. VSTACK is thus best suited to modelling the sound field near the source.

Appendix D. Methods and Parameters

This section describes the specifications of the seismic source that was used at all sites and the environmental parameters used in the propagation models.

D.1. Estimating Range to Thresholds Levels

Sound level contours were calculated based on the underwater sound fields predicted by the propagation models, sampled by taking the maximum value over all modelled depths above the sea floor for each location in the modelled region. The predicted distances to specific levels were computed from these contours. Two distances relative to the source are reported for each sound level: 1) R_{max}, the maximum range to the given sound level over all azimuths, and 2) $R_{95\%}$, the range to the given sound level after the 5% farthest points were excluded (see examples in Figure D-1).

The $R_{95\%}$ is used because sound field footprints are often irregular in shape. In some cases, a sound level contour might have small protrusions or anomalous isolated fringes. This is demonstrated in the image in Figure D-1(a). In cases such as this, where relatively few points are excluded in any given direction, R_{max} can misrepresent the area of the region exposed to such effects, and $R_{95\%}$ is considered more representative. In strongly asymmetric cases such as shown in Figure D-1(b), on the other hand, $R_{95\%}$ neglects to account for significant protrusions in the footprint. In such cases R_{max} might better represent the region of effect in specific directions. Cases such as this are usually associated with bathymetric features affecting propagation. The difference between R_{max} and $R_{95\%}$ depends on the source directivity and the non-uniformity of the acoustic environment.

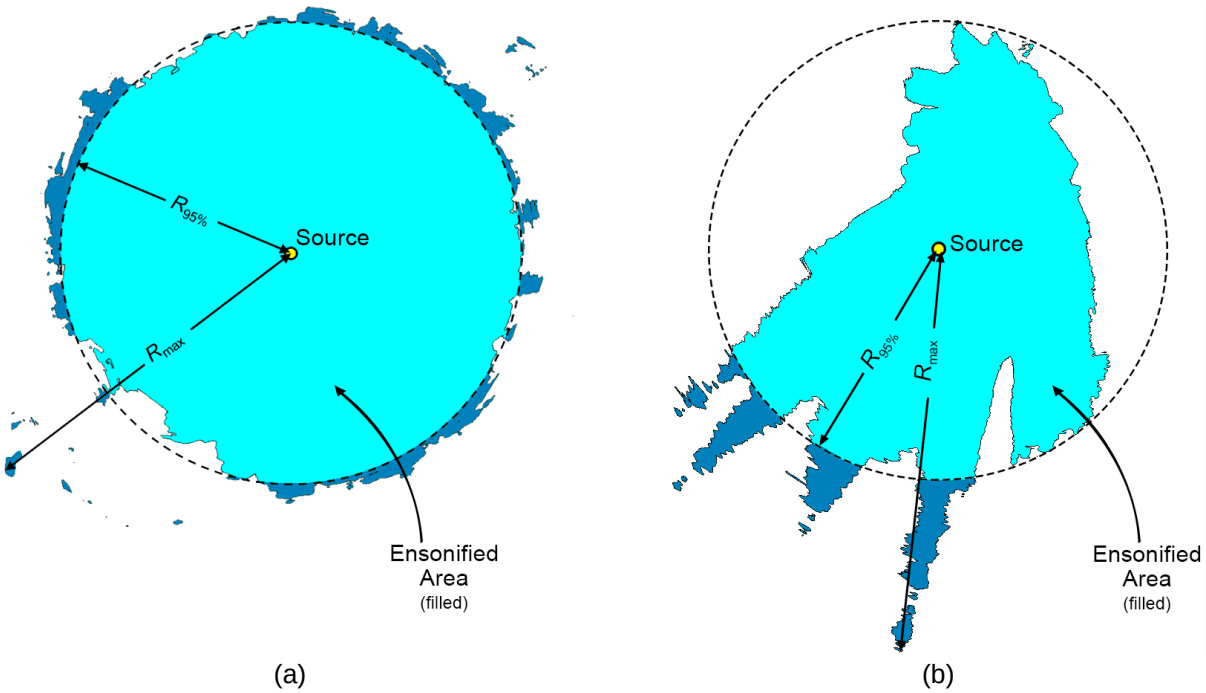

Figure D-1. Sample areas ensonified to an arbitrary sound level with R_{max} and $R_{95\%}$ ranges shown for two different scenarios. (a) Largely symmetric sound level contour with small protrusions. (b) Strongly asymmetric sound level contour with long protrusions. Light blue indicates the ensonified areas bounded by $R_{95\%}$; darker blue indicates the areas outside this boundary which determine R_{max}.

D.2. Estimating SPL from Modelled SEL Results

The per-pulse SEL of sound pulses is an energy-like metric related to the dose of sound received over the pulse's entire duration. The pulse SPL on the other hand is related to its intensity over a specified time interval. T_{90} is the 90% time window, the time interval often applied to assess seismic pulses (Appendix A). Seismic pulses typically lengthen in duration as they propagate away from their source, due to seafloor and surface reflections, and other waveguide dispersion effects. The changes in pulse length, and therefore T_{90}, affect the numeric relationship between SPL and SEL. Full-waveform modelling was used to estimate T_{90}, but this type of modelling is computationally intensive, and can be prohibitively time consuming when run at high spatial resolution over large areas.

For the current study, FWRAM (Appendix C.2) was used to model synthetic seismic pulses over the frequency range 10–2048 Hz. This was performed along broadside and endfire radials towards the deeper water depths to be conservative. FWRAM uses Fourier synthesis to recreate the signal in the time domain so that both the SEL and SPL from the source can be calculated. The differences between the SEL and SPL were extracted for all ranges and depths that corresponded to those generated from the high spatial-resolution results from MONM. A 125 ms fixed time window positioned to maximize the SPL over the pulse duration was applied. The resulting SEL -to-SPL offsets were averaged in 1 km range bins along each modelled radial and depth, and the 90th percentile was selected at each range to generate a generalised range-dependent conversion function for each site. The range- dependent conversion function was applied to predicted per-pulse SEL results from MONM to model SPL values. Figure D-2 shows the conversion offsets for four; the spatial variation is caused by changes in the received airgun pulse as it propagates from the source.

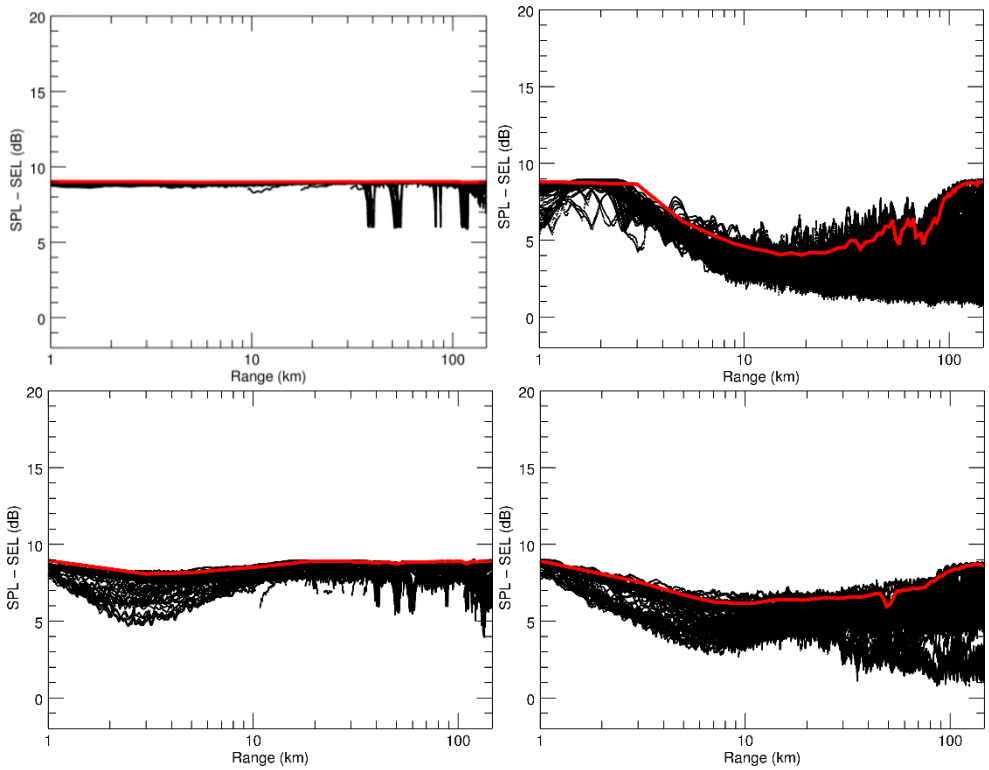

Figure D-2. Range-and-depth-dependent conversion offsets for converting SEL to SPL for seismic pulses. Slices are shown for the 3080 in^3 modelled Site 1 (upper left), Site 5 (upper right), Site 7 (lower left) and Site 12 (lower right). Black lines are the modelled differences between SEL and SPL across different radials and receiver depths; the solid red line is the 90th percentile of the modelled differences at each range.

D.3. Environmental Parameters

D.3.1. Bathymetry

Water depths throughout the modelled area were extracted from the Australian Bathymetry and Topography Grid, a 9 arc-second grid rendered for Australian waters (Whiteway 2009) for the region shown in Figure 1. Bathymetry data were extracted and re-gridded onto a Universal Transverse Mercator (UTM) coordinate projection (Zone 51 S) with a regular grid spacing of 100 × 100 m.

D.3.2. Sound speed profile

The sound speed profiles for the modelled sites were derived from temperature and salinity profiles from the U.S. Naval Oceanographic Office's *Generalized Digital Environmental Model V 3.0* (GDEM; Teague et al. 1990, Carnes 2009). GDEM provides an ocean climatology of temperature and salinity for the world's oceans on a latitude-longitude grid with 0.25° resolution, with a temporal resolution of one month, based on global historical observations from the U.S. Navy's Master Oceanographic Observational Data Set (MOODS). The climatology profiles include 78 fixed depth points to a maximum depth of 6800 m (where the ocean is that deep). The GDEM temperature-salinity profiles were converted to sound speed profiles according to Coppens (1981).

Mean monthly sound speed profiles were derived from the GDEM profiles within 200 km box radius of each modelling site. The July sound speed profile is expected to be most favourable to longer-range sound propagation across the entire year. As such, July was selected for sound propagation modelling to ensure precautionary estimates of distances to received sound level thresholds. Figure D-3. shows the resulting profile used as input to the sound propagation modelling.

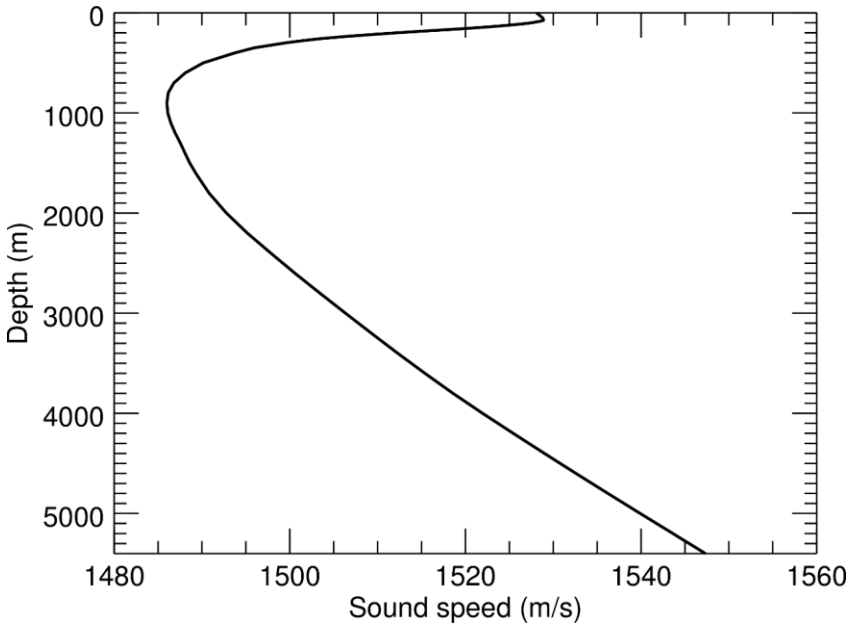

Figure D-3. The final sound speed profile (July) used for the modelling. Profiles are calculated from temperature and salinity profiles from GDEM V 3.0 (GDEM; Teague et al. 1990, Carnes 2009).

D.3.3. Geoacoustics

Acoustic transmission loss modelling requires the geoacoustic properties of the seabed and sub-bottom are as representative of the modelling area as possible. Four geoacoustic profiles were compiled for the modelling area based on available data for the depositional environment and lithology for the region.

The study area encompasses areas within the Northern Shelf Province, the Northwest Shelf Province, and Northwest Shelf Transition bioregions (Figure D-4)(Baker et al. 2008). In these areas, the morphology of the study area is dominated by coastal terrace, shelf and slope environments, which effectively define the lithological and sedimentary character of this environment. The dominant fractions of the surficial sediment within each region assist in deriving representative profiles.

Because the modelled area is large and geoacoustic information is limited, a simplified geoacoustic profile was constructed to represent the major features of the sediment column at the modelled sites. The geoacoustic properties for the modelled sites (Tables D-1 to D-4) were estimated from the average parameters based on the sediment model of Buckingham (2005). In the absence of other evidence, it was assumed that surficial sediment characteristics are largely constant with depth, at least to the depths of interest in transmission loss modelling. The profiles used for modelling assumed no distinct layering, which is similar to the majority of the stratigraphic profiles reviewed in this study

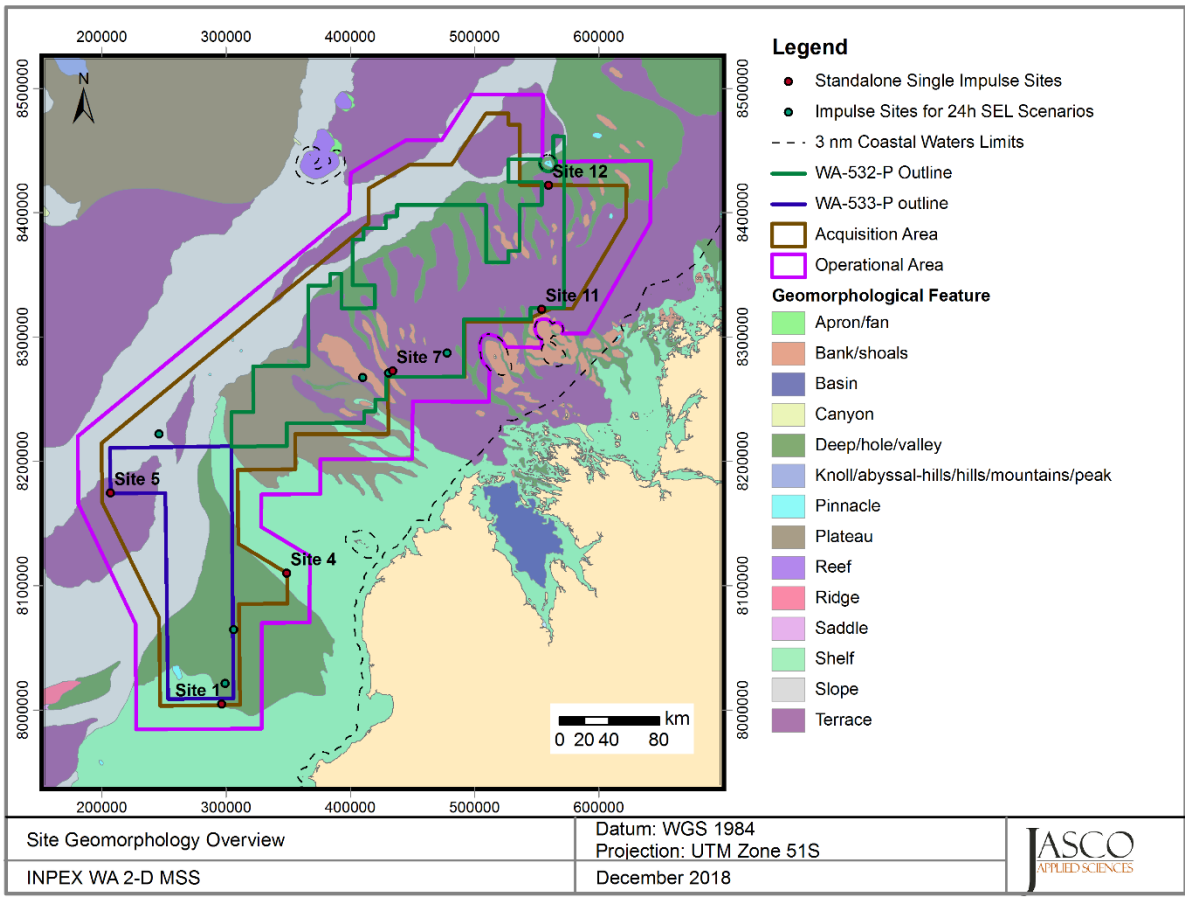

Figure D-4. The geomorphology of the study area.

Table D-1. Estimated geoacoustic profile for Sites 1–4, which represents a gravelly sand bottom. Within each depth range, each parameter varies linearly within the stated range. The compressional wave is the primary wave. The shear wave is the secondary wave.

Depth below seafloor (m)	Material	Density (g/cm³)	P-wave speed (m/s)	P-wave attenuation (dB/λ)	S-wave speed (m/s)	S-wave attenuation (dB/λ)
0–100.0	Increasingly consolidated carbonate sand	1.77–1.93	1646.0–1813.6	0.74–0.82	386.5	3.65
100.0–200.0		1.93–2.07	1813.6–1973.6	0.82–0.89		
200.0–300.0		2.07–2.19	1973.6–2126.2	0.89–0.96		
300.0–400.0		2.19–2.29	2126.2–2271.4	0.96–1.02		
400.0–500.0		2.29–2.38	2271.4–2409.0	1.02–1.08		

Table D-2. Estimated geoacoustic profile for Sites 5 and 6, which represents a muddy sand bottom. Within each depth range, each parameter varies linearly within the stated range. The compressional wave is the primary wave. The shear wave is the secondary wave.

Depth below seafloor (m)	Material	Density (g/cm³)	P-wave speed (m/s)	P-wave attenuation (dB/λ)	S-wave speed (m/s)	S-wave attenuation (dB/λ)
0–10	Muddy sand	2.04	1672	0.37	306	3.65
10–20		2.04	1788	0.76		
20–50		2.05	1850	0.94		
50–100		2.07	1968	1.22		
100–200		2.1	2094	1.45		
200–500		2.1	2243	1.73		
>500		2.1	2517	2.13		

Table D-3. Estimated geoacoustic profile for Sites 7–11, which represents a muddy sandy gravel bottom. Within each depth range, each parameter varies linearly within the stated range. The compressional wave is the primary wave. The shear wave is the secondary wave.

Depth below seafloor (m)	Material	Density (g/cm³)	P-wave speed (m/s)	P-wave attenuation (dB/λ)	S-wave speed (m/s)	S-wave attenuation (dB/λ)
0	Coarse sand	2.09	1827	0.65	350	3.65
10		2.09	2068	1.31		
20		2.09	2199	1.58		
50		2.09	2440	1.97		
100		2.09	2692	2.27		
200		2.09	3025	2.56		
500		2.09	3628	2.89		

Table D-4. Estimated geoacoustic profile for Site 12, which represents a gravelly muddy sand bottom. Within each depth range, each parameter varies linearly within the stated range. The compressional wave is the primary wave. The shear wave is the secondary wave.

Depth below seafloor (m)	Material	Density (g/cm³)	P-wave speed (m/s)	P-wave attenuation (dB/λ)	S-wave speed (m/s)	S-wave attenuation (dB/λ)
0	Medium sand	2.011	1733.5–1836	0.51–0.84	201.8	3.65
5		2.015	1836–1905.3	0.84–1.04		
10		2.018	1905.3–1998.1	1.04–1.26		
20		2.025	1998.1–2172.6	1.26–1.6		
50		2.047	2172.6–2359.1	1.60–1.86		
100		2.080	2359.1–2594.1	1.86–2.15		
200		2.097	2594.1–3010.2	2.15–2.54		
500		2.097	3010.2	2.54		

D.4. Seismic Sources

The layouts of the seismic sources considered in Appendix B are provided in Figures D-7 to D-5.

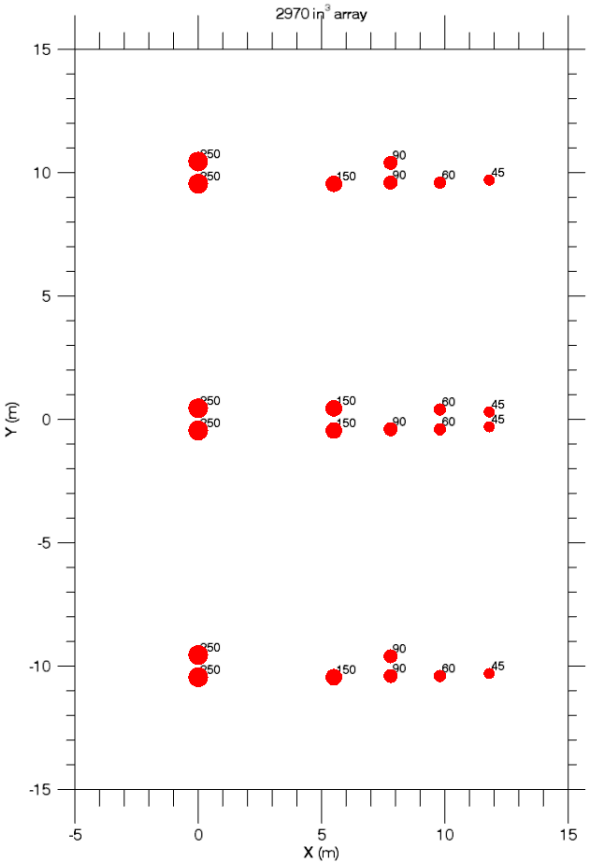

Figure D-5. Layout of the modelled 2970 in³ seismic source array. Tow depth is 7 m. The labels indicate the firing volume (in cubic inches) for each airgun. Also see Table D-7.

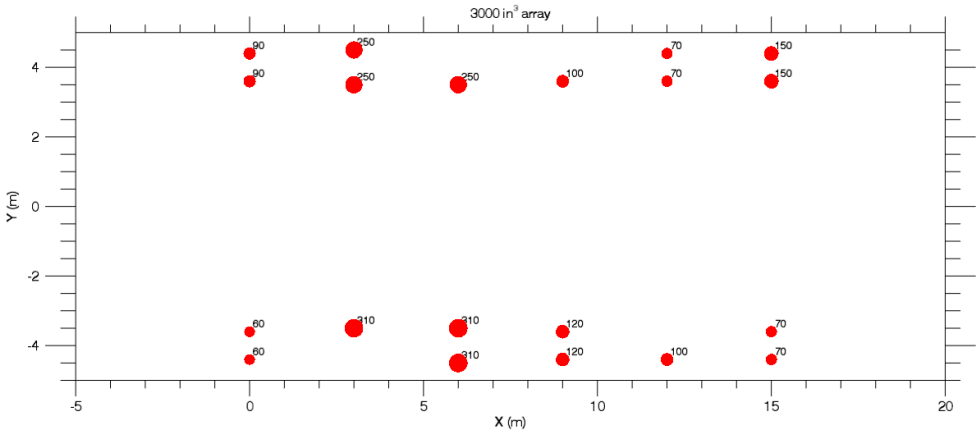

Figure D-6. Layout of the modelled 3000 in^3 seismic source array. Tow depth is 6 m. The labels indicate the firing volume (in cubic inches) for each airgun. Also see Table D-6.

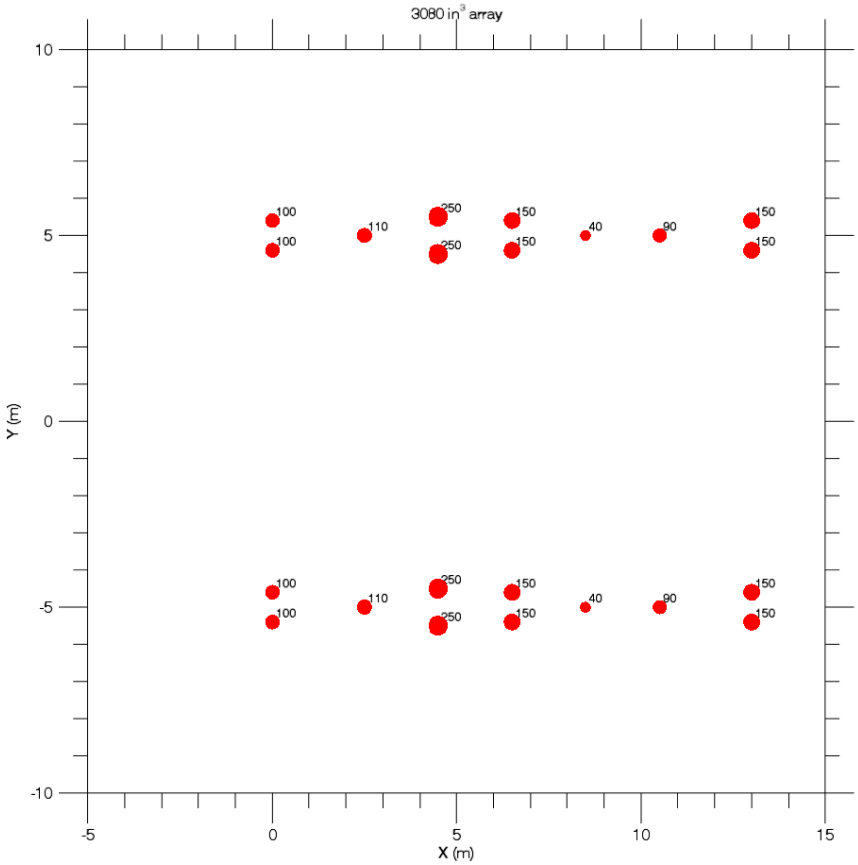

Figure D-7. Layout of the modelled 3080 in^3 seismic source array. Tow depth is 7 m. The labels indicate the firing volume (in cubic inches) for each airgun. Also see

Table D-5.

Table D-5. Layout of the modelled 3080 in^3 seismic source array. Tow depth is 7 m. Firing pressure for all guns is 2000 psi. Also see Figure D-7.

Gun	x (m)	y (m)	z (m)	Volume (in^3)	Gun	x (m)	y (m)	z (m)	Volume (in^3)
1	0	5.4	7	100	12	0	−4.6	7	100
2	0	4.6	7	100	13	0	−5.4	7	100
3	2.5	5	7	110	14	2.5	−5	7	110
4	4.5	5.5	7	250	15	4.5	−4.5	7	250
5	4.5	4.5	7	250	16	4.5	−5.5	7	250
6	6.5	5.4	7	150	17	6.5	−4.6	7	150
7	6.5	4.6	7	150	18	6.5	−5.4	7	150
8	8.5	5	7	40	19	8.5	−5	7	40
9	10.5	5	7	90	20	10.5	−5	7	90
10	13	5.4	7	150	21	13	−4.6	7	150
11	13	4.6	7	150	22	13	−5.4	7	150

Table D-6. Layout of the modelled 3000 in^3 seismic source array. Tow depth is 6 m. Firing pressure for all guns is 2000 psi. Also see Figure D-7.

Gun	x (m)	y (m)	z (m)	Volume (in^3)	Gun	x (m)	y (m)	z (m)	Volume (in^3)
1	0	4.4	6	90	11	0	−3.6	6	60
2	0	3.6	6	90	12	0	−4.4	6	60
3	3	4.5	6	250	13	3	−3.5	6	310
4	3	3.5	6	250	14	6	−3.5	6	310
5	6	3.5	6	250	15	6	−4.5	6	310
6	9	3.6	6	100	16	9	−3.6	6	120
7	12	4.4	6	70	17	9	−4.4	6	120
8	12	3.6	6	70	18	12	−4.4	6	100
9	15	4.4	6	150	19	15	−3.6	6	70
10	15	3.6	6	150	20	15	−4.4	6	70

Table D-7. Layout of the modelled 2970 in^3 seismic source array. Tow depth is 7 m. Firing pressure for all guns is 2000 psi. Also see Figure D-7.

Gun	x (m)	y (m)	z (m)	Volume (in^3)	Gun	x (m)	y (m)	z (m)	Volume (in^3)
1	0	10.45	7	250	13	9.8	0.4	7	60
2	0	9.55	7	250	14	9.8	−0.4	7	60
3	5.5	9.55	7	150	15	11.8	0.3	7	45
4	7.8	10.4	7	90	16	11.8	−0.3	7	45
5	7.8	9.6	7	90	17	0	−9.55	7	250
6	9.8	9.6	7	60	18	0	−10.45	7	250
7	11.8	9.7	7	45	19	5.5	−10.45	7	150
8	0	0.45	7	250	20	7.8	−9.6	7	90
9	0	−0.45	7	250	21	7.8	−10.4	7	90
10	5.5	0.45	7	150	22	9.8	−10.4	7	60
11	5.5	−0.45	7	150	23	11.8	−10.3	7	45
12	7.8	−0.4	7	90					

D.5. Model Validation Information

Predictions from JASCO's Airgun Array Source Model (AASM) and propagation models (MONM, FWRAM and VSTACK) have been validated against experimental data from a number of underwater acoustic measurement programs conducted by JASCO globally, including the United States and Canadian Artic, Canadian and southern United States waters, Greenland, Russia and Australia (Hannay and Racca 2005, Aerts et al. 2008, Funk et al. 2008, Ireland et al. 2009, O'Neill et al. 2010, Warner et al. 2010, Racca et al. 2012a, Racca et al. 2012b, Matthews and MacGillivray 2013, Martin et al. 2015, Racca et al. 2015, Martin et al. 2017a, Martin et al. 2017b, Warner et al. 2017, MacGillivray 2018, McPherson et al. 2018, McPherson and Martin 2018).

In addition, JASCO has conducted measurement programs associated with a significant number of anthropogenic activities which have included internal validation of the modelling (including McCrodan et al. 2011, Austin and Warner 2012, McPherson and Warner 2012, Austin and Bailey 2013, Austin et al. 2013, Zykov and MacDonnell 2013, Austin 2014, Austin et al. 2015, Austin and Li 2016, Martin and Popper 2016) .

Appendix E. Results

E.1. Additional Per-Pulse Sound Field Maps

Supplementary maps for Section 5.2.2.1, maps for six modelling sites included in the accumulated SEL scenarios, Figures E-1 to E-12.

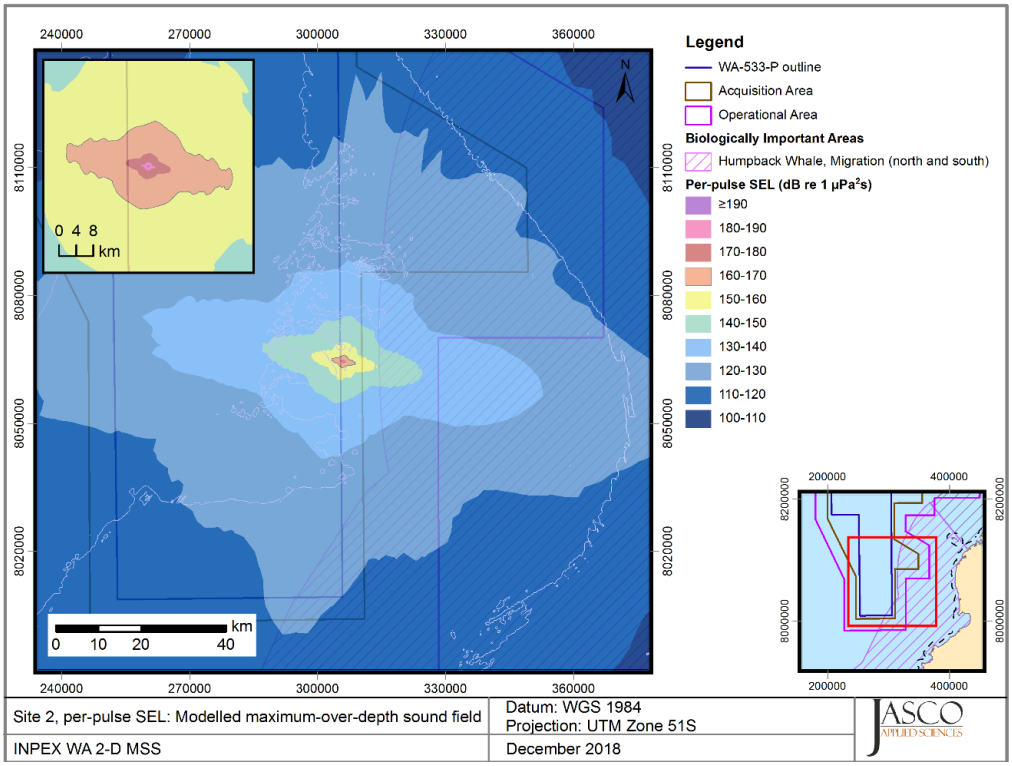

Figure E-1. *Site 2 (WA-533-P), per-pulse SEL*: Sound level contour map showing unweighted maximum-over-depth results.

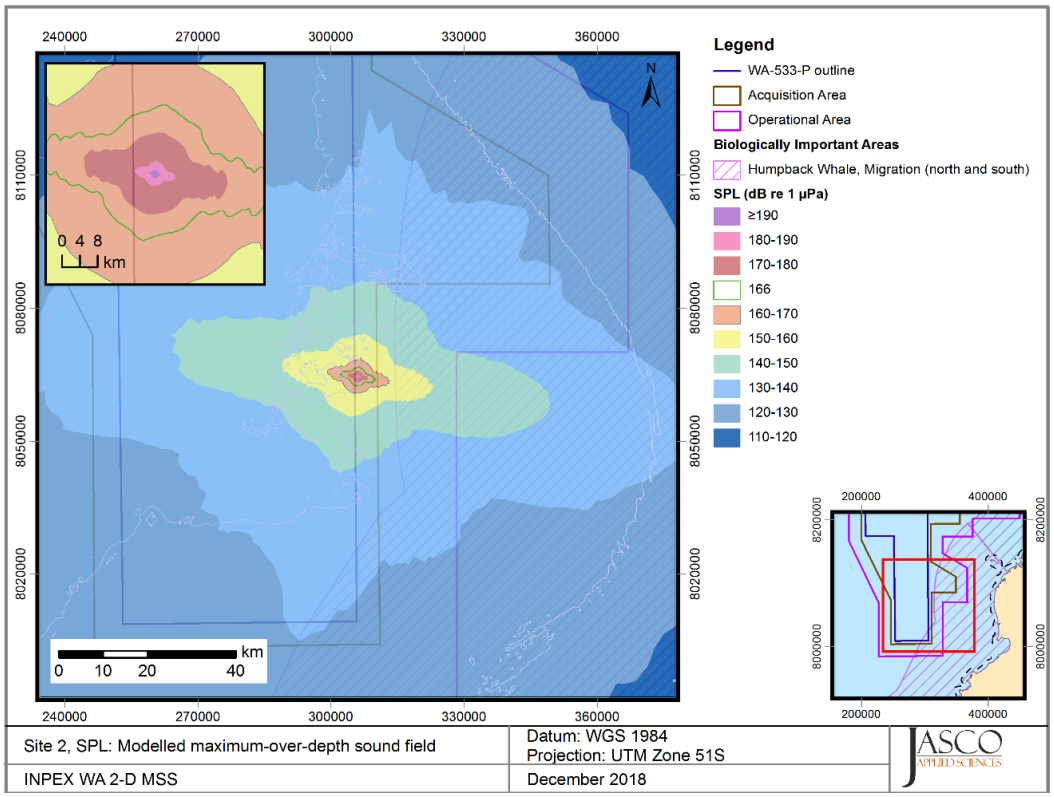

Figure E-2. *Site 2 (WA-533-P), SPL*: Sound level contour map showing unweighted maximum-over-depth results.

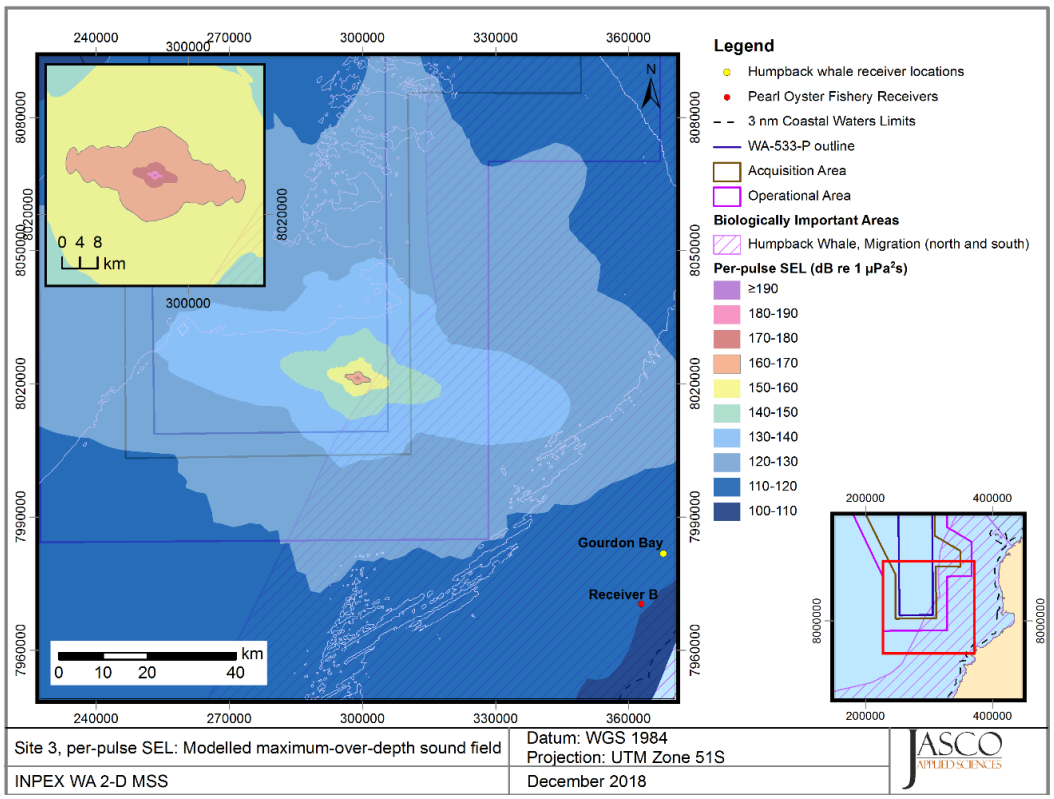

Figure E-3. *Site 3 (WA-533-P), per-pulse SEL*: Sound level contour map showing unweighted maximum-over-depth results.

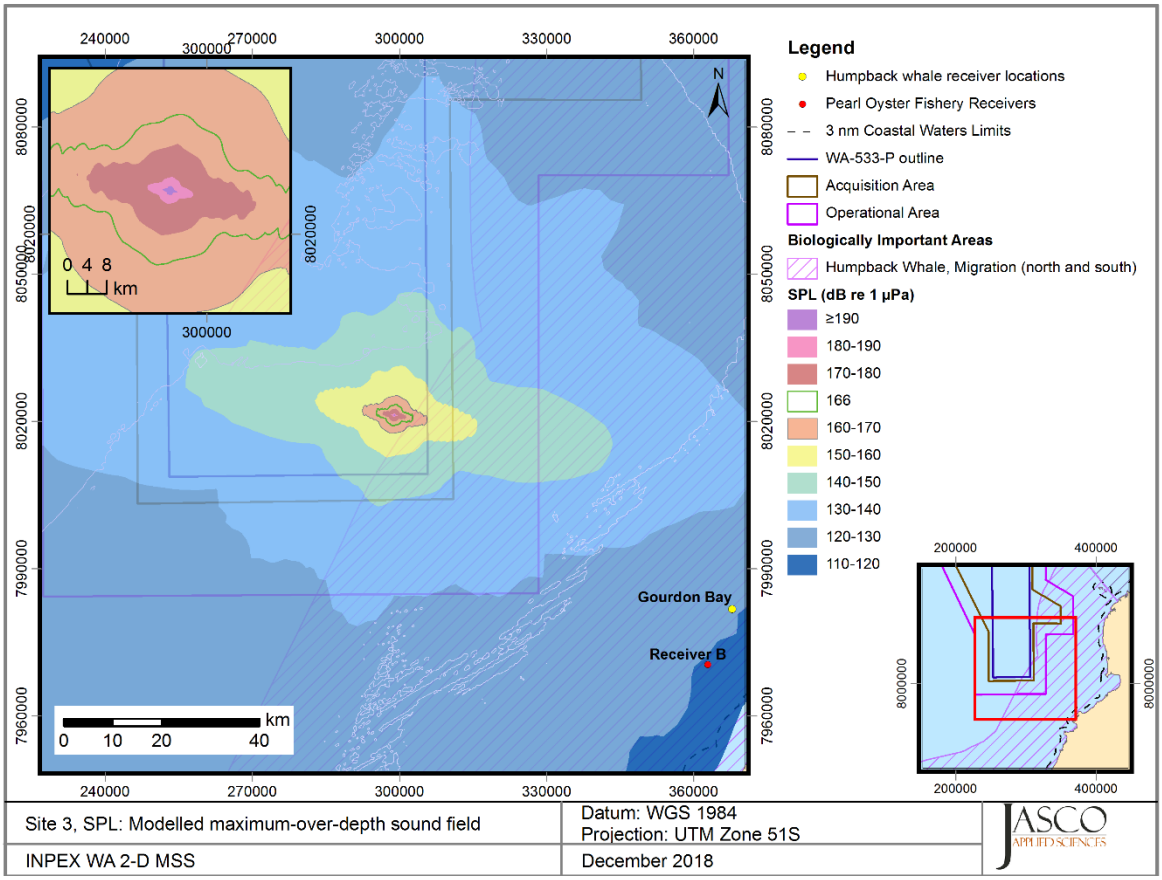

Figure E-4. *Site 3 (WA-533-P), SPL*: Sound level contour map showing unweighted maximum-over-depth results.

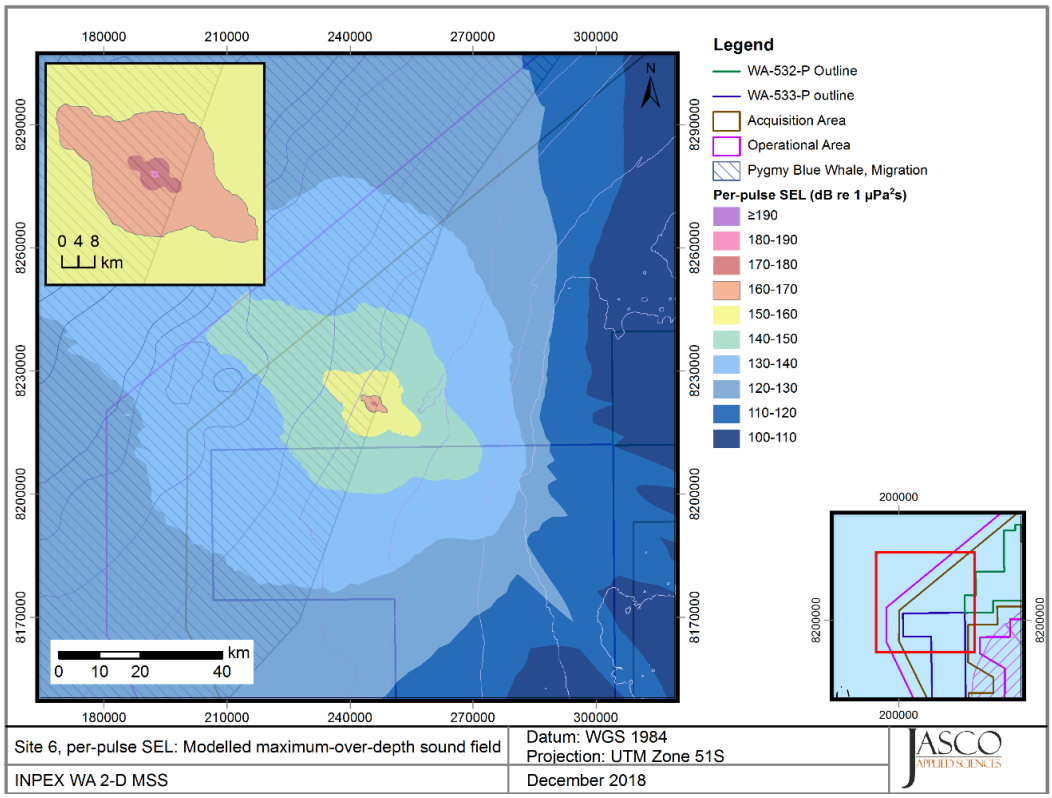

Figure E-5. *Site 6, per-pulse SEL*: Sound level contour map showing unweighted maximum-over-depth results.

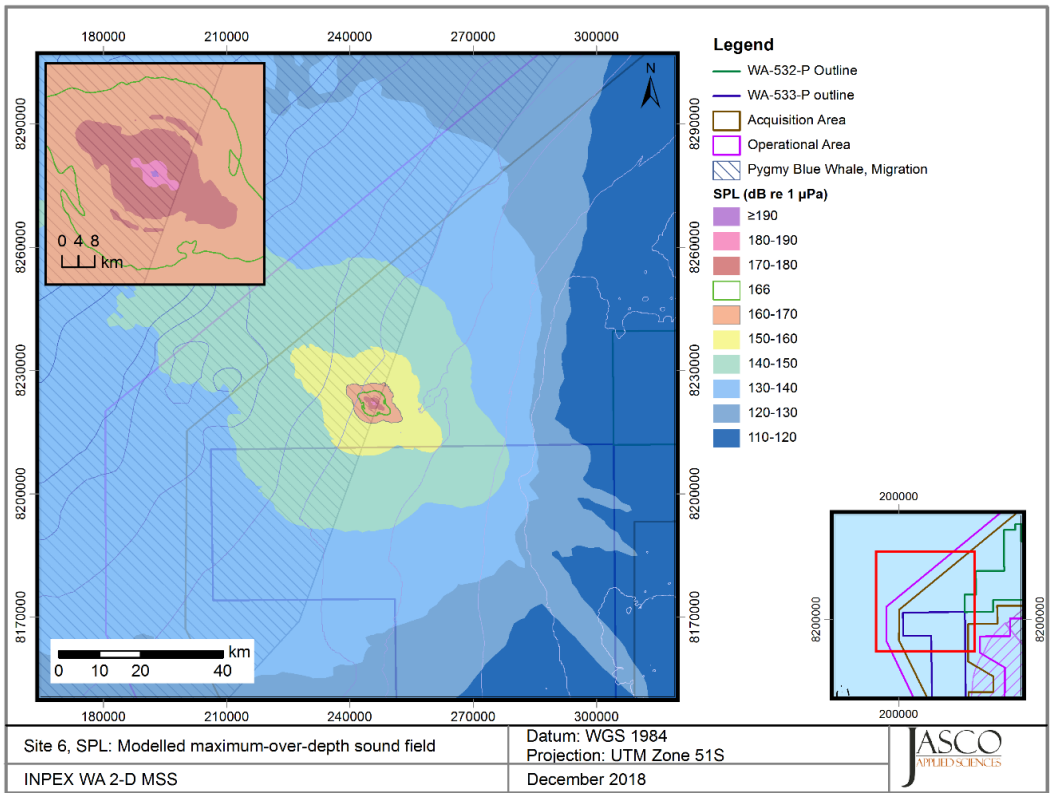

Figure E-6. *Site 6, SPL*: Sound level contour map showing unweighted maximum-over-depth results.

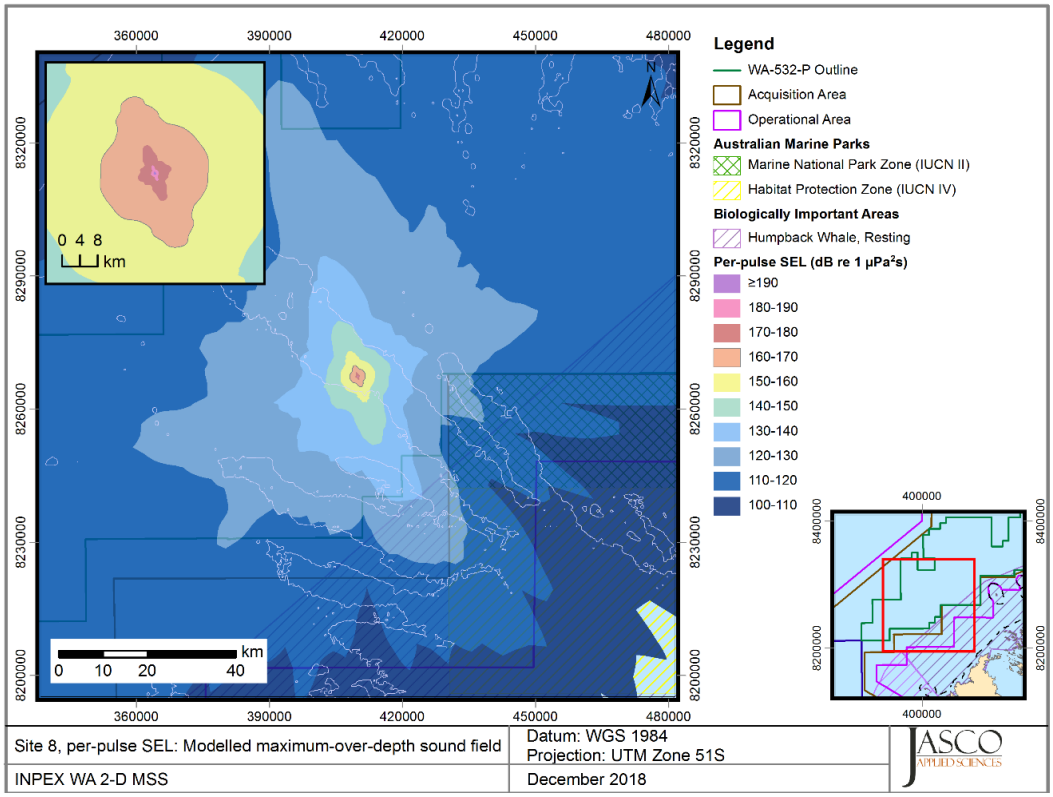

Figure E-7. *Site 8 (WA-532-P), per-pulse SEL*: Sound level contour map showing unweighted maximum-over-depth results.

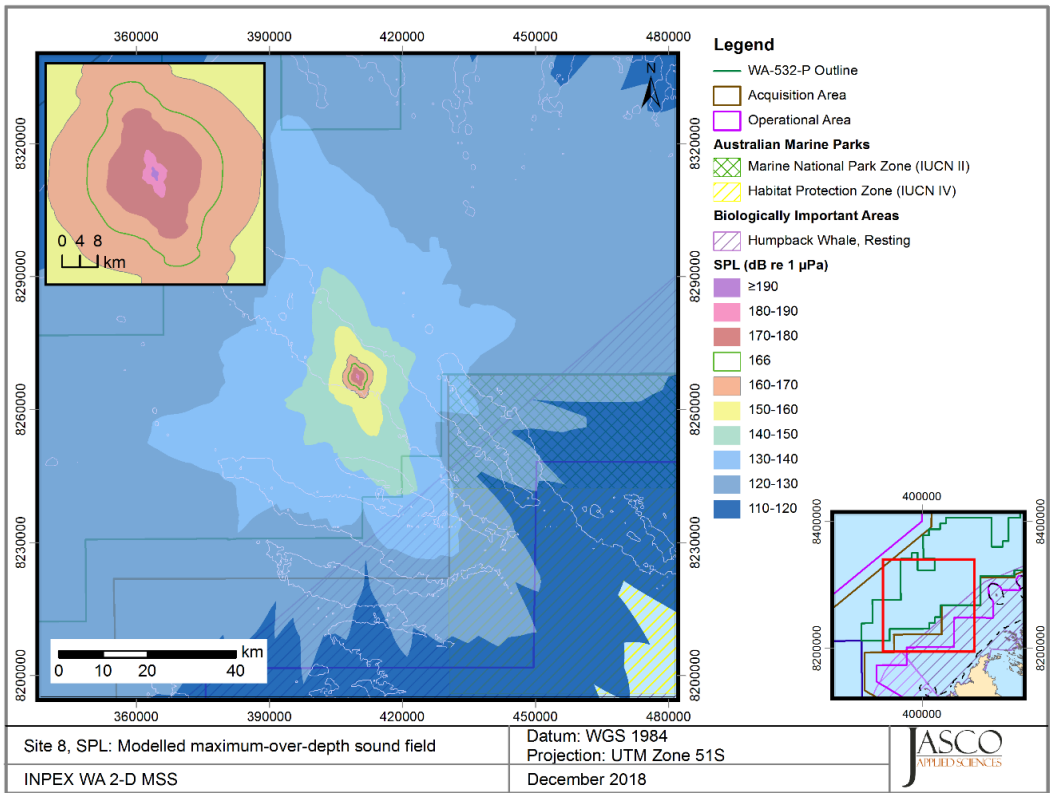

Figure E-8. *Site 8 (WA-532-P), SPL*: Sound level contour map showing unweighted maximum-over-depth results.

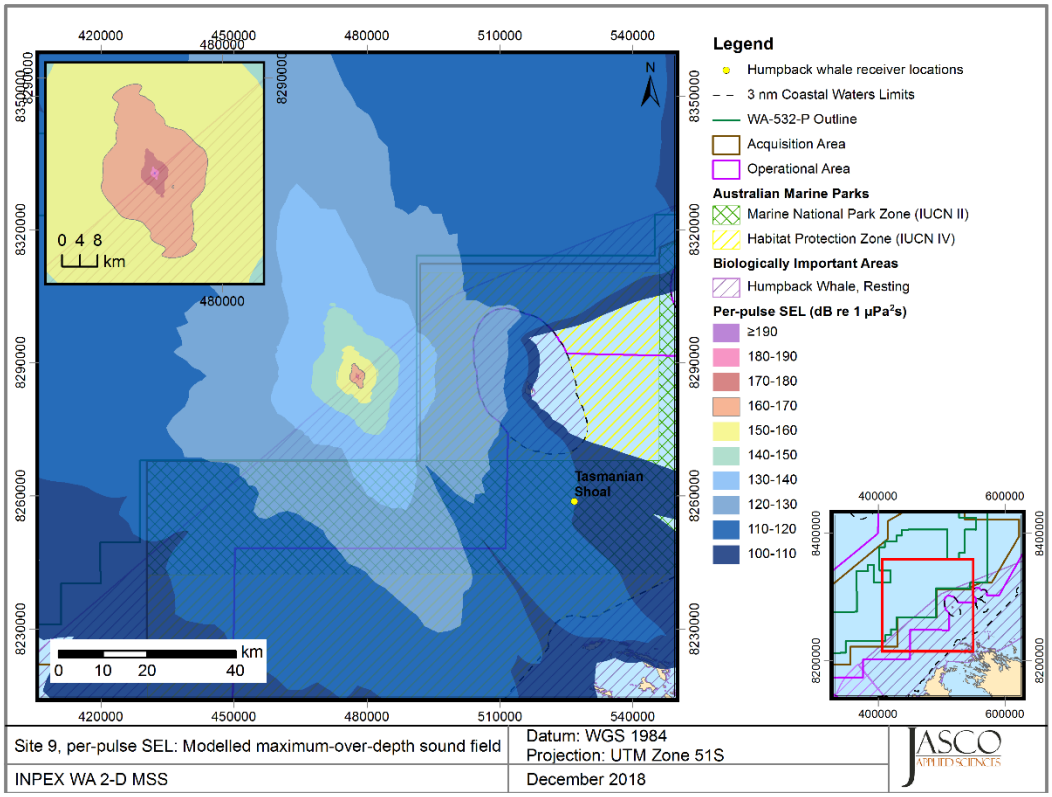

Figure E-9. *Site 9 (WA-532-P), per-pulse SEL*: Sound level contour map showing unweighted maximum-over-depth results.

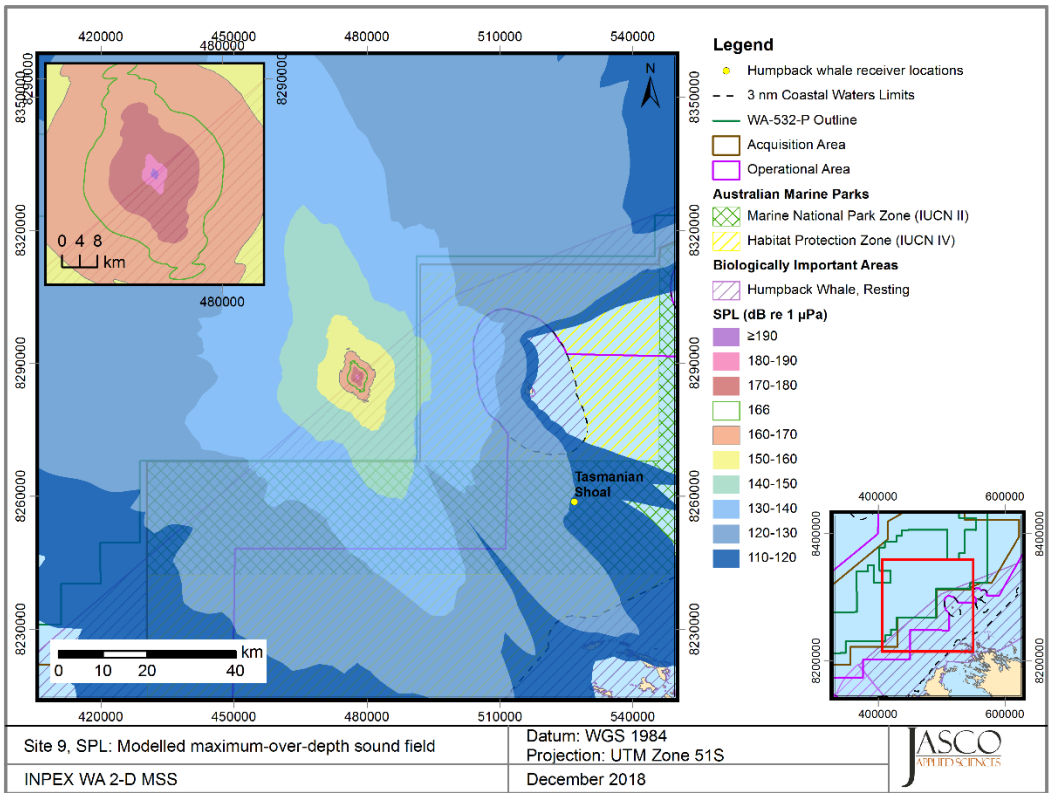

Figure E-10. *Site 9 (WA-532-P), SPL*: Sound level contour map showing unweighted maximum-over-depth results.

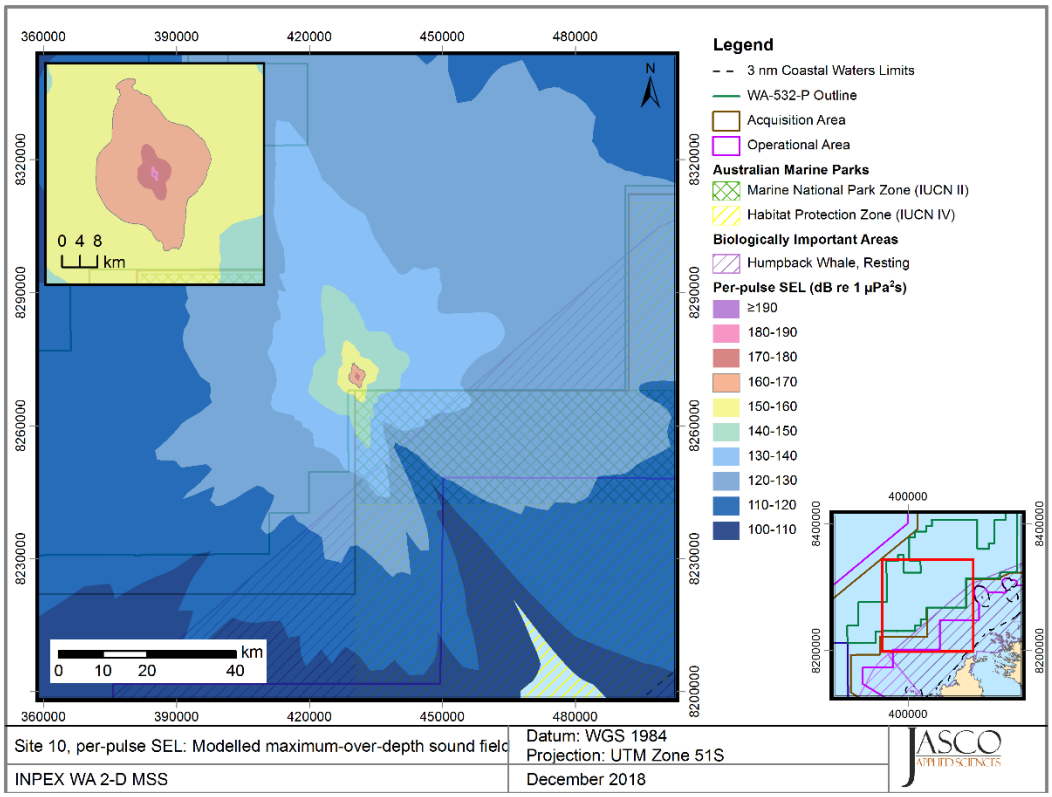

Figure E-11. *Site 10 (WA-532-P), per-pulse SEL*: Sound level contour map showing unweighted maximum-over-depth results.

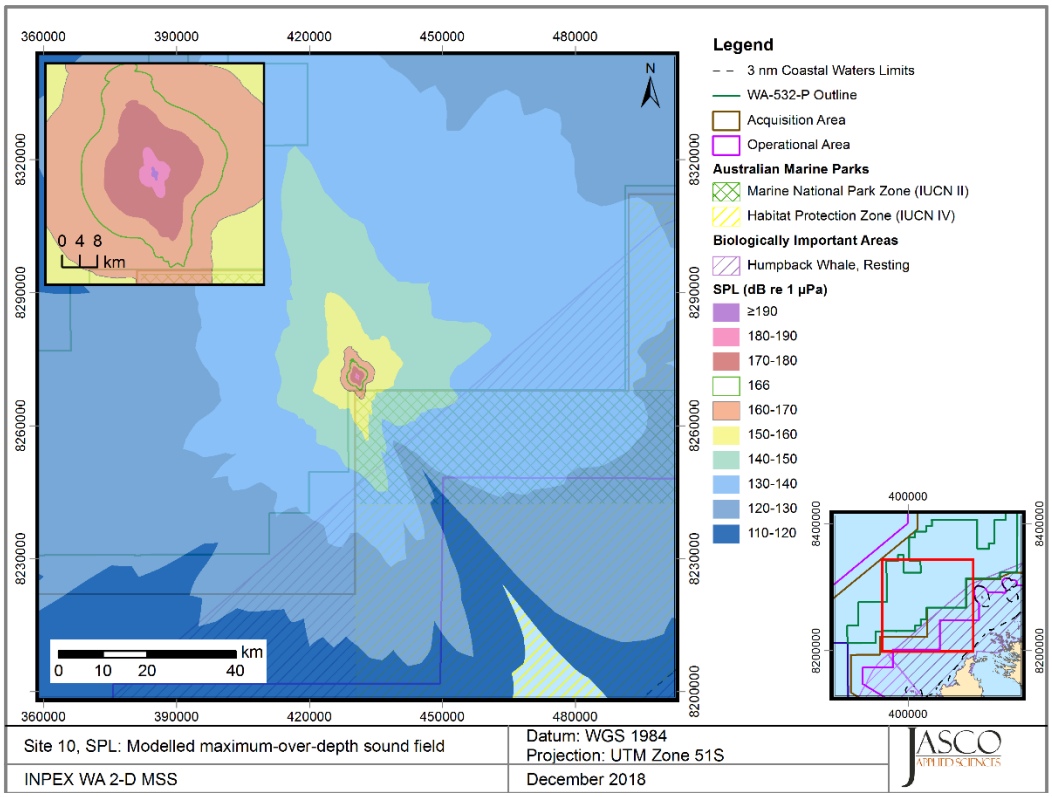

Figure E-12. *Site 10 (WA-532-P), SPL*: Sound level contour map showing unweighted maximum-over-depth results.

E.2. SPL Vertical Slice Plots

Supplementary maps for Section 5.2.2.2, vertical slices of the SPL sound fields, Figures E-13 to E-18.

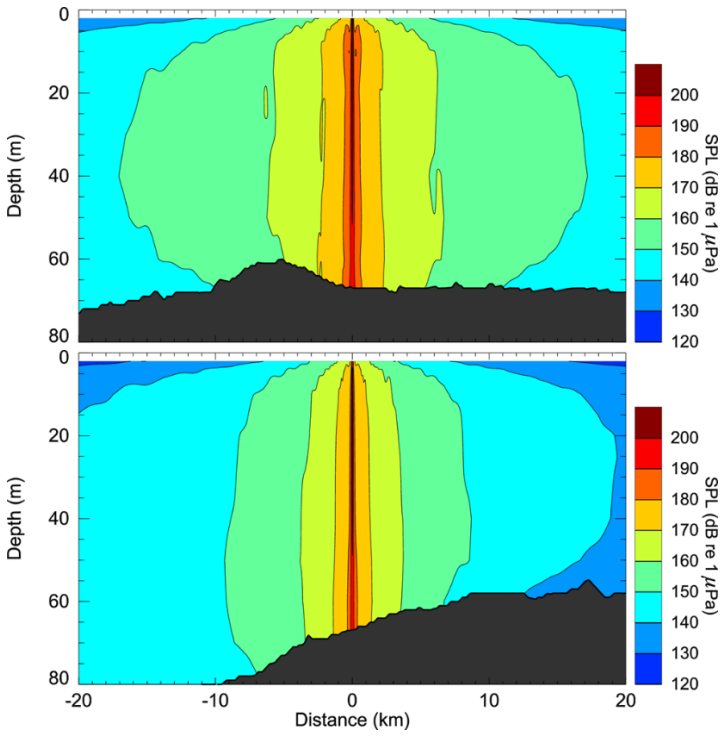

Figure E-13. *Site 1 (WA-533-P), SPL*: Vertical slice of the predicted SPL for the 3080 in^3 array. Levels are shown along the broadside (top) and endfire (bottom) directions.

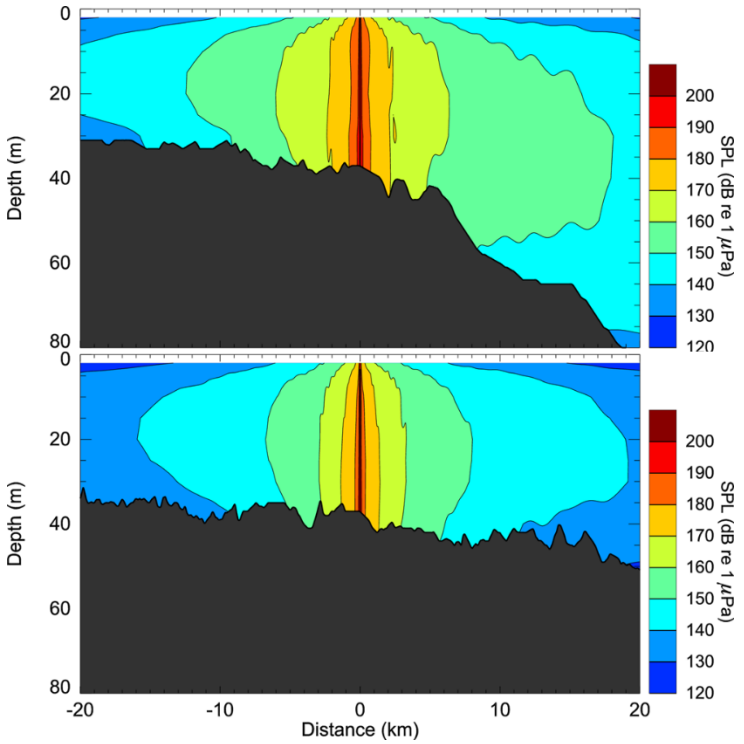

Figure E-14. *Site 4 (WA-533-P), SPL*: Vertical slice of the predicted SPL for the 3080 in^3 array. Levels are shown along the broadside (top) and endfire (bottom) directions.

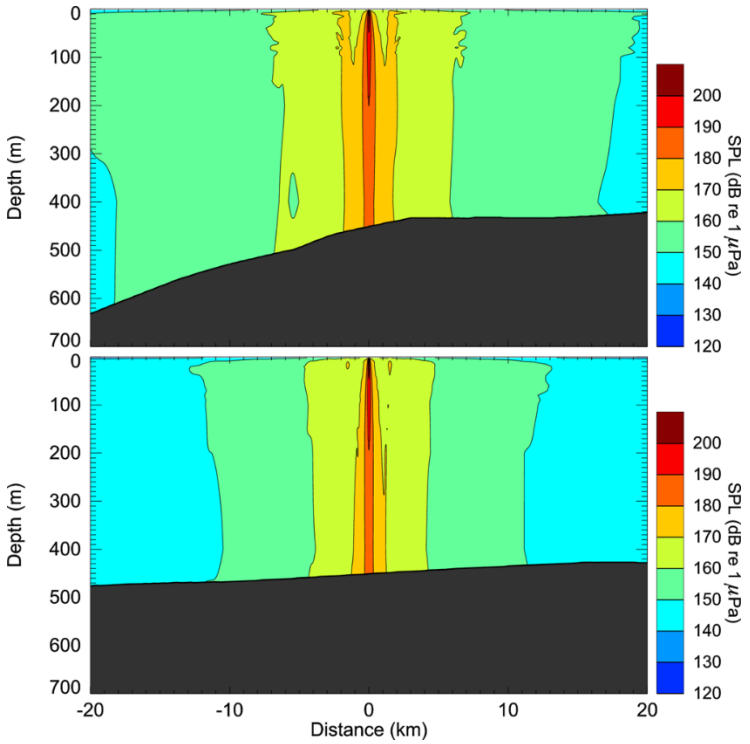

Figure E-15. *Site 5 (WA-533-P), SPL*: Vertical slice of the predicted SPL for the 3080 in3 array. Levels are shown along the broadside (top) and endfire (bottom) directions.

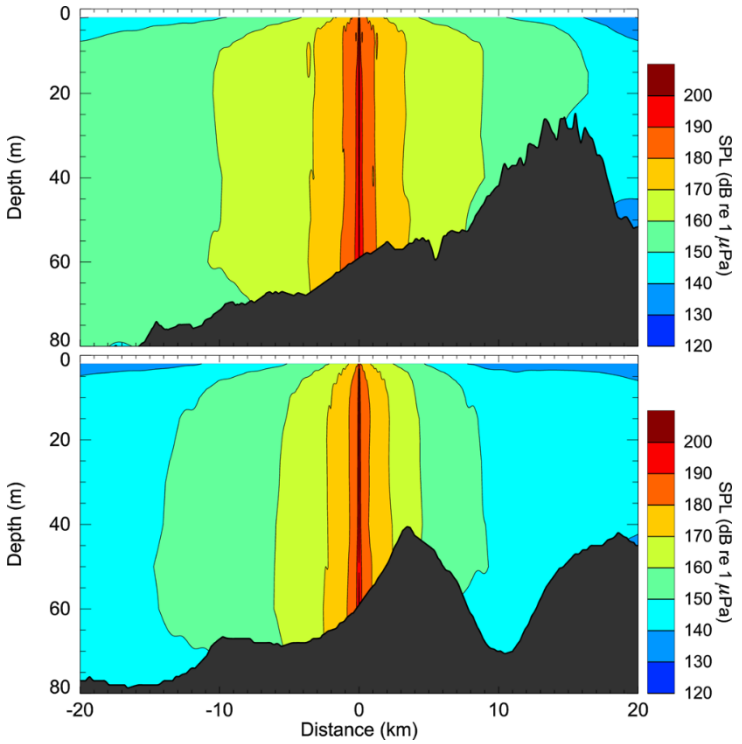

Figure E-16. *Site 7 (WA-532-P), SPL*: Vertical slice of the predicted SPL for the 3080 in3 array. Levels are shown along the broadside (top) and endfire (bottom) directions.

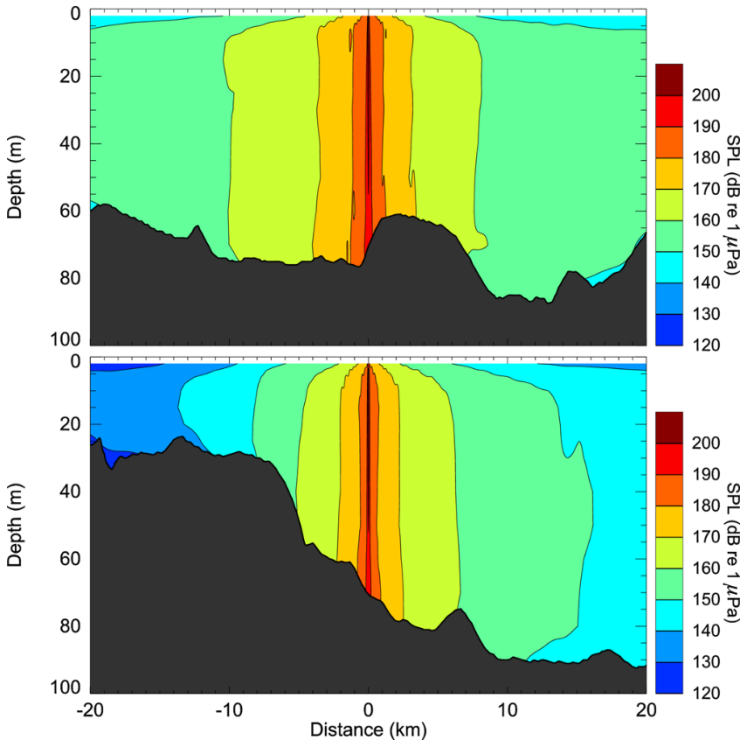

Figure E-17. *Site 11 (WA-532-P), SPL*: Vertical slice of the predicted SPL for the 3080 in3 array. Levels are shown along the broadside (top) and endfire (bottom) directions.

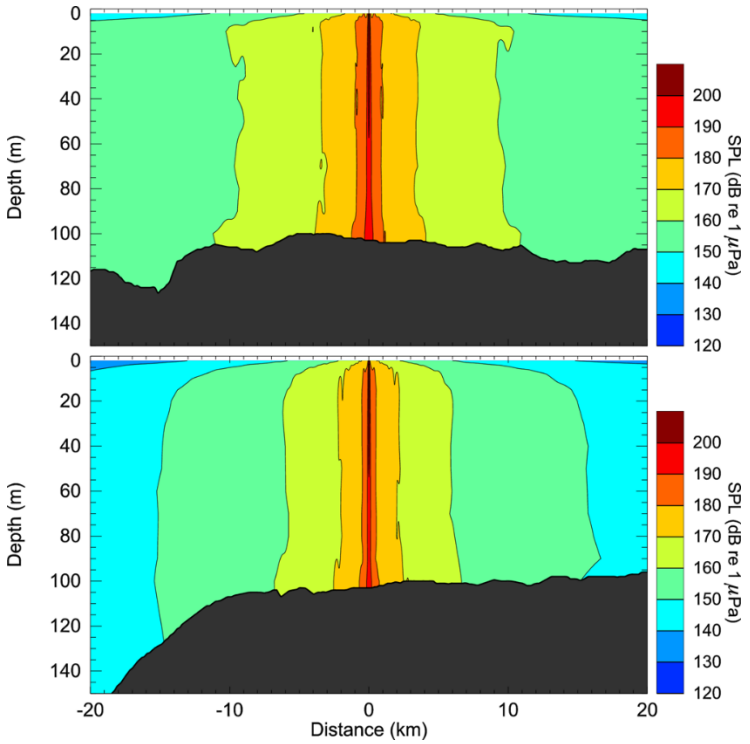

Figure E-18. *Site 12 (WA-532-P), SPL*: Vertical slice of the predicted SPL for the 3080 in3 array. Levels are shown along the broadside (top) and endfire (bottom) directions.